Oxygen and carbon isotope variations in precipitation and speleothem calcite from a northern California cave: Implications for paleoclimate reconstructions during the Late Pleistocene

By

Isabelle Ellis Weisman

Thesis
Submitted to the Faculty of the
Graduate School of Vanderbilt University
in partial fulfillment of the requirements
for the degree of

MASTER OF SCIENCE
in
Earth and Environmental Science
August 11, 2017
Nashville, Tennessee

Approved:

Jessica L. Oster, Ph.D.
Marisa Luisa S.P. Jorge, Ph.D.

ACKNOWLEDGEMENTS

This thesis would not have been possible without the support and help from a great number of people, however a few require special thanks.

I would first like to thank my advisor Dr. Jessica Oster for her persistent guidance, patient mentorship, and constant encouragement over the past two years. I would like to thank the Oster Lab Group, namely Nick Hermann and Elli Ronay, for generously encouraging my research and providing constructive feedback. Thank you to my second reader Dr. Malu Jorge for the insightful feedback and subsequent improvements. Thank you to Dr. John Ayers for serving on my committee and for communicating geochemistry in such an exciting and thoughtful manner. I would also like to thank Dr. Ralf Bennartz, Dr. Naomi Marks, Dave Mundt and the Lake Shasta Caverns Staff for their contributions to this thesis. I would lastly like to thank the faculty and graduate students of the EES department for making Vanderbilt a fantastic place to be a graduate student. A special thanks to my family, Michelle Foley, Brandt Gibson, Jennifer Bradham, Jewell Beasley-Stanley, and the Rock ‘Em Sock ‘Em softball team.

TABLE OF CONTENTS

LIST OF TABLES

LIST OF FIGURES

CHAPTER 1

INTRODUCTION

Over the past decade, California has dealt with extreme hydroclimate, water's interaction with soil, rocks, biota and humans, oscillations. Between 2012 and 2015, California experienced a drought considered to be the most severe in the last 1200 years (Griffin and Anchukaitis 2014). Droughts of this scale, and in this region, have significant economic consequences for this highly populated, water-stressed state. In 2016 alone, there was an estimated total value loss of $600 million and 7,400 full and part time jobs in agriculture statewide due to the drought (Medellin-Azura et al., 2016). Conversely, in 2017, northern California experienced its wettest winter on record, as the state was bombarded by winter storms that brought drenching rain and feet of snow in the Sierras Nevada Mountains. Although the wetter winter of 2017 resulted in landslides, road closures, power outages, and coastal flooding, it also increased streamflow, refilled reservoirs and increased the mountain snowpack throughout California, providing much needed relief to the state (NOAA). This drastic hydroclimate change, however, is not uncommon in California, as the state is known to deal with drought, followed by flooding, on multi-annual timescales. Similar, extreme hydroclimatic changes are also suggested by the paleo record, but at different timescales.

Paleoclimate records point to analogously large hydroclimatic changes in the Western US during the Late Pleistocene (Oster et al., 2015). Across the last glacial-interglacial transition, proxy records from Western North America (WNA; See Appendix A for list of abbreviations) document major dry and wet intervals, marked by the growth and decline of pluvial lakes, alluvial fan aggradation, speleothems and pollen records (Lyle 2012; Oster et al., 2009; Wagner et al., 2010; Asmerom et al., 2010; Antinao and McDonald 2013; Ibarra et al., 2014). However, these abrupt climate shifts were not spatially homogenous across California and the western US. Precipitation paleoclimate records and proxy reconstructions from northern California indicate different hydroclimatic responses than those apparent in southern California, the Great Basin and the American Southwest (Lyle, 2012; Munroe and Laabs, 2013, Oster et al., 2015, Kirby, 2013). Recent work in this region describes a precipitation dipole pattern during the Last Glacial Maximum (LGM) with a wet southwest and dry northeast separated by and a northwest to southeast trending transition zone across the northern Great Basin (Figure 1; Oster et al., 2015a). Similarly, modern studies of WNA hydroclimatic change related to the El Niño Southern Oscillation (ENSO) and the Pacific Decadal Oscillation (PDO) have identified a north-south dipole pattern of inter-annual and decadal precipitation variability between the Pacific Northwest and Desert Southwest (Wise, 2010; Redmond and Koch, 1991; Dettinger et al., 1998). The centers of the north and south region tend to be characterized by an opposite association with ENSO and PDO variability; meaning when one is anomalously wet the other is anomalously dry. Results indicate that the ENSO/PDO transition zone and the LGM precipitation dipole zone are located around the 40-42°N latitude.

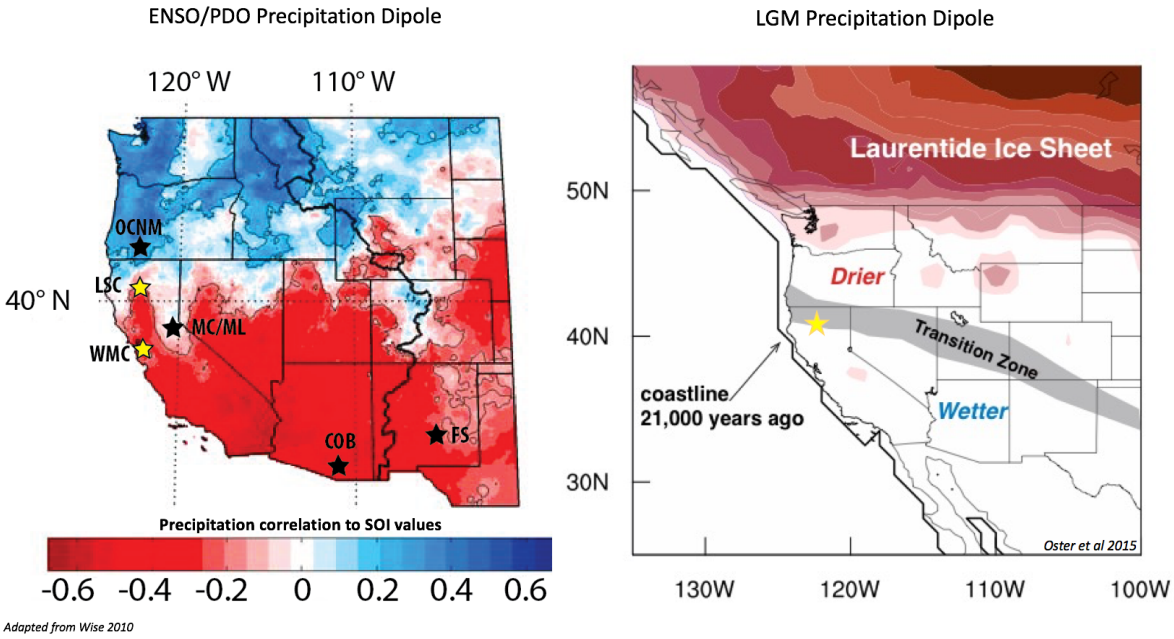

Figure 1. (Left) Map of western North America shaded according to precipitation correlation to Southern Oscillation Index (SOI) values. Speleothem records in progress indicated by yellow stars (LSC - Lake Shasta Caverns, WMC - White Moon Cave). Previously published speleothem records indicated by black stars (OCNM - Oregon Caves National Monument (Vacco et al., 2005); COB - Cave of the Bells (Wagner et al., 2010); FS - Fort Stanton (Feng et al., 2014). Red shading indicates negative correlation to SOI and blue shading indicates a positive correlation to the SOI. (Right) LGM precipitation dipole with Transition Zone shaded in gray. Location of LSC illustrated by yellow star.

Speleothem records, which can be precisely dated by U-Series dating methods often have the necessary chronological control, resolution and continuity to allow detailed investigations of hydroclimatic change (Fairchild and Baker, 2012). Recently, several speleothem records from across the western US have provided insight into precipitation amount, balance and source variation during the last deglacial, but relatively few speleothem records from the western US provide adequate coverage of this key transition zone at the last glacial-interglacial transition. In this study, I develop an oxygen ($\delta^{18}O$) and carbon ($\delta^{13}C$) isotope record from a speleothem that grew between ~35 and 14 ka from Lake Shasta Caverns, (40.8043°N, -122.3040°W; LSC) located in the region that seems to be a key hinge point in the pattern of hydroclimatic responses across the west on multiple timescales. The new record from LSC provides a high-resolution record of Late Pleistocene climate and precipitation variability and will complement previously published, temporally overlapping, paleo-precipitation proxies and modeling studies in WNA (Figure 2). The speleothem from LSC is well situated to investigate the stability of these patterns over time, and make it possible to evaluate the potential influence of climate oscillations in driving abrupt hydroclimatic changes during the last deglaciation. To aid in my interpretation of this multi-proxy paleorecord I also conduct a modern precipitation and cave drip water analysis of oxygen ($\delta^{18}O$) and hydrogen ($\delta^{2}H$) to identify the controls on the isotopic composition of precipitation in Northern California. Together, this project paints a fuller picture of hydroclimate change through the last glacial and deglaciation (~35 ka – ~14 ka), and refines the location and movement of the hydrologic transition zone through time.

Project Overview

This study uses this multi-proxy speleothem and rain and drip water analysis to address the following questions:

1. What controls the isotopic ($\delta^{18}O$ and $\delta^{2}H$) composition of precipitation in northern California? Is it moisture source, temperature, or a different parameter?
2. How did the hydroclimate of Northern California change across the last deglaciation?
3. How do changes at LSC fit into the regional picture of hydroclimatic change across the last glacial-interglacial?
4. Does the location of the transition zone change through time?

In order to accurately interpret the LSC proxy records, I conduct a modern precipitation and cave drip water analysis of oxygen ($\delta^{18}O$) and hydrogen ($\delta^{2}H$) to identify the controls on the isotopic composition of precipitation in Northern California because the relative influence of temperature and moisture source are unique to each cave site. To extend this temporally-limited LSC rainwater dataset and make my dataset a more comprehensive representation of precipitation over time, I supplement this work with $\delta^{18}O$ and $\delta^{2}H$ data from precipitation samples collected weekly from National Atmospheric Deposition Program (NADP) site near LSC. I compare this data to weather data from a nearby weather station to determine the respective potential influence of temperature on precipitation and cave drip water. I compare weekly and monthly-integrated rainwater isotopes across this interval with back-trajectory analyses to elucidate the potential influence of moisture transport to LSC in the present day. A more complete understanding of the controls on modern precipitation isotopic signatures will answer my first research question and ultimately aid in the interpretation of my paleorecord.

With a firm understanding of the controls on modern $\delta^{18}O$ and $\delta^{2}H$ precipitation, I have developed a continuous, high resolution $\delta^{18}O$ and $\delta^{13}C$ records from LSC, sample LSC3. U-Th dating of LSC3 indicate that it grew during the end of the last glacial cycle (~14.3-35.9 ka). Oxygen isotope ratios in speleothems should reflect meteoric water values. Stable carbon isotopes are typically taken alongside $\delta^{18}O$ measurements in speleothem geochemical analyses. Variability in carbon isotopes can arise from modification of dissolved inorganic carbon in seepage water that happens in the soil and epikarst. Over time, changes in the ratio of C_3 to C_4 plants above the cave, fluid-rock interaction, and prior calcite precipitation (PCP) can alter drip water and therefore speleothem $\delta^{13}C$ signatures (Oster et al., 2009; Fairchild and Baker, 2012).

Integration of this new paleoclimate record from LSC with ongoing and previously published work, temporally overlapping speleothem records of rainfall variability in WNA will create a continuous record along the west coast, expose how LSC compares with other regional records of change and enable me to determine how, and if, the pivoting transition zone has moved through the last glacial-deglacial. The LSC record will also help paint a fuller picture of Northern California hydroclimate change during the glacial-deglacial, and constrain how, and if, the hydrologic transition zone has moved thorough time.

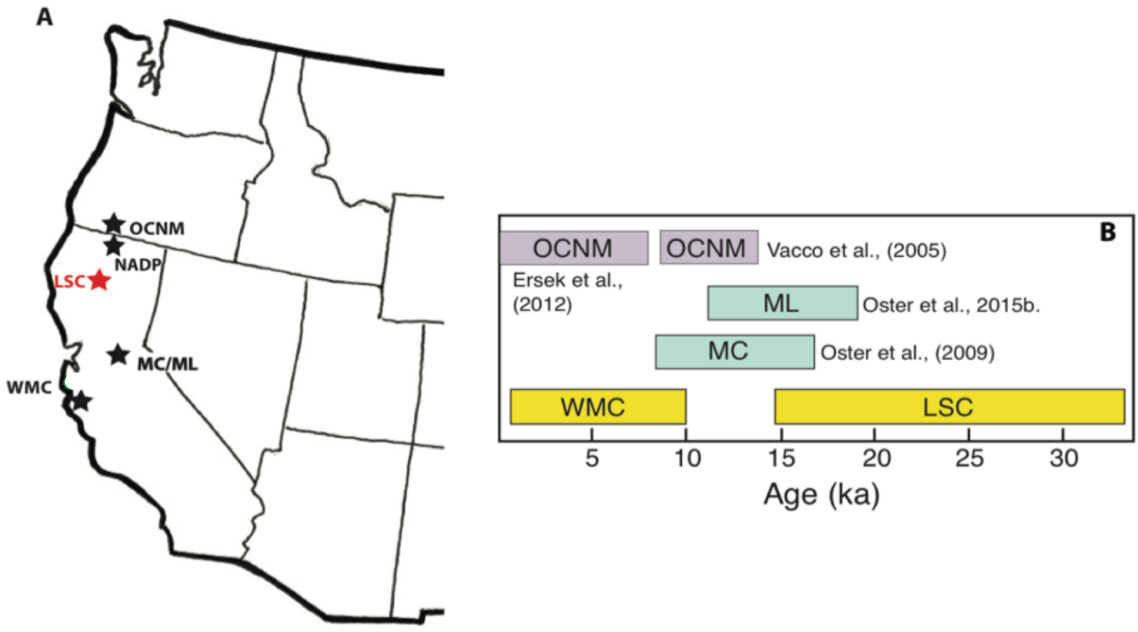

Figure 2. A) Location of cave records on map as black stars. NADP site CA-76 also located with black star. B) Age ranges of speleothem records under development at Lake Shasta Caverns (LSC) and White Moon Cave (WMC) and previously published records from Moaning and McLean's Caves (MC/ML) (Oster et al., 2009, 2015) and Oregon Caves (OCNM) (Vacco et al., 2005; Ersek et al., 2012).

Site and Sample Description

LSC is a commercial cave located approximately 32 km north of Redding, California, on the east side of the McCloud arm of Shasta Lake (40.8043°N, 122.3040°W). The McCloud limestone crops out in a north-south belt in the Shasta Lake area. The McCloud Limestone is Early Permian in age and ranges in thickness from less than 30m to about 800m. The eastern part of the Shasta Lake area is characterized by a large east-dipping monocline with folds and faults that warp and displace the limestone by 2000 feet or more locally. In most places, the McCloud Limestone is separated from the underlying Baird Formation (tuffaceous rocks and adjoining sandstones and shales), by a sill of mafic quartz diorite of uneven thickness, and dikes – likely offshoots of the sill – intrude the McCloud in many locations (Dimmerian and Harbaugh, 1965). There are a number of small caves as well as three large cave systems developed in the McCloud Limestone (LSC, Potter Creek, and Samwel Cave). Of the three, the largest and most complex cave system is LSC.

Cool wet winters and hot, dry summers characterize the climate above LSC. Between 1981 and 2010, Redding, California, experienced an average yearly rainfall of 879 mm. Approximately 90% of annual precipitation falls between October and May. The annual average high temperature is 24°C and annual average low temperature is 9.7°C, with an average annual temperature of

16.8°C (US Climate Data). Natural drip-water flow within the cave increases substantially during the winter season (up to 5 ml/min) and almost entirely ceases (1-2 drips/min) during the summer.

Sample LSC3 was collected in 2006 from the Thompson room (Figure 3). LSC3 is ~17.3cm tall (Figure 12). LSC3 contains a variety of calcite fabrics, with regions of dense translucent calcite, thin white calcite bands (1mm), and thin brownish detritus rich bands.

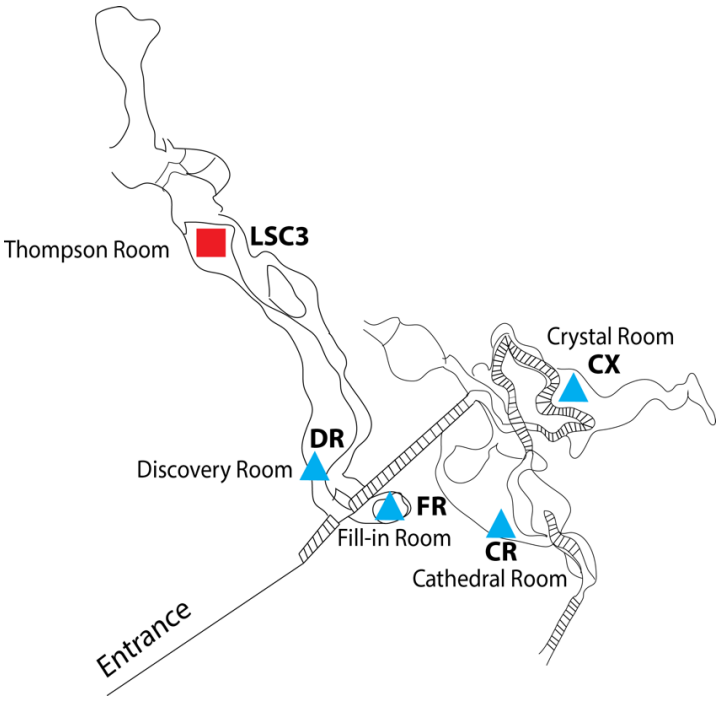

Figure 3. Map of LSC with blue triangles at drip water locations. LSC3 was collected from the Thompson Room (red square) in 2006.

CHAPTER 2

METHODOLOGY

Understanding the Modern Environment

In order to constrain paleorecords, it is critical to understand how the cave responds to modern environmental conditions. I have collaborated with the staff at LSC to collect monthly integrated precipitation and cave drip water. I supplemented this dataset with weekly-integrated precipitation samples collected between March 2010 through the February 2017, from the National Atmospheric Deposition Program (NADP) site CA-76 in Montague, California (~80 miles north of LSC). To investigate how precipitation $\delta^{18}O$ and $\delta^{2}H$ varies in the modern day, I compared daily temperature data from the University of California Integrated Pest Management (UC-IPM) weather station in Yreka, California to the $\delta^{18}O$ and $\delta^{2}H$ from precipitation samples from the NADP site CA-76 and at LSC. In order to determine if temperature controls the isotopic ($\delta^{18}O$ and $\delta^{2}H$) signature of precipitation in Northern California, I compare the $\delta^{18}O$ and $\delta^{2}H$ data with daily temperature data from the UC-IPM site in Yreka, California (the closest UC-IPM weather station to LSC and ~6 miles west of the NADP site). This precipitation study will be paired with HYSPLIT back-trajectory analyses (see HYSLPIT back trajectory section) to determine if moisture source influences the isotopic ($\delta^{18}O$ and $\delta^{2}H$) signature of precipitation that falls in Northern California.

NADP Precipitation

To better quantify the controls on precipitation $\delta^{18}O$ and $\delta^{2}H$ values, archived precipitation samples were obtained from the NADP site CA-76 in Montague, California (Figure 4). Previous work has demonstrated that the NADP collection and archiving protocol is sufficient for isotopic analysis (Harvey and Welker, 2000; Welker, 2000; Harvey, 2001; Vachon et al., 2007, 2010b, 2010a, Berkelhammer et al., 2012). A total of 140 precipitation samples were used for this study. The water samples were sent to be measured at the Stable Isotope Ratio Facility for Environmental Research (SIRFER) at the University of Utah. Microliter quantities of water were injected directly into a ThermoFinnigan Delta Plus XL isotope ratio mass spectrometer. Hydrogen and oxygen isotope ratios were both obtained from the analyses. Isotope ratios are expressed as ‰ as:

$$\delta^{N}E = ((R_{sample} / R_{standard}) - 1) \times 1000 \quad (1)$$

Where N is the heavy isotope of element E and R is the ratio of the heavy to light isotope ($^{18}O/^{16}O$ of $^{2}H/^{1}H$). The δ values are reported relative to V-SMOW. Long-term precision is 1.56‰ ($\delta^{2}H$) and 0.19‰ ($\delta^{18}O$).

Cave drip water

Drip water samples were collected at four locations within LSC between December of 2015 and March of 2017 (Figure 3). These drip sites were chosen because they are the most consistently

wet areas in the cave. The drips fall from draperies ranging from 10 m to less than 1m above collection site. Drip water sample collection began in December 2015 and will continue until December 2020. Through a collaboration with the staff at LSC, drip waters are sampled from the four drip locations monthly. The group of drips are less than 300 m apart. Water samples for stable isotope analysis ($\delta^{18}O$, $\delta^{2}H$ and $\delta^{13}C_{DIC}$) were collected in acid-cleaned 30 ml LDPE vials and capped with minimal headspace to reduce the potential for evaporative bias. Due to slow drip rates, it was not always possible to collect samples, especially during the late summer and autumn. Drip water samples for cation concentrations (Ca, Mg, Sr) and carbon isotope analysis of DIC and trace were filtered through 0.2 micron sterile filters and injected in the field into He flushed Labco vials containing phosphoric acid. Drip rate (in drips/minute) was measured at location CX using a stopwatch for one minute per visit during 2 visits in March and July 2016. Drip water samples were analyzed at the Santa Clara University Stable Isotope Laboratory (see following section for methods).

LSC monthly integrated precipitation

Integrated monthly precipitation samples were collected at LSC following the methods of Friedman et al. (1992). One-liter Nalgene containers were pre-filled with a 1-cm thick layer of mineral oil to eliminate the potential for evaporation after precipitation events and covered with a metal mesh filter to minimize debris entering the sample container. Each month, collectors were sealed, replaced and transported upright to the Santa Clara University Stable Isotope Laboratory for processing. Water samples were extracted from beneath the oil layer with a syringe and passed through multiple paper filters to eliminate oil contamination of the water sample. The stable isotope composition of drip and meteoric water samples was determined using off-axis integrated cavity output spectroscopy with a Los Gatos Research TWIA-45EP water isotope analyzer. Each measurement consisted of five preparatory injections to minimize memory effects and five measured injections. Samples were measured in at least triplicate and corrected using internal and external (USGS) reference water standards. $\delta^{18}O$ and $\delta^{2}H$ values are reported relative to Vienna Standard Mean Ocean Water (VSMOW). Replicate analyses demonstrated the typical precision of this technique to be <0.2 ‰ for $\delta^{18}O$ and <1 ‰ for $\delta^{2}H$ (1σ).

HYSPLIT back trajectory analysis

To track the moisture sources of precipitation at LSC, back trajectories of particle movements were created for 72 h periods using the registered version of the Hybrid Single Particle Langrangian Integrated Trajectory (HYSPLIT) Model (Draxler and Hess 1998) in collaboration with Dr. Ralf Bennartz. Backward trajectories tracking air masses over the previous 72 hours were generated at every 12 hours for ~5 years from March 25, 2010 to October 20, 2015 using NCAR/NCEP reanalysis data. The trajectories were run between 500 and 7500 m at 1000 meter increments. A total of 128 trajectories were created at Montague and processed using a batch file script to create 32 trajectory plots for each variable: $\delta^{18}O$, $\delta^{2}H$, $\delta^{2}H$ excess, and precipitation rate (mm/day). The plotted trajectories utilize data from 140 precipitation samples collected weekly from NADP site CA-76 in Montague, CA and precipitation data from the University of California Statewide Integrated Pest Management Program weather station in Yreka, CA (~6.4 miles west of the NADP site in Montague, CA).

Statistical Tests

In order to examine the sign and strength of relationships among drip water geochemical parameters and environmental factors, Pearson's product moment correlation coefficients ("*r*") and one-tailed tests of significance ("p") between pairs of measured parameters were calculated using the statistics program R 2.14.1 (http://www.r-project.org/). "*P*" values of <0.05 were accepted as statistically significant.

Constructing a Paleoclimate Record

A speleothem deposit is formed as a result of the interaction between percolating meteoric water and ions in soil and limestone bedrock. High carbon dioxide partial pressures (pCO_2) manifest in soil due to plant respiration and the decomposition of organic matter. Percolating water reaches and interacts with carbonate minerals as it travels through the epikarst zone, increasing the calcium concentration in solution. At some point, it reaches an air space with lower pCO_2. The water solution degasses CO_2 and tends to precipitate $CaCO_3$. This study relies on the collection of three types of geochemical data, stable oxygen and carbon isotope ratios, and U-Th isotope ratios from LSC3. Oxygen and carbon stable isotopes will be used to trace atmospheric source of precipitation, and groundwater mixing or flow changes (Lachniet 2009; Oster et al., 2009; Fairchild and Baker 2012). U-Th isotope ratios will be used to date and calculate LSC3 growth rates. This multi-proxy approach will paint a full picture of environmental variability at this site through time. This record, paired with the modern study, will help me answer research questions 2, 3 and 4.

Oxygen Isotopes ($\delta^{18}O$)

Oxygen isotope ratios in speleothems should reflect meteoric water values. However, if the residence time of water within the soil and epikarst is long, mixing effects between the meteoric water and groundwater, and evaporative effects in the uppermost soil zone, can alter or erase isotopic signals before the water reaches the speleothem site (Lachinet, 2009). Measurements of $\delta^{18}O$ in cave drip waters and rainwater $\delta^{18}O$ will determine the degree to which cave drip waters reflect meteoric isotope signals in the modern and what the dominant controls on meteoric water $\delta^{18}O$ are at LSC.

Stable Carbon Isotopes ($\delta^{13}C$)

Stable Carbon isotopes are typically taken alongside $\delta^{18}O$ measurements in speleothem geochemical analyses. Variability in carbon isotopes arise from modification in the soil, specifically the ratio of C_3 to C_4 plants above the cave, bedrock composition, cave ventilation fluid-rock interaction, and prior calcite precipitation (PCP) (Oster et al., 2009; Fairchild and Baker, 2012). Stable carbon isotopes can be useful for identifying if PCP has taken place within the system. PCP occurs when carbonate saturated waters precipitate carbonate within the soil, epikarst or cave, before reaching the site of speleothem growth (Oster et al., 2009; Fairchild and Baker, 2012). The amount of PCP depends on the path the water takes to the speleothem or changes in

the amount of soil moisture. For instance, a long flow path will increase the likelihood of PCP to occur. An increased residence time in the soil/epikarst means that the water has more of an opportunity to come into contact with pockets of gas or water, which can lead to PCP if the pCO_2 of the pocket is lower than the soil environment with which the water was equilibrated (Fairchild and Baker, 2012). Furthermore, PCP is an important control on the $\delta^{13}C$ of the dissolved organic carbon (DIC) (Fairchild et al., 2006). During the precipitation of carbonate, CO_2 gas is released. Since this degassing process favors ^{12}C, the $\delta^{13}C$ signal of DIC in solution, and thus the speleothem, will become more enriched in ^{13}C and more positive.

Speleothem proxy record construction

Samples for stable isotope analysis ($\delta^{18}O$ and $\delta^{13}C$) were milled along the growth axis from one face of the halved stalagmite using a CM-2 micromill, housed at Vanderbilt University, at 100μm spatial resolution (data to ~30.8 ka or 93.32mm is currently available). For the faster growing portion of the speleothem, I have analyzed samples at 100-micron resolution throughout the slowly growing section, between ~30.8 ka and 18.5 ka (93.32 to 52.15mm), and at 300-micron resolution for the quickly growing portions between ~18.4 ka to ~14.9 ka (51.83 – 23.31mm) and ~35.9 ka to ~30.8 ka (175.54 – 93.32mm). In doing so, I achieve ~30-year resolution throughout the entire speleothem. Stable isotope samples were packed in weigh paper envelopes, and sent to the Stable Isotope Biogeochemistry Lab at Stanford University. There, the samples were analyzed using a Thermo Finnigan Deltaplus XL coupled to a GasBench. Typical precision of stable isotope measurements is <0.2 ‰ for both oxygen and carbon. Final $\delta^{13}C$ and $\delta^{18}O$ values are expressed relative to the international standard V-PDB (Vienna PeeDee Belemnite)

U-Series Dating (U-Th Dating)

Unstable isotopes undergo radioactive decay until they achieve a stable state. The decay process for a particular nuclide has a characteristic half-life that corresponds to the amount of time it takes for half of the initial amount of an atom to decay into its stable product, or "daughter" isotope (Bourdon et al., 2013). By measuring the amount of radioactive parent vs. daughter isotope in a sample, I can measure the amount of decay that has taken place and calculate an age. ^{234}U undergoes alpha decay to form ^{230}Th with a half-life of ~245,000 years. Uranium (U) is soluble in oxidizing environments, and is able to travel with groundwater until reaching the speleothem site. Once there, the U is precipitated within the calcite mineral structure and is immobile. Thorium (Th) is not soluble in water under oxidizing conditions, and is assumed to not be incorporated into the calcite structure. However, detrital grains may introduce Th to the deposit, and a correction factor is used to ensure minimal impact on age determination by measuring the $^{230}Th/^{232}Th$ ratio to compare detrital ^{232}Th with radiogenically produced ^{230}Th (Fairchild and Baker, 2012).

This study includes ten subsamples for $^{230}Th/U$ dating collected from LSC3. U-series samples powder samples were dissolved in 7N HNO_3 and equilibrated with a mixed spike containing ^{229}Th, ^{233}U, and ^{236}U. Separation of U and Th was completed with a two stage HNO_3-HCl cation exchange procedure, preceded by treatment with a mixture of HNO_3 and $HClO_4$ to remove any residual organic material. U and Th fractions were analyzed on a Thermo Neptune Plus Multi-collector ICP-MS at the Berkeley Geochronology Center. Measured peak heights were

corrected for peak tailing, multiplier dark noise/Faraday baselines, instrumental backgrounds, ion counter yields, mass fractionation, interfering spike isotopes, and procedural blanks. Mass fractionation was determined using the gravimetrically determined $^{233}U/^{236}U$ ratio of the spike. Activity ratios and ages were calculated using the half-lives of Jaffey et al. (1971) for ^{238}U, Holden (1989) for ^{232}Th, and Cheng et al. (2013) for ^{230}Th and ^{234}U. Correction for U and Th from detritus was made assuming detritus with activity ratios of $(^{232}Th/^{238}U) = 0.67 \pm 0.34$, $(^{230}Th/^{238}U) = 1.0 \pm 0.1$, and $(^{234}U/^{238}U) = 1.0 \pm 0.1$, which were determined by comparing detritus rich samples to pure calcite samples within WMC1. An age model was generated using the COPRA algorithm (Breintenbach et al., 2012).

CHAPTER 3

RESULTS

Water Analysis

Precipitation

The precipitation data set includes weekly integrated precipitation samples from the NADP site CA-76 in Montague, California collected between March 2010 through October 2015 and monthly integrated precipitation samples from LSC collected between December 2015 through February 2017. The data set also includes precipitation amount and temperature data from the University of California Integrated Pest Management Site (UC-IPM) in Yreka, California, ~6 miles west of the NADP site, and a weather station in Shasta Lake run by usclimatedata.com (Figure 4). Precipitation amount data from both sites between January 2015 and December 2015 indicate that rainfall occurs at the same time at these sites, but at different magnitudes. The UC-IPM site in Yreka, CA receives less rainfall than Shasta Lake (Figure 5.) The NADP and LSC precipitation $\delta^{18}O$ and $\delta^{2}H$ fall along the Global Meteoric Water Line (GMWL) and Local Meteoric Water Line (LMWL; Kendall and Coplen 2001; Figure 6), suggesting that the NADP precipitation samples have not undergone evaporation within the collector and the NADP sampling techniques are sufficient for analysis and subsequent interpretation.

The $\delta^{18}O$ and $\delta^{2}H$ of the NADP weekly integrated precipitation samples collected demonstrate seasonal fluctuations of, at most, ~17‰, between ~-20‰ and -3‰, and ~140‰, between ~-168‰ and ~-24‰, respectively. Overall, NADP CA-76 rainwater $\delta^{18}O$ and $\delta^{2}H$ are more negative during the winter and spring and less negative during the summer and autumn, with the exception of individual Atmospheric River precipitation events. The most positive $\delta^{18}O$ and $\delta^{2}H$ precipitation falls during the spring and summer months, May through September, while the most negative $\delta^{18}O$ and $\delta^{2}H$ precipitation falls during the autumn and winter months, October through April (Figure 7). This finding suggests that temperature may exert a control on the $\delta^{18}O$ and $\delta^{2}H$ signature of precipitation at this site over time. This seasonal trend is similar to that seen at Black Chasm Cave in the Sierra Nevada Foothills, California (Oster et al., 2012).

Weekly average maximum, minimum and median temperatures from rain days recorded by the UC-IPM weather station were compared to the NADP CA-76 precipitation $\delta^{18}O$ and $\delta^{2}H$ signatures (Appendix A). Spearman's Rho "r" values were calculated for $\delta^{18}O$ and weekly average minimum, median and maximum temperatures (0.40, 0.42 and 0.42 respectively with $p<.001$) indicating that temperature has a significant moderate control on the $\delta^{18}O$ of precipitation that falls in Northern California in the modern day (Figure 8). A speleothem and precipitation study at Oregon Caves National Monument (OCNM) in the in the Klamath Mountains interpreted changes in speleothem $\delta^{18}O_C$ to be positively correlated to surface air temperature changes (Figure 2; Ersek et al., 2010). However, Ersek et al., (2010) also suggest that moisture source may also cause temporal variations in the $\delta^{18}O$ of precipitation ($\delta^{18}O_P$) at this site.

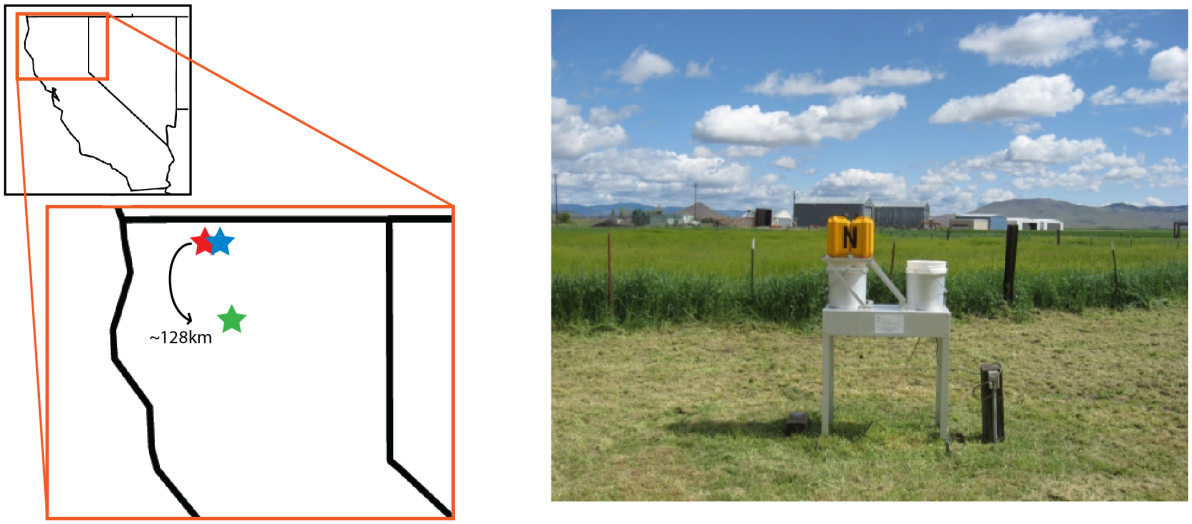

Figure 4. (Left) Map of Northern California. Lake Shasta Caverns represented as the green star. Location of National Atmospheric Deposition Program (NADP) site CA-76 in Montague, CA represented as the blue star. University of California Integrated Pest Management (UC-IPM) site in Yreka, CA represented at red star. The NADP and UC-IPM site are located ~128 km north of LSC. (Right) NADP site CA-76 in Montague, CA (photo courtesy of NADP).

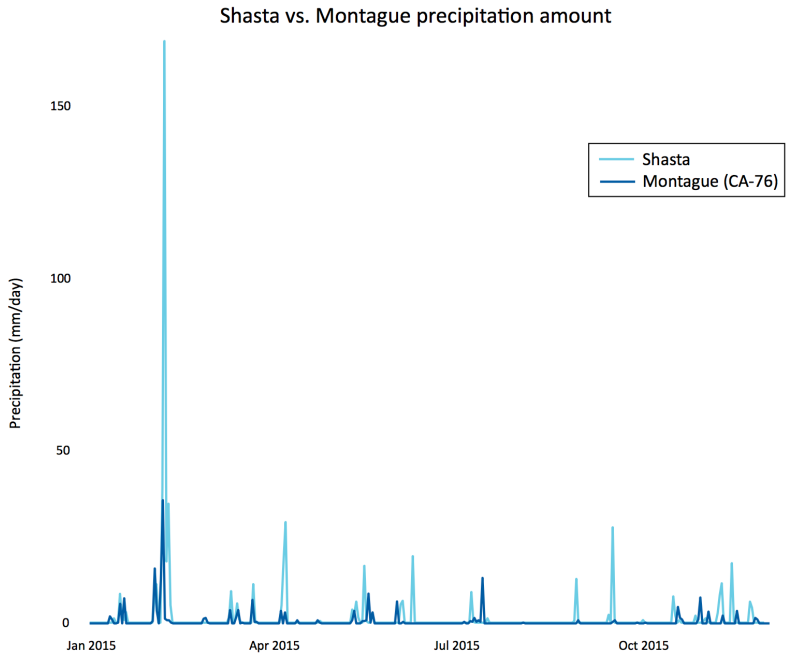

Figure 5. Precipitation amount (mm) at Lake Shasta Caverns (light blue) vs. at the NADP site CA-76 (dark blue) in Montague, CA between January 2015 through December 2015. Shasta precipitation data courtesy of usclimatedata.com

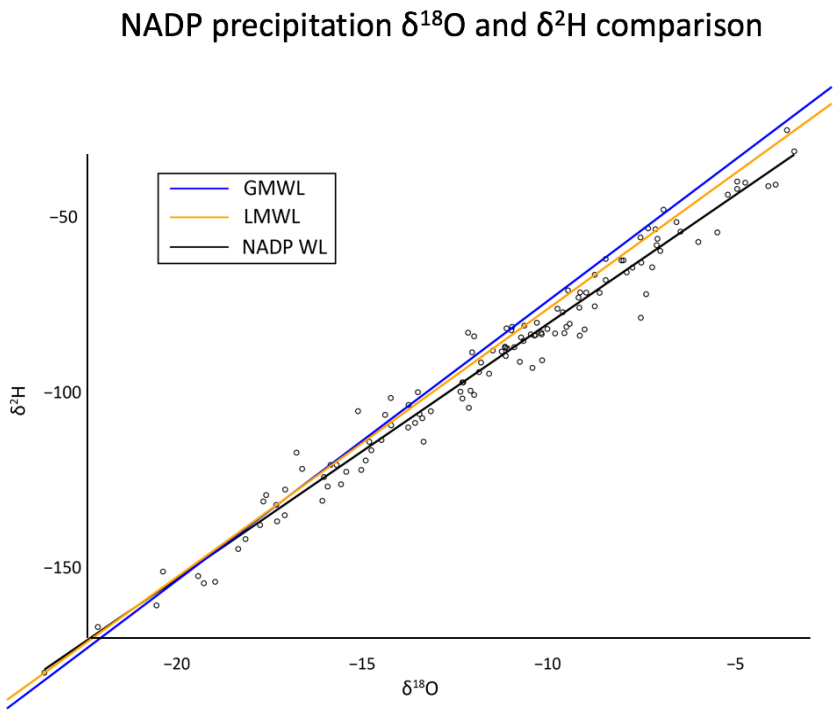

Figure 6. Plotted $\delta^{18}O$ and $\delta^{2}H$ from NADP site CA-76 in Montague, CA. The Global Meteoric Water Line (GMWL) is shown in blue, the Local Meteoric Water Line for Northern California (LMWL; Kendall and Coplen, 2001) is shown in orange and the regression line calculated from this data shown in black.

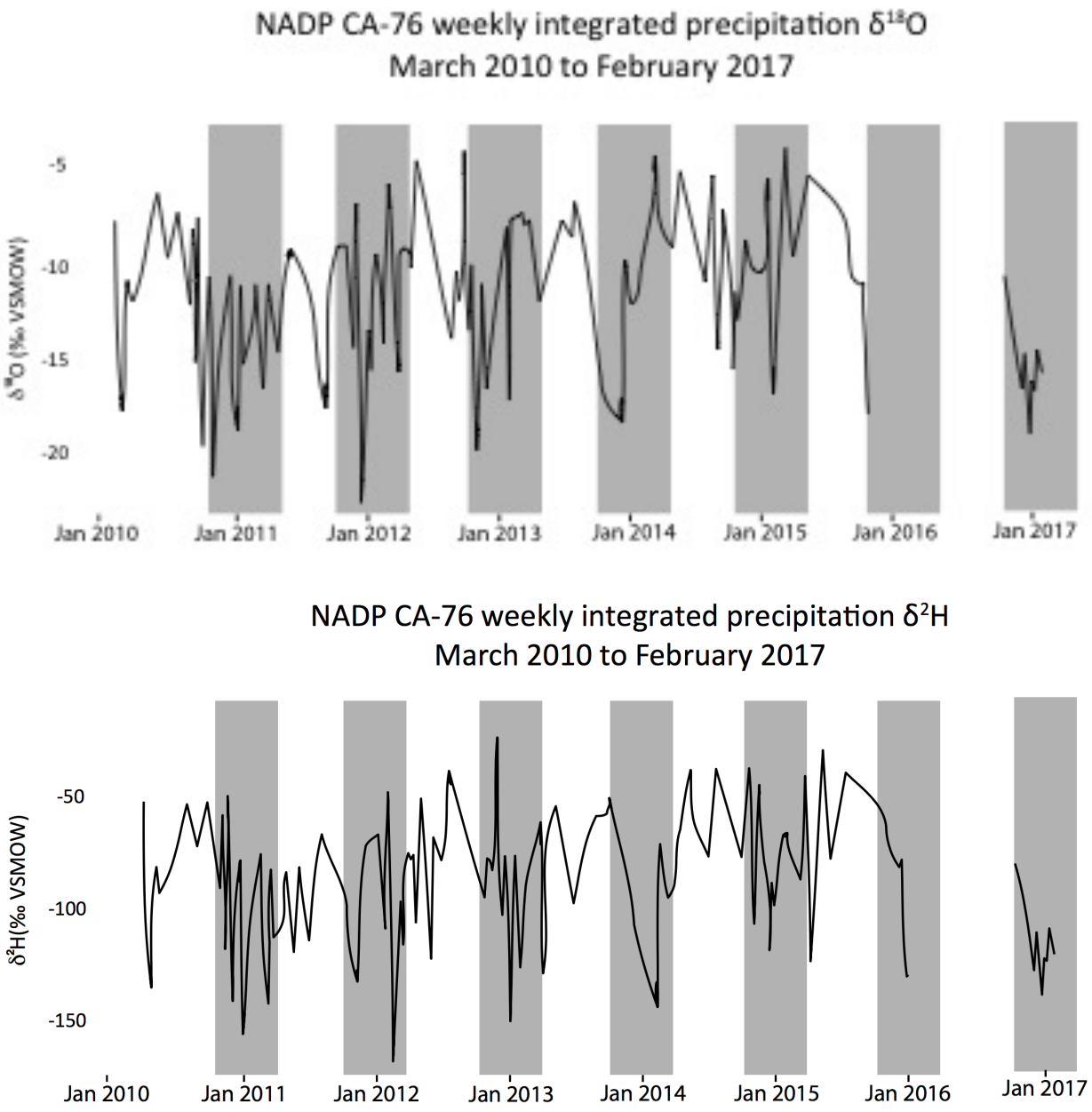

Figure 7. (Top) $\delta^{18}O$ of weekly integrated precipitation samples from NADP site CA-76 from March 2010 through February 2017. (Bottom) Equivalent plot of $\delta^{2}H$. Winter months (Oct-March) highlighted by gray shaded bars.

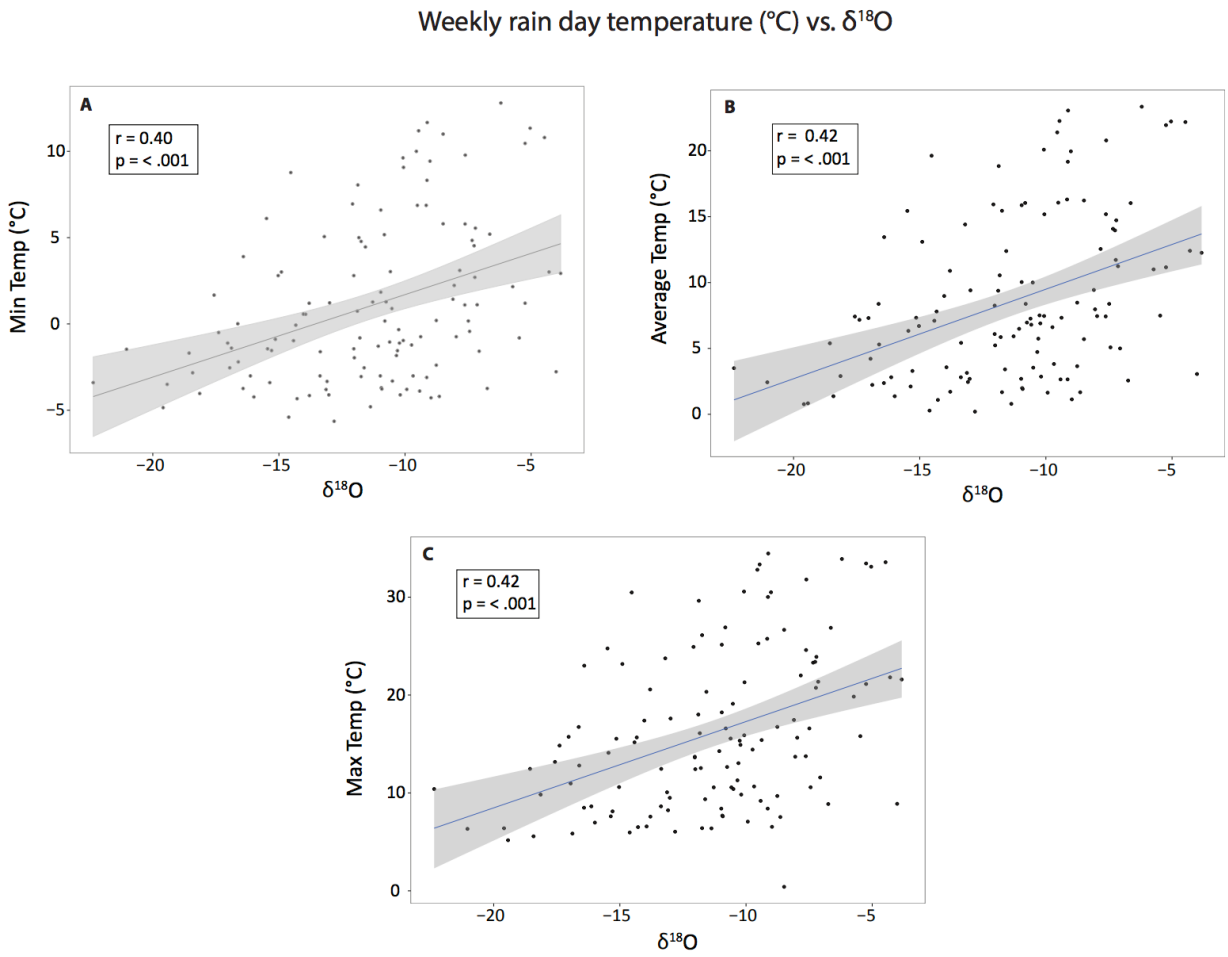

Figure 8. Weekly average minimum(A), average (B) and maximum rain day temperatures (°C) vs. $\delta^{18}O$ of NADP site CA-76 weekly average precipitation samples. Spearman's Rho ("r") and one-tailed tests of significance ("p") in boxes on plots. Linear regression and 95% confidence interval illustrated by blue line and gray shading respectively.

Drip water

Through a collaboration with the staff at LSC, the four drip sites have been sampled for oxygen/hydrogen isotopic composition monthly beginning in December 2015. During two trips to LSC, on December 5, 2015 and March 8, 2016, drip waters were sampled for trace elements and $\delta^{13}C$. To date, the drip water samples have been analyzed for $\delta^{18}O$ collected on December 5, 2015, March 8, 2016 and July 16, 2016 (Figure 10). The drip water $\delta^{18}O$ and $\delta^{2}H$ fall along the GMWL and in line with monthly integrated precipitation samples collected at LSC (Figure 9). The average $\delta^{18}O$ of drip water collected on March 8, 2016 is -9.46‰ with a standard deviation of 0.035‰. The average $\delta^{18}O$ of drip waters collected on July 16, 2016 is -9.27‰ with a standard deviation of 0.45‰. The $\delta^{18}O$ of drip water collected on December 5, 2015 scatter from -10‰ to -7.14‰, with an average of -8.55‰ and a standard deviation of 1.18‰. Drip water samples collected on December 5, 2015 have been analyzed for $\delta^{13}C$ (Table 1). The average $\delta^{13}C$ is -9.77‰, with a

standard deviation of 2.14‰. The drip water collected on March 8, 2016 has not yet been analyzed for trace elements and $\delta^{13}C$ and the drip water collected on December 5, 2015 has not yet been analyzed for trace elements. The drip water samples collected for $\delta^{18}O$ via the LSC staff between October 2016 through February 2017 are awaiting analysis.

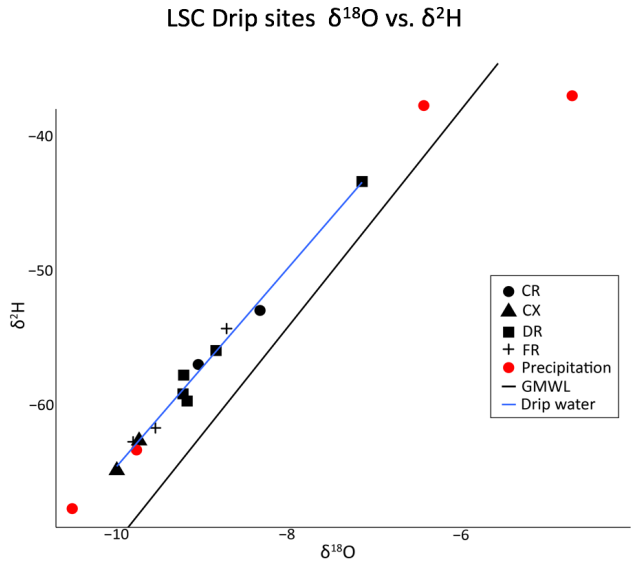

Figure 9. $\delta^{18}O$ vs. $\delta^{2}H$ of LSC drip water vs. precipitation (red). Drip water water line in blue and Global Meteoric Water Line in black. Monthly integrated precipitation sample collected in March falls below the meteoric waterline suggesting evaporation prior to analysis.

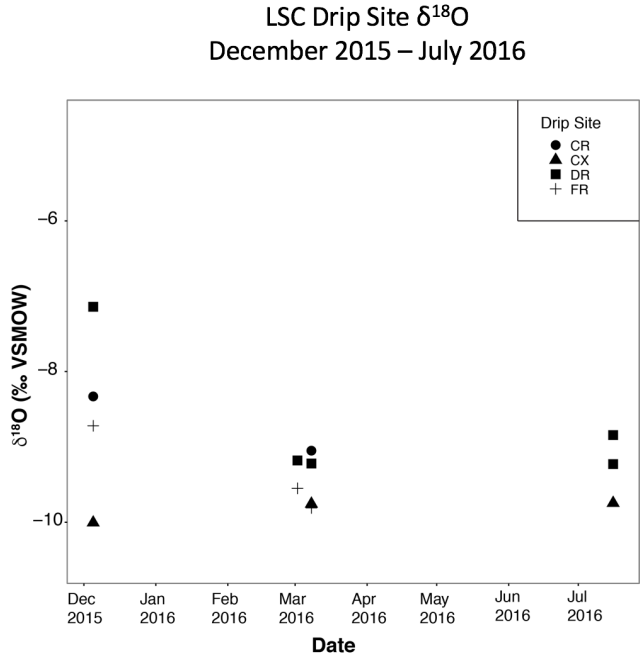

Figure 10. Drip water $\delta^{18}O$ collected from Lake Shasta Caverns (LSC) between December 2015 and July 2016.

Table 1
$\delta^{13}C$ data from three drip water sites and one pool of water (* denoted). Water samples collected on 12/5/2015.

Drip Site	$\delta^{13}C$
CR-1	-11.79
CR-3*	-7.41
DR-1	-7.53
FR-1	-9.98
samples collected 12/5/2015 *denotes pool water sample	

HYSPLIT Back Trajectories

Results of NOAA HYSPLIT model backward trajectories reaching the CA-76 Montague site between March 2010 and October 2015 show that precipitation $\delta^{18}O$ and deuterium excess are related to changes in moisture source. The deuterium excess, d, defined as:

$$d\ (‰) = \delta^{2}H - 8 \times \delta^{18}O \quad (2)$$

where $\delta^{2}H$ and $\delta^{18}O$ denote the deuterium and ^{18}O abundance relative to VSMOW, is a second-order isotope parameter that is specifically sensitive to the conditions during the evaporation of water from the ocean surface. Relative humidity is linearly correlated to deuterium excess, meaning when relative humidity is high, deuterium excess is low and vice versa (Merlivat and Jouzel, 1979; Johnsen et al., 1989; Pfahl and Wernli, 2008). The results of the 72-hour back trajectory analysis at 2500 and 3500m above sea level suggest that cool season storms originating in the subtropical pacific (roughly below 40°N) have lower deuterium excess, indicating humid conditions (blue circles, Figure 11 A, B). These back trajectories are also associated with more positive precipitation $\delta^{18}O$ values (red circles; Figure 11. C, D). Conversely, storms sourced in the North Pacific (roughly above 40°N) have higher deuterium excess (red circles; Fig. 11 A, B), indicating lower humidity during evaporation, and generally more negative but also highly variable $\delta^{18}O$ values (blue circles, Fig. 11C, D). As such, the isotopic composition of precipitation in Northern California is in part related to the source of moisture delivered to the region. There did not appear to be any clear relationship between the results of the back-trajectory analyses and the precipitation rate (mm/day).

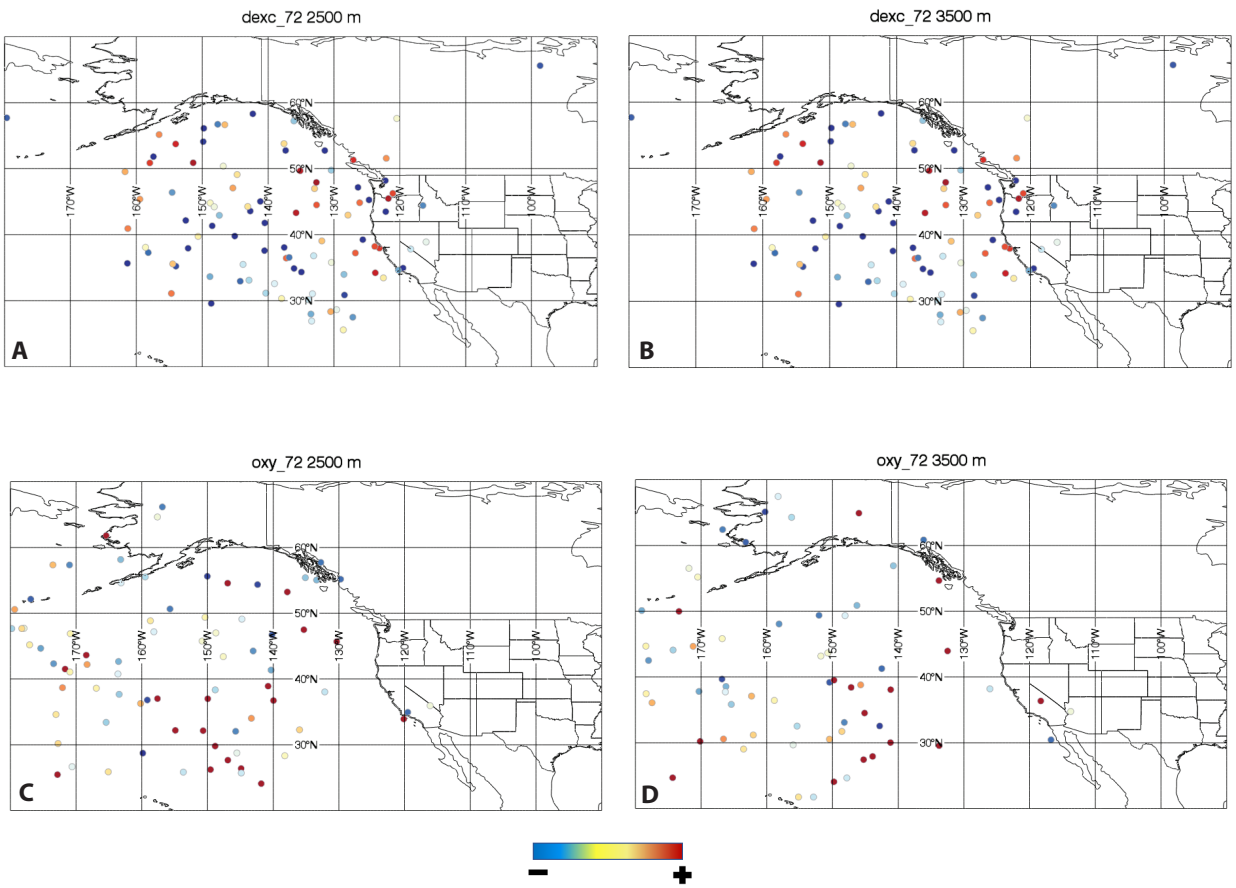

Figure 11. HYSPLIT back trajectories of deuterium excess plots using the 72h model at 2500m (A) and 3500m above sea level (B) between October and March. Equivalent plots of oxygen isotope value, using the 72h model at 2500m (C) and 3500m (D) above sea level between October and March (2010 through 2015). The red shading represents more positive values, while the blue shading represents more negative values.

Stalagmite Records

U-Series

Analytical results and calculated ages for LSC3 samples are presented in Table 2. All errors are 2σ. Measured U concentrations range from 58 to 102 ppb in LSC3 samples. Dates from the LSC3 stalagmite preserve stratigraphic order within uncertainties (Figure 12). The LSC3 stalagmite precipitated from ~35.9 to ~14.3 ka, spanning the last deglaciation, including Heinrich Stadials 1-3, and the Bølling-Allerød.

Table 2
U-series analytical data and ages for LSC3.

Sample name	Sample wt. (mg)	U (ppb)	^{232}Th (ppb)	(^{230}Th/^{232}Th)	(^{232}Th/^{238}U)	± (%)	(^{230}Th/^{238}U)	± (%)	(^{234}U/^{238}U)	± (%)	Uncorrected age, error (ka)		Corrected age, error (ka)		Initial (^{234}U/ ^{238}U)	
LSC3-0.1 cm	198.60	102.5	0.9655	43.54	0.00272	0.12	0.1336	1.73	1.0697	0.20	14.80	±0.28	14.30	±0.30	1.073	±0.002
LSC3-2 cm	193.42	101.5	0.6248	67.35	0.00167	0.11	0.1350	0.86	1.0577	0.61	14.92	±0.17	14.73	±0.18	1.060	±0.007
LSC3-2.9 cm	186.78	59.51	0.2884	89.02	0.00108	0.08	0.1406	2.71	1.0737	0.36	15.78	±0.46	15.19	±0.45	1.077	±0.004
LSC3-5.2 cm	197.56	58.41	0.8608	35.40	0.00419	0.54	0.1702	2.21	1.0724	0.22	19.27	±0.47	18.46	±0.49	1.077	±0.002
LSC3-7.6 cm	198.30	52.53	0.7325	53.31	0.00387	0.11	0.2421	1.31	1.0750	0.84	28.20	±0.51	27.42	±0.52	1.081	±0.010
LSC3-8.1 cm	187.40	49.93	0.4225	92.77	0.00210	0.09	0.2562	1.06	1.0835	0.24	29.80	±0.37	29.14	±0.38	1.091	±0.003
LSC3-10.6 cm	194.76	55.90	0.6288	76.61	0.00305	0.06	0.2809	1.38	1.1025	0.29	32.32	±0.53	31.68	±0.54	1.112	±0.003
LSC3-12.9 cm	195.62	99.28	0.4284	195.4	0.00108	0.23	0.2747	0.91	1.0625	0.25	32.76	±0.36	32.43	±0.36	1.069	±0.003
LSC3-15 cm	197.99	77.50	0.3792	176.2	0.00121	0.22	0.2809	0.77	1.0597	0.52	33.46	±0.37	33.38	±0.37	1.066	±0.006
LSC3-17.3 cm	197.38	93.23	0.4268	202.4	0.00115	0.22	0.3020	0.83	1.0706	0.24	36.23	±0.37	35.90	±0.37	1.078	±0.003

All isotope ratios are activity ratios. Uncertainties are given at 2 standard deviations. Uncorrected ages are calculated from measured ratios. Corrected ages were corrected for initial ^{230}Th using (^{232}Th/^{238}U) = 1.21 ± 0.50 , (^{230}Th/^{238}U) = 1.0 ± 0.1, and (^{234}U/^{238}U) = 1.0 ± 0.1. Decay constants are those of Jaffey (1971) for ^{238}U and Cheng et al. (2013) for ^{230}Th and ^{234}U. Initial (^{234}U/^{238}U) is back-calculated from the measured ratio and the corrected ^{230}Th age.

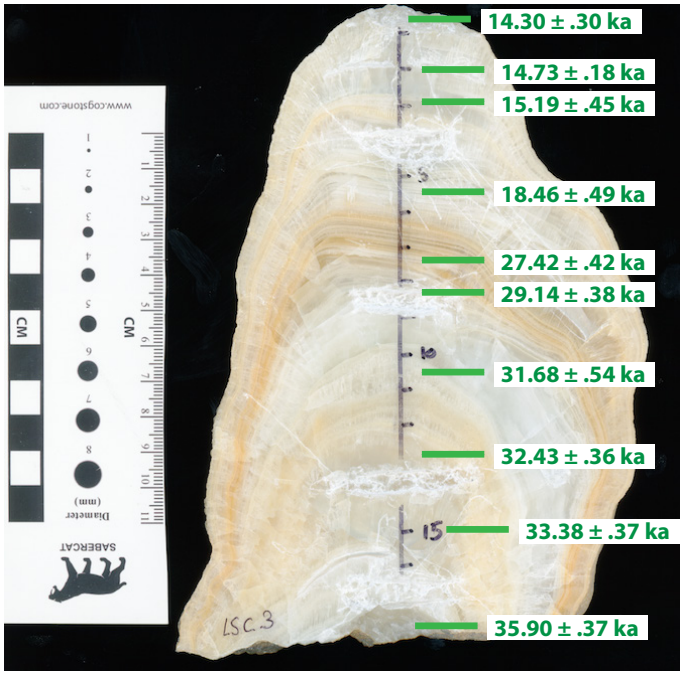

Figure 12. LSC3 speleothem with U-Th dates and errors. LSC3 is ~17.3cm in length.

Age-depth modeling

An age model for LSC3 was constructed using the MATLAB package, Constructing Proxy Records from Age models (COPRA) (Breitenbach et al., 2012; Figure 13). The COPRA interface-based proxy reconstruction software allows the detection and interactive handling of age reversals and hiatuses, depth-age modeling, and proxy-record reconstruction. Monte Carlo simulation and a translation procedure are used to assign a precise time scale to climate proxies (Breitenbach, 2012).

Our COPRA age model was optimized with a pchip interpolation of 2000 Monte Carlo simulations by inputting proxy depth and the depth, age, and 2σ uncertainty associated with each U-series analysis.

Growth rate

There are no visible growth hiatuses in the LSC3 speleothem. Growth rates varied between 12.5µm/year (or 8yr/100µm) and 4.2µm/year (or 24yr/100µm) through the period of speleothem growth. From ~35.9 ka to ~30.8 ka growth rates were ~12.5µm/year. The growth rate slowed to ~4.2µm/year and remained low between ~30.8 ka and ~18.5 ka. The growth rate increased to ~12.5µm/year from ~18.4 ka to ~14.9 ka. The faster growth rate during the Bølling Allerød (BA; ~14.7-12.7 ka) corresponds with more negative $\delta^{18}O$, while the slower growth rate during Marine Isotope Stage 2 (MIS2; (~25-19 ka)) corresponds with more positive $\delta^{13}C$, as I discuss in more detail below.

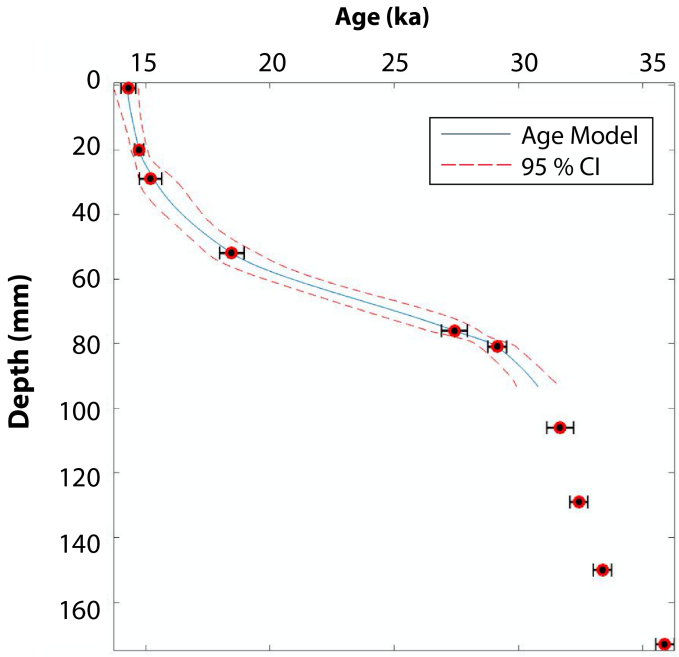

Figure 13. COPRA (Breintenbach et al., 2012) generated age model of LSC3. Samples run at the Berkeley Geochronology Center. Data currently only available until ~30.8 ka. Remaining samples awaiting analysis.

Stable Isotopes

The stable isotope time-series developed for the LSC3 stalagmite offer multi-decadal (30 year) resolution based on U-Th constrained calcite growth rates calculated using the COPRA age model. The $\delta^{18}O$ values fluctuate with clearly defined rises and falls between -10.43‰ and -8.04‰. The $\delta^{13}C$ values also fluctuate with clearly defined rises and falls between -7.37‰ and -3.24‰ (Figure 14).

The LSC3 $\delta^{18}O$ record increases by ~1‰ from ~31-29 ka and then decreases by ~1‰ from ~29-28 ka. The $\delta^{18}O$ then exhibits rapid centennial-scale increases of ~1.5‰ during three Dansgaard-Oeschger events, occurring at approximately 28, 27 and 23 ka, but is otherwise relatively stable between 28 and 24 ka. The $\delta^{18}O$ exhibits a ~1‰ decrease during Heinrich Stadial 2 (HS-2; 26-23 ka; Gutjahr and Lippold, 2011) and then further decreases to a local minimum of ~-9.25‰ between 23-21 ka. The $\delta^{18}O$ record rebounds just prior to the onset of the LGM at ~21 ka, and increases and then decreases by ~1‰ during the LGM (between 21 and 19 ka). Following the LGM and during HS-1 the LSC3 $\delta^{18}O$ record decreases by 1.5‰ between 19-18 ka and then increases more gradually by 1.5‰ between 18-16.5 ka. The LSC3 $\delta^{18}O$ record then decreases step-wise by 1‰ between 16.5 ka and 15.5 ka to the records' minimum of ~-10.5‰ at ~14.6 ka. The record then displays a ~1.5‰ increase during the BA, until the record ends at ~14.3 ka.

The LSC3 $\delta^{13}C$ record decreases by ~2‰ from ~31-30 ka, during HS-3, and then remains relatively constant between 30 and 28 ka. The $\delta^{13}C$ then increases rapidly by ~2‰ from 28-27 ka before decreasing to a local minimum of ~-7.3‰ at 27 ka. The $\delta^{13}C$ then increases by ~4‰ between 27 and 24.5 ka. The $\delta^{13}C$ record reaches a local maximum of ~-3‰ during HS-2 (around 24 ka). The $\delta^{13}C$ then decreases slightly, to ~-4.5‰ and remains relatively constant during the LGM, between 21-19 ka. Following the LGM, during HS-1, the LSC3 $\delta^{13}C$ record decreases by ~2‰ to the records minimum of ~-7.5‰, between 19-18 ka and then increases more gradually 2‰ between 18-16.5 ka, in conjunction with the LSC3 $\delta^{18}O$ record. The LSC3 $\delta^{13}C$ record remains around ~-6‰ between 16.5 ka and ~14.5 ka before increasing by ~3‰ during the BA and until the records ends at ~14.3 ka

The $\delta^{18}O$ and $\delta^{13}C$ values exhibit a significant, moderate and positive down-axis correlation (Spearman's $r = 0.43$, $p<0.001$). The moderate positive down-axis correlation could indicate kinetically driven non-equilibrium fractionation (Hendy 1971). Nonequilibrium fractionation can occur during rapid CO_2 degassing and calcite precipitation driven by decreased drip rates, increased evaporation, and/or changing cave pCO_2 (Mickler et al. 2004, 2006; Dreybrodt and Scholz 2011, Deininger et al. 2012, Oster et al. 2015). However, rapid precipitation of calcite can result in equilibrium $\delta^{18}O$ values (Feng et al. 2012), and covariation between $\delta^{18}O$ and $\delta^{13}C$ in stalagmites has been documented, and result from environmental processes that influence both isotopic compositions (Genty et al. 2003; Fleitmann et al. 2004; Oster et al. 2009, 2014, 2015).

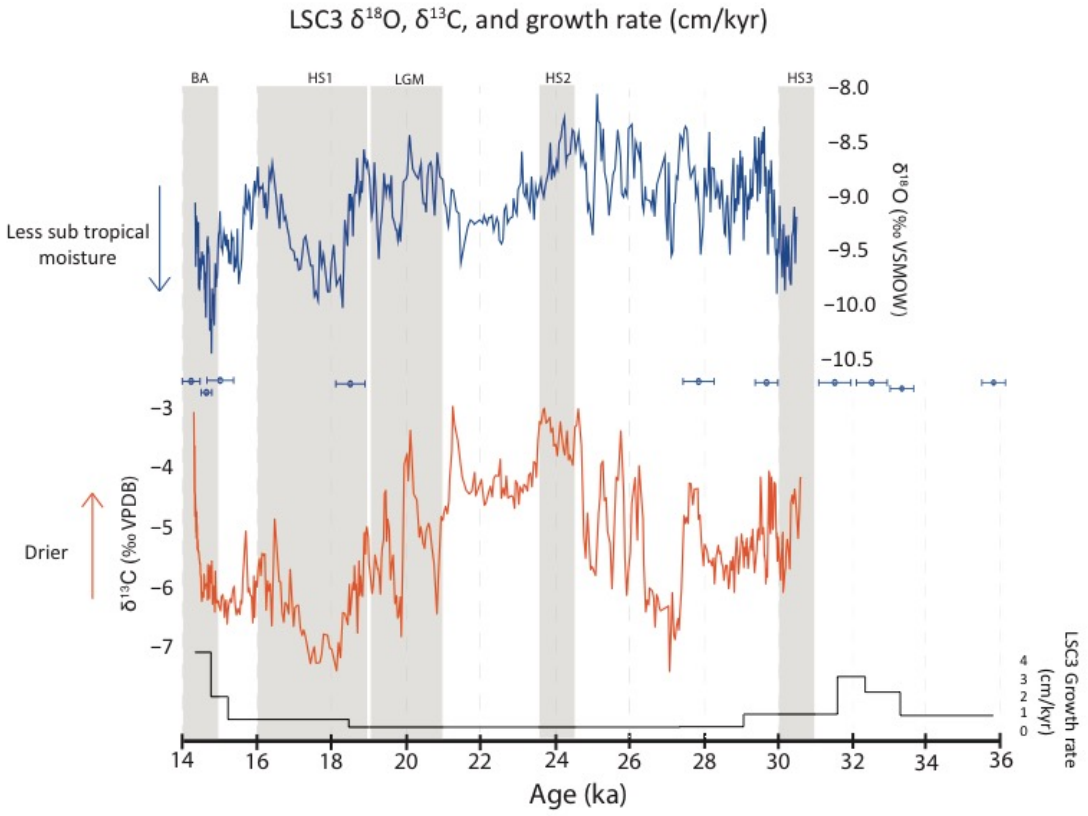

Figure 14. LSC3 stacked $\delta^{18}O$ (blue), $\delta^{13}C$ (orange) and growth rate (cm/kyr; black) records. LSC3 U-series ages with 2σ errors plotted in blue. Interpretation of increases and decreases in each record is annotated with arrows.

CHAPTER 4

DISCUSSION

Rain Water Variability

The observed trend of more negative $\delta^{18}O$ and $\delta^{2}H$ values of NADP site CA-76 rainwater during the colder and wetter winter and early spring, and less negative values during the warmer and drier late spring through late autumn/early winter suggest that rainwater isotopes are influenced by seasonal variation in surface air temperature. Spearman's statistical tests between daily temperature data from the UC-IPM weather station in Yreka, California weather station and weekly-integrated precipitation from the NADP site CA-76 in Montague, CA demonstrate that temperature has a significant, moderate control on the $\delta^{18}O$ and $\delta^{2}H$ of precipitation that falls in northern California (Figure 8). There is also a significant, weak negative relationship between rain $\delta^{18}O$ or $\delta^{2}H$ and rainfall amount ($r_s = -0.26$ and $p = .0036$, and $r_s = -0.23$ and $p = 0.011$ respectively). Because the direct relationship between rainfall $\delta^{18}O$ and air temperature on rainy days is stronger, these observations agree with the work from Oregon Caves that suggests that temperature rather than rainfall amount controls rainfall $\delta^{18}O$ in the Pacific Northwest (Ersek et al., 2010).

The isotopic composition of NADP CA-76 rainwater also appears to vary with water vapor source, as tropical-sourced water vapor is associated with less depleted $\delta^{18}O$ values and high deuterium excess (Figure 11). Back-calculated particle trajectories for rainfall events in northern California using the NOAA Hybrid Single Particle Lagrangian Integrated Trajectory Model (HYSPLIT) and global reanalysis data indicate that the $\delta^{18}O$, $\delta^{2}H$ and deuterium excess composition of rainfall in this region is influenced by water vapor source. Particle back-trajectories between October and March for deuterium excess and $\delta^{18}O$ suggest that storms originating in the subtropical pacific (roughly below 40°N) have lower deuterium excess, indicating humid conditions at the time of evaporation, and more positive $\delta^{18}O$ values. These are characteristic qualities of Atmospheric River (AR) storms. Because the isotopic composition of precipitation that falls in northern California is moderately a function of water vapor source, the LSC3 speleothem $\delta^{18}O$ should reflect moisture source; meaning a relatively negative $\delta^{18}O$ represents increased north pacific moisture and/or colder temperatures and a relatively positive $\delta^{18}O$ represents increased tropical pacific moisture and/or warmer temperatures. If $\delta^{18}O$ is controlled by moisture source, then positive $\delta^{18}O$ trends in the LSC3 record could indicate increased AR events.

Northern California is known to experience AR events, which occur when the jet stream taps into warm, wet air from the tropical Pacific and funnels it up to the west coast of North America. These storms are uncharacteristically warm and wet for California winter precipitation (Dettinger, 2004). For example, one AR storm passed over the cave between late November and early December of 2012 (November 27- December 3). Weekly integrated precipitation collected from the NADP site CA-76 in Montague, CA between November 27 and December 4, 2012 recorded a $\delta^{18}O$ value of -4.01‰. Comparatively, during the week prior, November 20-27, 2012, the $\delta^{18}O$ of weekly integrated precipitation was -10.35‰. During the week following the AR event, the $\delta^{18}O$ of weekly integrated precipitation collected between December 4–11, 2012, had a $\delta^{18}O$

value of -13.09‰. The relatively positive $\delta^{18}O$ and $\delta^{2}H$ isotopic signature of precipitation recorded during the AR event is expected of precipitation derived from a more tropical source. HYSPLIT back trajectories calculated during this November/December AR event also suggest a subtropical moisture source (Figure 15). Studies of rainfall $\delta^{18}O$ in central and southern California have identified similar relationships between $\delta^{18}O$ and moisture source (Oster et al., 2012 and Berkelhammer et al., 2012). In a precipitation analysis of event-based rainfall $\delta^{18}O$ in SW Oregon, no relationship with moisture source was identified, however, it was revealed that temperature was the dominant factor controlling the isotopic variability of rainwater in that region. (Ersek et al., 2010).

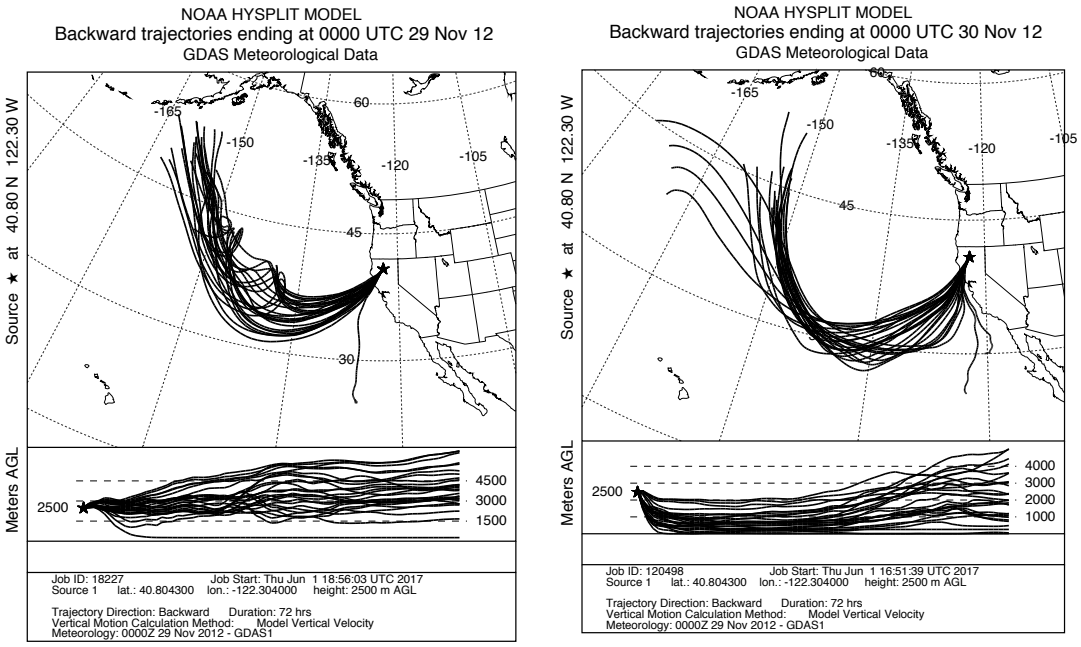

Figure 15. 72-hour HYSPLIT back trajectories run on November 29, 2012 (left) and November 30, 2012 (right) during the Atmospheric River event that hit northern California between November 27 – December 5, 2012. The trajectories indicate a subtropical moisture source that should result in precipitation with a relatively positive $\delta^{18}O$ signature.

Drip Water Variability

Drip rate in Lake Shasta Caverns may be tied to rainfall above the cave, with drip rates near zero in the dry summer months due to the lack of water recharge from the surface. Drip rates increase in the spring and summer (March 8, 2016 drip rate was 5ml/min). The instillation of drip rate loggers in the future will elucidate the potential control of rainfall amount and duration of rain event.

Though at present data is limited, shifts in drip water $\delta^{18}O$ and $\delta^{2}H$ appear to be controlled by rainfall event intensity (amount of rain delivered per unit of time) and timing of the precipitation event (the time of year when the rain falls, during the wet or the dry season; Figure 16). The average $\delta^{18}O$ of drip water collected in March and July 2016 show a small variability, while there is a large range of $\delta^{18}O$ variability in drip water collected in December 2015. The low variability

of drip water $\delta^{18}O$ and $\delta^{2}H$ relative to that of the rainwater in March and July suggests that there is some mixing of rainwater recharge with the older stored waters within the epikarst. Such rainwater storage, however, likely consists of waters recharged during each rainy season given that drip water ceases to enter the cave during the late summer months. The storage and mixing of rainwater in the epikarst within each season, however, likely dampens the effect of singular variations in water vapor source (ie. atmospheric rivers compared to North Pacific sourced storms). In order for changes in vapor source to have a significant long-term effect on drip waters, recorded by speleothems stable isotopic compositions, the shifts would need to be sustained throughout a rainy season, and possibly for several years depending on stalagmite growth. Sustained differences in the stable isotopic composition of autumn, winter and spring rainfall due to temperature likely have a greater influence on drip water stable isotopes. The continuation of this study and cooperation of the LSC staff will allow us to further investigate the controls on the drip rate and the isotopic signature of drip water at LSC.

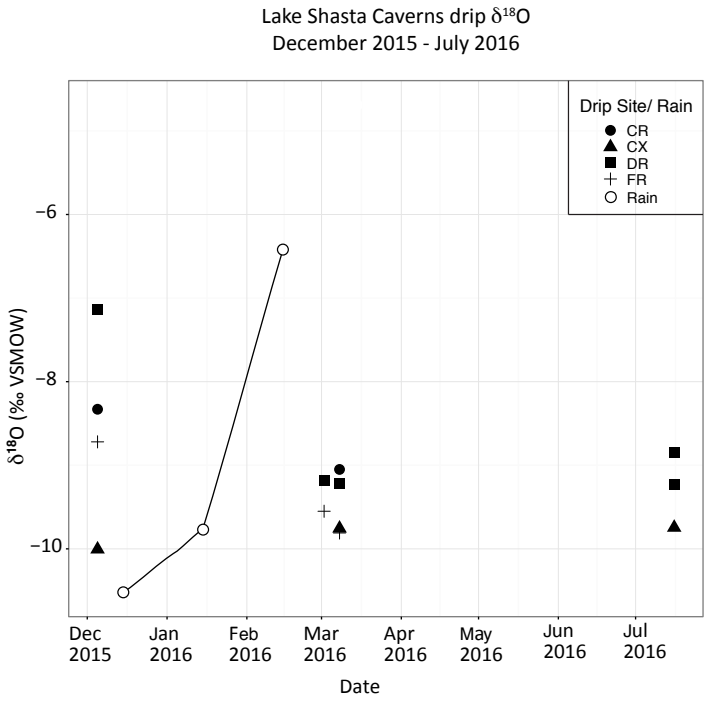

Figure 16. Drip water $\delta^{18}O$ collected from Lake Shasta Caverns (LSC) between December 2015 and July 2016, compared to monthly integrated precipitation collected at LSC. The monthly integrated precipitation sample collected in March is not included because the sample was evaporatively enriched.

Interpretation of LSC Proxy Records

The LSC3 isotopic records display long-term trends and abrupt shifts across the end of the last glacial period that show distinct similarities and some dissimilarities with regional climate changes as recorded in other paleoclimate archives (Figure 17). LSC3 $\delta^{18}O$ and $\delta^{13}C$ records display centennial and millennial scale oscillations of ~1-2‰ and ~1-4‰ respectively throughout the entire record. Of note, the LSC3 $\delta^{18}O$ record captures rapid centennial-scale increases of ~1.5‰ coeval with three Dansgaard-Oeschger (DO) events, occurring roughly around 28, 27 and

23 ka, in agreement with NGRIP and the Fort Stanton speleothem record. DO events are rapid climate fluctuations in polar Northern Hemisphere marked by rapid warming, followed by slow cooling (Bond et al., 1992). During MIS2 (~25-19 ka) the LSC3 $\delta^{13}C$ record reaches its most positive $\delta^{13}C$ values, ~-3‰, and remains relatively positive from HS-2 (~26-23 ka) to the end of the LGM (Figure 14). Following the LGM and during HS-1 the LSC3 $\delta^{18}O$ and $\delta^{13}C$ records decrease by 1.5‰ and 2‰ respectively between 19-18 ka and then increase more gradually by 1.5‰ and 2‰ respectively between 18-16.5 ka, in agreement with the Fort Stanton and Cave of the Bells speleothem $\delta^{18}O$ records. We use the modern precipitation data to aid in our interpretation of the variations captured in this proxy record.

$\delta^{18}O$

Six years of observations of stable isotopes in rain from nearby Montague, CA and temperature data from Yreka, CA reveal a significant, positive moderate correlation between rain $\delta^{18}O$ and surface air temperature, and show a significant, negative weak relationship between $\delta^{18}O$ and rainfall amount. Moisture source and trajectory influence rain $\delta^{18}O$ and deuterium excess, with storms sourced in the subtropical Pacific having higher $\delta^{18}O$ and more negative deuterium excess than storms that originate in the North Pacific. During intense rain events (October-March) it appears that changes in rainwater $\delta^{18}O$ are likely transferred to cave drip water. The drip water samples collected during a strong rain event in December (between December 1 and 5 it rained 4.3 cm; usclimatedata.com) display the greatest $\delta^{18}O$ variation, suggesting that the water has not been stored and mixed in the epikarst, which may suggest that some drips transfer the isotopic signature of rain events more quickly than others (Figure 16). Otherwise, changes in $\delta^{18}O$ appear to be dampened due to mixing with stored water in the epikarst (Figure 16). Increases in rainfall amount have a significant, weak relationship $\delta^{18}O$ of precipitation, thus increases in rainfall may also result in in negative $\delta^{18}O$ drip water. We interpret changes in modern drip water in LSC $\delta^{18}O$ to reflect changes in temperature, rainfall amount, and potentially changes in moisture source. However, more drip water data will assist in evaluating this hypothesis.

Modeling work through the Paleoclimate Modeling Intercomparison Project (PMIP2 and PMIP3) indicate that the region was colder during the LGM compared to present day. The ensemble average of 21ka simulations conducted as part of PMIP2 and 3 suggests that Lake Surprise and Tule Lake in north/northwest California were colder during the LGM by 6.41°C± 2°C and 5.88°C ± 2°C respectively. Lake Chewaucan in southern Oregon was colder by 6.46°C ± 2°C (Oster et al., 2015). Based on the water-calcite fraction factor:

$$1000\ln\alpha = 16.1\left(10^{3}T^{-1}\right) - 24.6 \quad (3;\ \text{Tremaine et al., 2011})$$

and a fractionation temperature dependence of:

$$\Delta\delta^{18}O/\Delta T = -0.177‰/°C \quad (4;\ \text{Tremaine et al., 2011})$$

in-cave effect of a temperature-decrease of this magnitude would cause the $\delta^{18}O$ of the LSC3 speleothem to be slightly more positive, by 1.04‰ to 1.14‰ (based on the Tule Lake 5.88°C and Lake Chewaucan 6.46°C boundaries). Furthermore, based on the temperature effect on rainwater, and therefore dripwater,

$$T = .14\delta^2 - 4.3\delta + 16.5 \text{ (5; Epstein et al., 1953)}$$

a maximum temperature-decrease of 6.46°C or minimum decrease of 5.88°C would result in the $\delta^{18}O$ to be more negative, by ~1.93‰ to ~1.79‰ respectively. In terms of the LSC3 $\delta^{18}O$ paleorecord, this would manifest as a transition from more negative $\delta^{18}O$ values during the LGM to more positive $\delta^{18}O$ values after the LGM (by ~.8‰). The PMIP2 and 3 temperatures are estimates of the average annual temperature, so the calculations above should be interpreted as an informed estimate. The LSC3 $\delta^{18}O$ record displays the opposite trend as what is predicted by the water-calcite fractionation factor and temperature effect on rainwater calculations, with relatively more positive $\delta^{18}O$ values occurring during the LGM (21-19 ka) and more negative $\delta^{18}O$ following the LGM (19-16 ka; Figure 14). Because we see $\delta^{18}O$ changes that are over two times greater than the in-cave effect, over 1.5 times greater than the rainwater water effect of changing temperature, and the inverse relationship between $\delta^{18}O$ and temperature during the LGM, changes in LSC3 $\delta^{18}O$ likely in part reflect sustained changes in moisture source across the last deglaciation.

Overall, there is a multi-millennial-scale, increasing and decreasing trend throughout the $\delta^{18}O$ record between ~31 and 21 ka, the onset of the LGM. This interval, however, includes three, rapid $\delta^{18}O$ increases of ~1.5‰, which align with DO event recorded in NGRIP. Beginning at the LGM, and until the end of the record, the $\delta^{18}O$ record displays cyclical millennial-scale increases and decreases of ~2‰. The $\delta^{18}O$ record reaches a local maximum, ~-8.5‰, at the onset of the LGM which lasts until ~18.5 ka.

The overall long-term patterns of change in $\delta^{18}O$ suggest periods of increased North Pacific moisture between 31-30 ka, 18-17.5 ka and briefly at ~14.5 ka. Between ~30 ka and ~19 ka, LSC3 displays relatively positive $\delta^{18}O$ values with rapid, noisy, fluctuations of ~1‰, suggesting an increased contribution of subtropical moisture during HS-2. Three DO events are captured in the LSC3 $\delta^{18}O$ record, seen as millennial-scale increases in $\delta^{18}O$ by ~1.5‰ occurring at ~28, 27 and 23 ka (Figure 18). The increase in $\delta^{18}O$ between ~18 ka to ~16 ka, ~-10‰ to ~-8.5‰, followed by the decrease of $\delta^{18}O$ from ~16 ka to ~14.4 ka, ~-8.5‰ to ~-10.5‰, suggest a sustained increase and then decrease in subtropical moisture respectively during HS-1. Following ~14.4 ka, $\delta^{18}O$ increases by ~1.5‰, from ~-10.5‰ to ~-9.0 until the end of the record at ~14.3 ka, suggesting increased subtropical moisture during the later part of the BA.

$\delta^{13}C$

Pollen and plant macrofossil from the nearby Siskiyou Mountains provide evidence that there is no significant portion of C_4 flora in this region during the last glacial and deglaciation (Briles et al., 2005). Carbon isotope values in LSC3 should therefore reflect a combination of changes in soil respiration and prior calcite precipitation (PCP). Both of these processes shift speleothem $\delta^{13}C$ in the same direction in response to changes in water availability over the cave. Increased rainfall should lead to increased soil respiration and decreased PCP, causing a negative shift in speleothem $\delta^{13}C$ record, and vice versa, as has been noted in drip water and speleothem records from the central Sierra Nevada and Oregon (Oster et al., 2009, 2012, 2014, 2015; Ersek et al., 2012).

Overall, there is a broad increasing and decreasing trend throughout the LSC3 $\delta^{13}C$ record, upon which there are periods of rapid, large decreases and increases and periods of stability. In general, the shorter-term trends coincide with Heinrich stadials 1-3 and interstadials with values rising from minimum values in a given stadial through the remainder of the stadial to maximum values in the subsequent interstadial. $\delta^{13}C$ values decrease rapidly to new minimum values in the early portions of the following stadial interval. Preliminary $\delta^{13}C$ data from HS-3 (~29-30 ka) record a transition from relatively high $\delta^{13}C$ values (-4‰), to relatively low values (~-6‰) during the middle of HS-3, suggesting wet and/or potentially high soil respiration between 31-30 ka. Highest $\delta^{13}C$ values, suggesting the overall driest conditions and/or potentially the least soil respiration, occur between HS-2 (~26-23 ka) and the end of the LGM, ~24.2 ka to ~19 ka respectively and from 14.4 to 14.3 ka. The peak in $\delta^{13}C$ occurs between 23.8-24.2 ka, during HS-2. A prominent shift toward substantially more negative $\delta^{13}C$ values occurs during the first half of HS-1, between ~19-18 ka. During the second half of HS-1, ~17-16 ka, $\delta^{13}C$ prominently increases and stabilizes until ~14.4 ka, during the first part of the BA. The LSC record then displays a rapid, large increase in $\delta^{13}C$, by nearly 3‰, between 14.4 and 14.3ka, suggesting a shift from wetter to drier conditions during the BA.

LSC3 growth rate calculations complement the proxy record interpretations. LSC3 grew quickly between ~33.3-31.6 ka and ~15.1-14.3 ka, at ~2-3cm/kyr and ~~2-4cm/kyr respectively, which suggests increased water availability/wetter conditions. LSC3 grew slowly between ~29-18.3 ka, <1cm/kyr, which suggest drier conditions during HS-2 and the LGM (Figure 14). The LSC3 record will cover HS-3 and beyond, to ~35.9 ka, once the remaining samples are analyzed.

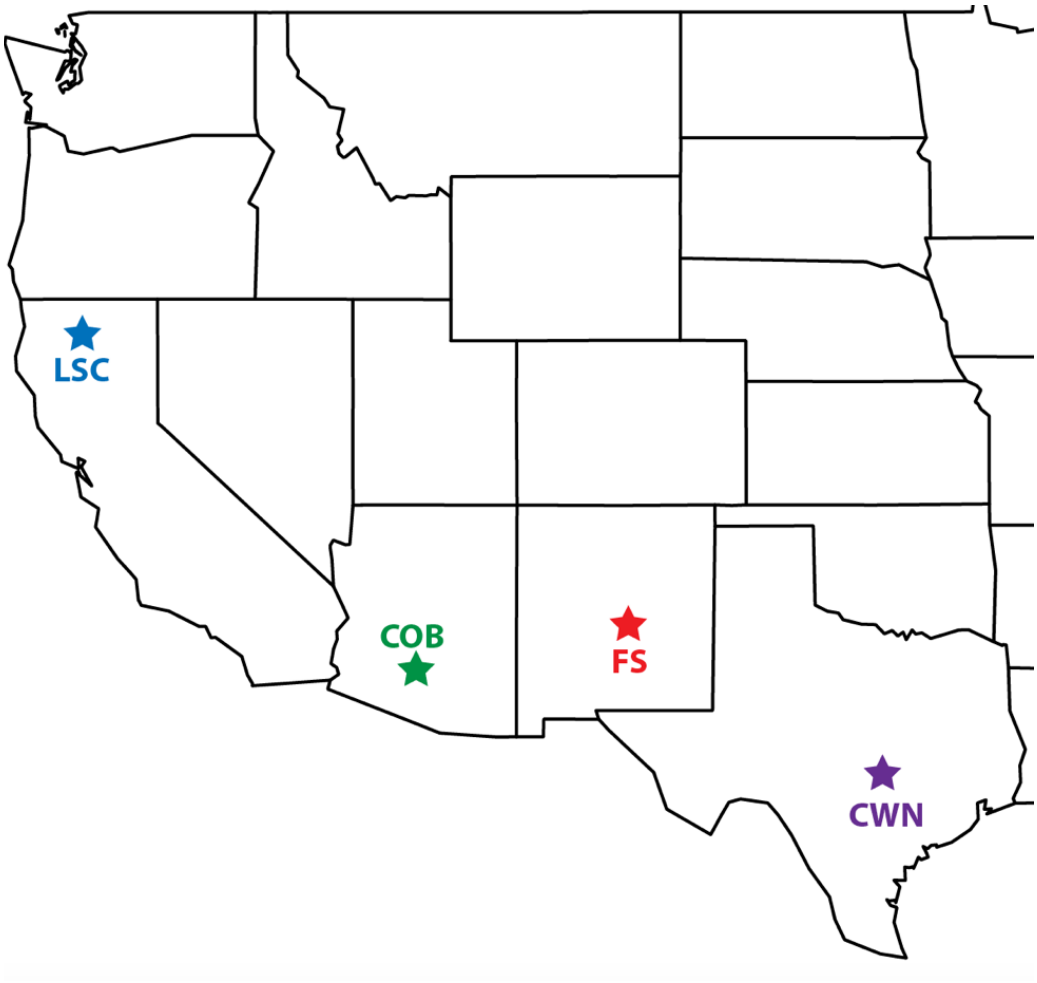
LSC
COB
FS
CWN

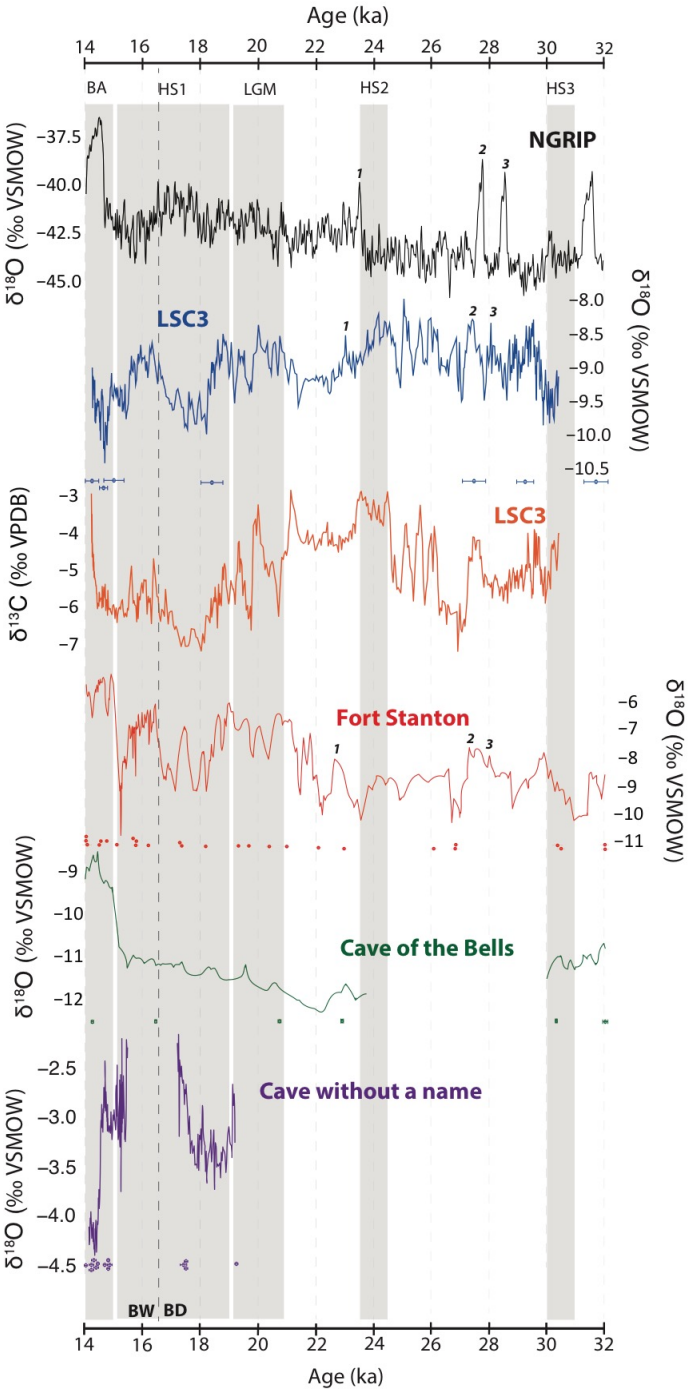

Figure 17. Map of speleothem records in Western North America that cover the Late Pleistocene (above, page 29). Stacked $\delta^{18}O$ and $\delta^{13}C$ records color coordinated with map (below). From Top to bottom: NGRIP – Greenland ice core (North Greenland Ice Core Project members, 2004); LSC – Lake Shasta Caverns; Fort Stanton (Asmerom and Polyak et al., 2010); Cave of the Bells (Wagner et al., 2010); Cave without a Name (Feng et al., 2014). Black italicized numbers above peaks in the $\delta^{18}O$ record represent DO events. BA – Bølling Allerød, HS – Heinrich Stadial, LGM – Last Glacial Maximum. BD – Big Dry, BW- Big Wet. U-Series ages and 2σ errors are plotted below each corresponding isotope record.

Regional Climate Change During the Last Deglaciation

Collectively, late Pleistocene paleoclimate proxies from WNA indicate large-amplitude changes in temperature and water availability (Asmerom et al., 2010; Wagner et al., 2010; Ibarra et al., 2014; Oster et al., 2015). This study relies on the LSC3 speleothem which, through U-Series age dating, captures the late Pleistocene/LGM period of hydroclimate change. We place the LSC3 record, and its interpretation, into the broader context of WNA paleo-precipitation studies covering the last deglaciation.

The broad climate evolution of WNA is linked to large-scale North Hemisphere changes associated with global climatic events (Lora et al., 2016). The polar Northern Hemisphere was punctuated by rapid climate fluctuations known as Dansgaard-Oeschger (DO) events (Bond et al., 1993). DO events are marked by rapid warming, followed by slow cooling. The most prominent cooling's, known as Heinrich Stadials (HS), were associated with massive iceberg discharge into the North Atlantic Ocean (Bond et al., 1992). The release of massive quantities of meltwater and icebergs into the North Atlantic reduced meridional overturning circulation and increased ocean stratification, leading to extensive winter sea ice formation (Cheng et al., 2009; Denton et al., 2010). The vast sea ice cover created extreme seasonality in the North Atlantic region, most notably in Greenland (Denton et al., 2010; Cross et al., 2015). The DO events are expressed as sharp positive excursions, followed by relatively gradual decreases in $\delta^{18}O$ of Greenland ice cores (Johnsen et al., 1992). DO events are also seen in approximately synchronous shifts in several western US proxy records, especially in speleothems, indicating that robust teleconnections exist between the two regions (Asmerom et al., 2010; Wagner et al., 2010; Figure 17).

The $\delta^{18}O$ record of LSC3 shows changes that correspond to DO events as seen in NGRIP and the Fort Stanton, NM Speleothem record (Figure 17). Three distinguishable DO interstadials (1, 2 and 3) are present in the LSC3 record, seen as $\delta^{18}O$ peaks occurring at approximately 28.1 ka, 27.5 ka and 23 ka (Figure 17).

In the Great Basin, higher lake levels are associated with HS-1 and the Younger Dryas (Munroe and Laabs 2013a, Oviatt, 1997; Ibarra et al., 2014). Speleothems from the southwestern United States also show clear responses to Heinrich Events (HS-1-HS-5) (Asmerom et al., 2010; Musgrove et al., 2001; Wagner et al., 2010). Asmerom et al., (2010) interpret the negative $\delta^{18}O$ excursions in speleothem calcite, seen leading up to the BA and during HS-4, from Fort Stanton Cave to be a result of increased Pacific-dominated (winter) precipitation and higher annual precipitation due to variations in meridional temperature gradients that drove changes in atmospheric circulation and influenced the strength, position and moisture sources of the winter westerly storm track in western North America (Asmerom et al., 2010). Other proposed mechanisms that explain negative $\delta^{18}O$ excursions reference the influence of Milankovich orbital forcings, which include changes in winter and summer insolation and thickness and extent of continental ice sheets and sea ice (Lachniet et al., 2014; COHMAP Members, 1988; Hostetler and Benson, 1990). Asmerom et al., (2010) also interpret the positive $\delta^{18}O$ excursions in the Fort-Stanton speleothem to be a result of DO events, specifically a smaller contribution of Pacific-dominated winter precipitation due to the northward shift of the polar jet stream and the Intertropical Convergence Zone (ITCZ) which modulated the position of the winter storm track over North America.

In regards to the Heinrich Events, LSC3 records changes in $\delta^{18}O$ that are correlated and anticorrelated with NGRIP and other regional records through time. During HS-2, LSC3 and FS $\delta^{18}O$ decrease by ~1.5‰ (Figure 17). During HS-1, NGRIP, LSC3 and FS show centennial to millennial, synchronous rises and falls (the magnitude of NGRIP fluctuations is relatively more muted). A distinctive feature of Great Basin lake reconstructions is the widespread lake expansion following the discharge of icebergs in the North Atlantic during HS-1 and HS-2 (Munroe and Laabs, 2013; Ibarra et al., 2014). Evidence suggests that the climate of HS-1 in western North America can be divided into two distinct phases. Based on pluvial lake records from New Mexico, Broecker et al., (2009) divided HS-1 into an earlier dry phase (the Big Dry, 17.5-16.3 ka), and a later wet phase (the Big Wet, 16.3-15 ka). However, evidence for "Big Dry" and the "Big Wet" at this time is not consistent across the region.

Some WNA proxy records indicate a transition from drier conditions to wetter conditions in the middle of HS-1. Dry conditions are suggested during the earlier portion of HS-1 by a paired speleothem $\delta^{13}C$ and $\delta^{234}U$ record from Fort Stanton Cave in New Mexico (Polyak et al., 2012). During the latter part of HS-1 many lakes, including Lake Franklin (in northeast Nevada; Broecker and Putnam, 2012), Lake Bonneville (in northwest Utah; Munroe and Laabs, 2013), and Lake Surprise (in northeast California; Ibarra et al., 2014) reached highstands, and this period has been described as the wettest period in the Great Basin in the past 30,000 years (Figure 18). The Fort Stanton speleothem $\delta^{234}U$ record also shows a transition to wetter conditions around 16.1 ka (Polyak et al., 2012). The Lake Elsinore leafwax $\delta^{2}H$ record suggests a brief shift to colder/wetter conditions (Kirby et al., 2013), and cold and wet conditions are also noted at Swamp Lake on the west side of the Sierra Nevada during the latter part of HS-1 (Street et al., 2012; Figure 18).

The LSC3 record shows evidence of a two-phased HS-1, with wetter conditions above LSC3 between 16.5 and 17.5 ka - during the "Big Dry" - and a shift to drier conditions at 16.5 ka – during the "Big Wet" (Figure 14). We see the opposite transition as Broecker et al., (2009), as we interpret changes in the LSC $\delta^{13}C$ record to reflect a transition from wetter to drier conditions. The LSC3 $\delta^{13}C$ record is relatively negative (between ~-7 and -6‰) from 17.5-16.5 ka, suggesting wet conditions and/or increased soil respiration – in contrast to the Broecker et al. "Big Dry" phase. The LSC3 $\delta^{13}C$ stabilizes, and increases slightly, between ~16.4-15 ka, suggesting drier and/or decreased soil respiration – in contrast to the Broecker et al., "Big Wet" phase. The $\delta^{13}C$ rapidly increases at ~14.4 ka, suggesting a decrease in water availability at the end of the record during the BA (Figure 17).

Oxygen isotope records from Cave of the Bells (in Arizona) and Fort Stanton Caves display large and abrupt increases at the onset of the Bølling Allerød (BA), which are interpreted as decreases in the proportion of winter, relative to summer, moisture in that region (Asmerom et al., 2010; Wagner et al., 2010). However, the Fort Stanton $\delta^{234}U$ record indicates wet conditions persisted through this interval in New Mexico (Polyak et al., 2012). Together, these records suggest decreased winter precipitation and enhanced summer moisture to the southwest, which is consistent with a Texas speleothem from Cave Without a Name record suggesting greater moisture transport from Gulf of Mexico during this time (Figure 17; Feng et al., 2014). The Lake Elsinore leaf wax $\delta^{2}H$ record points to drier conditions, or an increase in subtropical moisture across this interval (Kirby et al., 2013; Figure 18). Great Basin lakes show evidence of desiccation at this time, however lake levels are also influenced by evaporation, which likely increased with rising

summer insolation at this time (McGee et al., 2012; Munroe and Laabs, 2013). We interpret LSC3 $\delta^{18}O$ to reflect sustained changes in moisture source and $\delta^{13}C$ to reflect water availability and/or soil respiration. The transition out of HS-1 into the BA in the LSC3 record is marked by a small decrease followed by a small increase in $\delta^{18}O$, which is consistent with a shift from more north pacific to more subtropical sourced moisture, and a shift from a steady, relatively negative $\delta^{13}C$ to less negative, suggesting a shift from wetter conditions and/or increased soil respiration to drier and/or less soil respiration near the end of the record during the BA. Together, the LSC3 proxy record indicate a relatively wet climate following HS-1 and a shift to drier conditions during the BA at the end of the record.

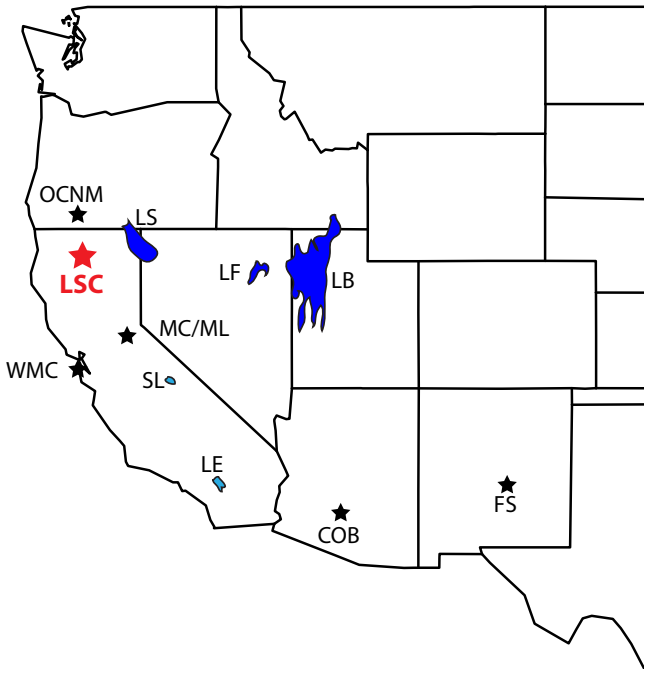

Figure 18. A map of paleoclimate records discussed in the text: Speleothem records indicated by stars. LSC = Lake Shasta Caverns; FS = Fort Stanton Cave (Asmerom et al., 2010); COB = Cave of the Bells (Wagner et al., 2010); OCNM = Oregon Caves National Monument (Vacco et al., 2005; Ersek et al., 2012); MC/ML = Moaning and McLean Cave respectively (Oster et al., 2009, 2012, 2015); LS = Lake Surprise (Ibarra et al., 2014); LF = Lake Franklin (Munroe and Laabs, 2013); (LB = Lake Bonneville (McGee et al., 2012); SL = Swamp Lake (Street et al., 2012); LE = Lake Elsinore (Kirby et al., 2013). Dark blue indicates lake Pleistocene lake and light blue indicates modern lake.

The integration of the LSC3 record into the regional network of published proxy records allows for an evaluation of the spatiotemporal variability of the hydrologic transition zone. The term "transition zone" denotes the area separating the wet and dry end members of the dipole precipitation pattern separating the Pacific Northwest and the Desert Southwest, seen in response to both ENSO forcing and forcing by the ice sheet during the LGM. The transition zone is spatially limited to west of the continental divide, and consists of a narrow zone within the 40-42° latitude band. Modeling work indicates that the strength and location of the dipole transition zone are modulated by ocean-atmosphere conditions which have varied over time (Wise et al., 2010). In California, the center of the transition zone has ranged from 37-42°N, between 1926-2007. The

LSC3 record is from a cave located within this transition zone, at ~40.8°N, and, by comparing the stable isotope record with previously published records from regions below the transition zone (central California, Arizona, New Mexico, and Texas) we can capture the subtle movement of the hydrologic transition zone through time (~35.9 ka to 14.3 ka). Specifically, by comparing our interpretation of the LSC3 $\delta^{18}O$ and $\delta^{13}C$ record with the interpretation of the other speleothem records, we can determine if the transition zone was positioned above, at, or below LSC – and how that may have changed over time.

During HS-1 both the LSC3 and FS record display a shift toward substantially more negative $\delta^{13}C$ and $\delta^{18}O$ values, respectively, during the first half of HS-1, between ~19-18 ka and then a prominent increase in $\delta^{13}C$ and $\delta^{18}O$ during the second half of HS-1, ~17-16 ka. Decreases in the LSC3 $\delta^{13}C$ record are interpreted to represent "wetter" conditions. Polyak et al., (2012) interpret increases in the FS $\delta^{18}O$ record to represent less winter dominated precipitation (or more summer precipitation). The FS $\delta^{234}U$ record is interpreted as an independent proxy for precipitation (Polyak et al., 2012). During HS-1, the FS $\delta^{234}U$ increases, and stays high, between ~18.5-16.4 ka, and then decreases from ~16.4 ka until ~14.3ka. This two-phased $\delta^{234}U$ record is interpreted to represent a transition from dry conditions to wet conditions during HS-1. Together, the FS $\delta^{18}O$ and $\delta^{234}U$ indicate a transition from dry conditions with more winter precipitation to wetter conditions and more summer precipitation. The interpretation of the FS $\delta^{18}O$ and $\delta^{234}U$ record is consistent with the Big Wet (regional lake level highstands) and Big Dry, and inconsistent with the LSC3 $\delta^{18}O$ and $\delta^{13}C$ records. During HS-1 LSC3 records a shift from relatively wetter conditions and/or more soil respiration to drier and/or less soil respiration. The proxy disagreement between LSC3 and FS speleothems suggest that LSC3 showed behavior that may be more similar to the north, dry side of the dipole zone. Climate modeling suggests that the narrowing of the transition zone occurs when the Southern Oscillation Index (SOI) and the Pacific Decadal Oscillation (PDO) are in a constructive phase (SOI-/PDO+ or SOI+/PDO-) and during the negative Atlantic Meridional Oscillation (AMO-) phase (Wise et al., 2010). During the transition into the Bølling Allerød, we see a shift from LSC3 and FS proxy disagreement, to proxy agreement.

During the Bølling Allerød, LSC3 $\delta^{13}C$ stabilizes between ~17-15 ka, before $\delta^{13}C$ rapidly increases at ~14.3 ka by ~3‰, suggesting a shift from relatively wet conditions to drier conditions and/or less soil respiration. Similarly, FS2 $\delta^{13}C$ and $\delta^{234}U$ data show a transition to much drier conditions in the southwestern USA starting at 14.5 ka. The FS $\delta^{18}O$ record displays a ~4‰ decrease between 17-15 ka, followed by an abrupt, ~5‰ increase between ~15-14.3 ka, suggesting a rapid shift from increased winter precipitation to increased summer precipitation respectively. Because the LSC3 and FS record display similar interpretations, this may suggest that LSC behaves similar to the south side of the dipole during this interval. The LSC3 record, and future proxy data in the hydrologic transition zone, will allow benchmarking of the location and movement of the narrow transition zone band through time, thus aiding in the development of more robust climate models during periods of known hydroclimate change.

CHAPTER 5

CONCLUSIONS

I have conducted a modern precipitation and cave drip water analysis in Northern California and developed a precisely dated high-resolution $\delta^{18}O$ and $\delta^{13}C$ stable isotope record from a Lake Shasta Caverns speleothem that grew from 35.9 to 14.3 ka in Lakehead, California.

The modern precipitation and cave drip water study indicates that the NADP site CA-76 in Montague, CA and LSC receive precipitation at the same time, but at different magnitudes; with LSC receiving more precipitation during the congruent rain events. The $\delta^{18}O$ of the NADP samples falls along both the GMWL and the LMWL, with more negative $\delta^{18}O$ and $\delta^{2}H$ during the winter and spring and less negative during the summer and autumn, with the exception of individual Atmospheric River precipitation events. The most positive $\delta^{18}O$ and $\delta^{2}H$ precipitation falls during the spring and summer months, May through September, while the most negative $\delta^{18}O$ and $\delta^{2}H$ precipitation falls during the autumn and winter months, October through April, indicating that temperature provides some control on the $\delta^{18}O$ signature of precipitation. Through a comparison with maximum, average, and minimum average rain day temperatures and the $\delta^{18}O$ of precipitation, I found that the rain day temperature exerts a moderate control on the $\delta^{18}O$ of precipitation that falls in northern California. In addition to temperature, I also found that moisture source exerts a moderate control on the $\delta^{18}O$ of precipitation as well. HYSPLIT back trajectory analyses suggest that precipitation originating in the subtropical pacific results in rainfall with more positive $\delta^{18}O$ and lower deuterium excess, compared to precipitation originating in the north Pacific, and consistent with atmospheric river events. The preliminary drip water analyses reveal that drip water $\delta^{18}O$ falls along the GMWL and has a signature similar to monthly-integrated precipitation collected near the cave entrance. Further analysis drip water collected monthly through a collaboration with D. Mundt that began in December 2015 will shed light on the annual $\delta^{18}O$ fluctuation of cave drip water and how precipitation is transferred to the cave.

U-Th dating reveals that the LSC3 stalagmite precipitated from ~35.9 to ~14.3 ka, spanning the last deglaciation, including Heinrich Stadials 1-3, and the Bølling-Allerød. There are no visible growth hiatuses in the LSC3 speleothem. The speleothem grew quickly from ~35.9 ka to ~30.8 ka, slowly from ~30.8 ka and ~18.5 ka and quickly from ~18.4 ka to ~14.9 ka. We interpret increases in growth rate to represent wetter conditions. The stable isotope time-series developed for the LSC3 stalagmite offer sub to multi-decadal resolution based on U-Th constrained calcite growth rates calculated using the COPRA age model. The LSC3 $\delta^{18}O$ record captures three DO events occurring roughly around 28, 27 and 23 ka – seen as ~1.5‰ increases in $\delta^{18}O$ – and HS-1-3. We interpret changes in LSC3 $\delta^{18}O$ to reflect sustained changes in moisture source across the last deglaciation. We interpret changes in carbon isotope values in LSC3 to reflect a combination of changes in soil respiration and PCP, meaning relatively positive $\delta^{13}C$ values represent the driest conditions and/or times with potentially the least soil respiration. Main features of the stable isotope record point to a relatively dry LGM and a wet BA.

The most important product of this research is a high-resolution paleoclimate record from northern California; a product that does not exist currently. The LSC records cover approximately 20,000 years, during a period of drastic hydroclimate change. The LSC record also temporally overlaps with published records to the north and south. By building upon this network of work in the region and comparing to these coeval records, the new records from LSC will provide clarity regarding the ENSO and LGM related north-south dipole and contribute to refining our understanding hydroclimatic variability in the western U.S.

Appendix A.
List of terms and abbreviations as they appear in the text.

Term	Abbreviation
Western North America	WNA
Last Glacial Maximum	LGM
El Niño Southern Oscillation	ENSO
Pacific Decadal Oscillation	PDO
Southern Oscillation Index	SOI
Lake Shasta Caverns	LSC
Speleothem from Lake Shasta Caverns	LSC3
White Moon Cave	MWC
Oregon Caves National Monument	OCNM
Cave of the Bells	COB
Fort Stanton	FS
National Atmospheric Deposition Program	NADP
Prior calcite precipitation	PCP
Moaning and McLean Cave	MC/ML
Cave Without a Name	CWN
University of California Integrated Pest Management	UC-IPM
Hybrid Single Particle Langrangian Integrated Trajectory	HYSPLIT
Dissolved organic carbon	DIC
Local Meteoric Water Line	LMWL
Global Meteoric Water Line	GMWL
Bølling-Allerød	BA
Constructing Proxy Records from Age models	COPRA
Marine Isotope Stage 2	MIS2
Heinrich Stadial (1:5)	HS-1:5
Atmospheric Rivers	AR
Dansgaard-Oeschger	DO
North Greenland Ice Core Project	NGRIP
Lake Surprise	LS
Lake Franklin	LF
Lake Bonneville	LB
Swamp Lake	SL
Lake Elsinore	LE
Atlantic Meridional Oscillation	AMO
Big Wet	BW
Big Dry	BD
Inter Tropical Convergence Zone	ITCZ

Appendix B.

Precipitation amount and temperature data from the University of California Integrated Pest Management site in Yreka, CA. $\delta^{18}O$ and $\delta^{2}H$ data from weekly integrated precipitation samples collected at the National Atmospheric Deposition Program site CA-76 in Montague, CA. Samples analyzed by the ThermoFinnigan Delta Plus XL isotope ratio mass spectrometer at the Stable Isotope Ratio Facility for Environmental Research at the University of Utah. Long term precision is 1.56‰ ($\delta^{2}H$) and 0.19‰ ($\delta^{18}O$). Temperature data is reported as maximum, minimum and average temperatures recorded by the UC-IPM station on the days when is rained and during the week captured by the NADP sample. The rain isotope samples are collected weekly, so each day in the respective week will have the same $\delta^{18}O$ and $\delta^{2}H$ signatures, but different daily temperatures and precipitation amount values.

Date	Precip amount (mm)	$\delta^{2}H_{VSMOW}$ (‰)	$\delta^{18}O_{VSMOW}$ (‰)	Maximum Temperature (°C)	Minimum Temperature (°C)	Average Temperature (°C)
3/25/10	11.42	-52.92	-7.63	13.75	1.1	7.43
3/26/10	1.777	-52.92	-7.63	13.75	1.1	7.43
3/27/10	0	-52.92	-7.63	13.75	1.1	7.43
3/28/10	0.254	-52.92	-7.63	13.75	1.1	7.43
3/29/10	2.284	-52.92	-7.63	13.75	1.1	7.43
3/30/10	10.66	-52.92	-7.63	13.75	1.1	7.43
3/31/10	1.523	-113.58	-15.29	8.12	-1.54	3.29
4/1/10	0	-113.58	-15.29	8.12	-1.54	3.29
4/2/10	7.8	-113.58	-15.29	8.12	-1.54	3.29
4/3/10	15.48	-113.58	-15.29	8.12	-1.54	3.29
4/4/10	0.508	-113.58	-15.29	8.12	-1.54	3.29
4/5/10	3.807	-113.58	-15.29	8.12	-1.54	3.29
4/6/10	0.254	-113.58	-15.29	8.12	-1.54	3.29
4/7/10	0	-128.61	-16.61	12.8	-2.20	5.30
4/8/10	0	-128.61	-16.61	12.8	-2.20	5.30
4/9/10	0	-128.61	-16.61	12.8	-2.20	5.30
4/10/10	0	-128.61	-16.61	12.8	-2.20	5.30
4/11/10	0	-128.61	-16.61	12.8	-2.20	5.30
4/12/10	10.6	-128.61	-16.61	12.8	-2.20	5.30
4/13/10	3.046	-135.98	-17.57	13.17	1.67	7.42
4/14/10	0.508	-135.98	-17.57	13.17	1.67	7.42
4/15/10	0.508	-135.98	-17.57	13.17	1.67	7.42
4/16/10	0	-135.98	-17.57	13.17	1.67	7.42
4/17/10	0	-135.98	-17.57	13.17	1.67	7.42
4/18/10	0	-135.98	-17.57	13.17	1.67	7.42
4/19/10	0	-135.98	-17.57	13.17	1.67	7.42
4/20/10	10.15	-135.98	-17.57	13.17	1.67	7.42
4/21/10	5.076	-83.07	-11.28	10.57	1.27	5.92
4/22/10	2.538	-83.07	-11.28	10.57	1.27	5.92
4/23/10	0	-83.07	-11.28	10.57	1.27	5.92
4/24/10	0	-83.07	-11.28	10.57	1.27	5.92
4/25/10	0	-83.07	-11.28	10.57	1.27	5.92
4/26/10	0	-83.07	-11.28	10.57	1.27	5.92
4/27/10	28.42	-83.07	-11.28	12.65	1.28	6.96
4/28/10	7.107	-82.19	-10.75	12.65	1.28	6.96
4/29/10	8.3	-82.19	-10.75	12.65	1.28	6.96
4/30/10	1.523	-82.19	-10.75	12.65	1.28	6.96
5/1/10	0	-82.19	-10.75	12.65	1.28	6.96
5/2/10	0	-82.19	-10.75	12.65	1.28	6.96
5/3/10	0	-82.19	-10.75	12.65	1.28	6.96
5/4/10	0	-82.19	-10.75	12.65	1.28	6.96

5/5/10	0	-93.79	-11.83	16.1	5.0	10.55
5/6/10	0	-93.79	-11.83	16.1	5.0	10.55
5/7/10	0	-93.79	-11.83	16.1	5.0	10.55
5/8/10	0	-93.79	-11.83	16.1	5.0	10.55
5/9/10	0.254	-93.79	-11.83	16.1	5.0	10.55
5/10/10	0.761	-93.79	-11.83	16.1	5.0	10.55
5/11/10	3.046	-93.79	-11.83	16.1	5.0	10.55
5/12/10	0					
5/13/10	0					
5/14/10	0					
5/15/10	0					
5/16/10	0					
5/17/10	0					
5/18/10	0					
5/19/10	17.8					
5/20/10	1.269					
5/21/10	0					
5/22/10	0.508					
5/23/10	0.508					
5/24/10	0					
5/25/10	0					
5/26/10	1.777	-86.28	-11.57	20.33	4.46	12.39
5/27/10	0.761	-86.28	-11.57	20.33	4.46	12.39
5/28/10	6.345	-86.28	-11.57	20.33	4.46	12.39
5/29/10	0	-86.28	-11.57	20.33	4.46	12.39
5/30/10	0	-86.28	-11.57	20.33	4.46	12.39
5/31/10	22.2	-86.28	-11.57	20.33	4.46	12.39
6/1/10	21.7	-86.28	-11.57	20.33	4.46	12.39
6/2/10	0	-85.68	-10.06	21.30	9.07	15.18
6/3/10	1.777	-85.68	-10.06	21.30	9.07	15.18
6/4/10	9.645	-85.68	-10.06	21.30	9.07	15.18
6/5/10	1.269	-85.68	-10.06	21.30	9.07	15.18
6/6/10	0	-85.68	-10.06	21.30	9.07	15.18
6/7/10	0	-85.68	-10.06	21.30	9.07	15.18
6/8/10	0	-85.68	-10.06	21.30	9.07	15.18
6/9/10	0					
6/10/10	18.9					
6/11/10	0					
6/12/10	0					
6/13/10	0					
6/14/10	0					
6/15/10	0					
6/16/10	0					
6/17/10	0					
6/18/10	0					
6/19/10	21.1					
6/20/10	21.7					
6/21/10	0					
6/22/10	0					
6/23/10	0					
6/24/10	0					
6/25/10	0					
6/26/10	0					
6/27/10	0					
6/28/10	0					
6/29/10	0					
6/30/10	0					

7/1/10	0					
7/2/10	0					
7/3/10	0					
7/4/10	0					
7/5/10	0					
7/6/10	0					
7/7/10	0					
7/8/10	0					
7/9/10	0					
7/10/10	0					
7/11/10	0					
7/12/10	0					
7/13/10	0					
7/14/10	0					
7/15/10	0					
7/16/10	0					
7/17/10	0					
7/18/10	0					
7/19/10	0					
7/20/10	0	-54.14	-6.2	33.9	12.8	23.35
7/21/10	0	-54.14	-6.2	33.9	12.8	23.35
7/22/10	0	-54.14	-6.2	33.9	12.8	23.35
7/23/10	0	-54.14	-6.2	33.9	12.8	23.35
7/24/10	0	-54.14	-6.2	33.9	12.8	23.35
7/25/10	0	-54.14	-6.2	33.9	12.8	23.35
7/26/10	0	-54.14	-6.2	33.9	12.8	23.35
7/27/10	32.23	-54.14	-6.2	33.9	12.8	23.35
7/28/10	0					
7/29/10	0					
7/30/10	0					
7/31/10	0					
8/1/10	0					
8/2/10	0					
8/3/10	0					
8/4/10	0					
8/5/10	0					
8/6/10	0					
8/7/10	0					
8/8/10	0					
8/9/10	0					
8/10/10	0					
8/11/10	0					
8/12/10	0					
8/13/10	0					
8/14/10	0					
8/15/10	0					
8/16/10	0					
8/17/10	0	-72.88	-9.55	32.8	10	21.40
8/18/10	1.269	-72.88	-9.55	32.8	10	21.40
8/19/10	0	-72.88	-9.55	32.8	10	21.40
8/20/10	0	-72.88	-9.55	32.8	10	21.40
8/21/10	0	-72.88	-9.55	32.8	10	21.40
8/22/10	0	-72.88	-9.55	32.8	10	21.40
8/23/10	0	-72.88	-9.55	32.8	10	21.40
8/24/10	0	-72.88	-9.55	32.8	10	21.40
8/25/10	0					
8/26/10	0					

8/27/10	0					
8/28/10	0					
8/29/10	0					
8/30/10	0					
8/31/10	0.254					
9/1/10	0					
9/2/10	0					
9/3/10	0					
9/4/10	0					
9/5/10	0					
9/6/10	0					
9/7/10	0					
9/8/10	0					
9/9/10	0					
9/10/10	0					
9/11/10	0					
9/12/10	0					
9/13/10	0					
9/14/10	0	-53.3	-7.21	23.90	5.55	14.73
9/15/10	0	-53.3	-7.21	23.90	5.55	14.73
9/16/10	0	-53.3	-7.21	23.90	5.55	14.73
9/17/10	0	-53.3	-7.21	23.90	5.55	14.73
9/18/10	0	-53.3	-7.21	23.90	5.55	14.73
9/19/10	9.391	-53.3	-7.21	23.90	5.55	14.73
9/20/10	2.538	-53.3	-7.21	23.90	5.55	14.73
9/21/10	0	-53.3	-7.21	23.90	5.55	14.73
9/22/10	0					
9/23/10	0					
9/24/10	0					
9/25/10	0					
9/26/10	0					
9/27/10	0					
9/28/10	0					
9/29/10	0					
9/30/10	0					
10/1/10	0					
10/2/10	0					
10/3/10	0					
10/4/10	1.015					
10/5/10	0					
10/6/10	0					
10/7/10	0					
10/8/10	0					
10/9/10	0					
10/10/10	0					
10/11/10	0					
10/12/10	0					
10/13/10	0					
10/14/10	0					
10/15/10	0					
10/16/10	0					
10/17/10	0					
10/18/10	0					
10/19/10	0	-91.56	-12.03	13.70	2.80	8.25
10/20/10	0	-91.56	-12.03	13.70	2.80	8.25
10/21/10	0	-91.56	-12.03	13.70	2.80	8.25
10/22/10	0	-91.56	-12.03	13.70	2.80	8.25

10/23/10	6.853	-91.56	-12.03	13.70	2.80	8.25
10/24/10	44.67	-91.56	-12.03	13.70	2.80	8.25
10/25/10	18.78	-91.56	-12.03	13.70	2.80	8.25
10/26/10	0.761	-91.56	-12.03	13.70	2.80	8.25
10/27/10	0	-59.03	-8.05	13.70	2.23	7.97
10/28/10	7.36	-59.03	-8.05	13.70	2.23	7.97
10/29/10	6.599	-59.03	-8.05	13.70	2.23	7.97
10/30/10	13.3	-59.03	-8.05	13.70	2.23	7.97
10/31/10	15.6	-59.03	-8.05	13.70	2.23	7.97
11/1/10	0	-59.03	-8.05	13.70	2.23	7.97
11/2/10	0	-59.03	-8.05	13.70	2.23	7.97
11/3/10	0	-118.74	-15.03	10.6	2.8	6.7
11/4/10	0	-118.74	-15.03	10.6	2.8	6.7
11/5/10	0	-118.74	-15.03	10.6	2.8	6.7
11/6/10	0	-118.74	-15.03	10.6	2.8	6.7
11/7/10	15.48	-118.74	-15.03	10.6	2.8	6.7
11/8/10	7.8	-118.74	-15.03	10.6	2.8	6.7
11/9/10	0	-118.74	-15.03	10.6	2.8	6.7
11/10/10	5.838	-50.51	-7.44	10.58	-0.43	5.08
11/11/10	0.508	-50.51	-7.44	10.58	-0.43	5.08
11/12/10	0.761	-50.51	-7.44	10.58	-0.43	5.08
11/13/10	0	-50.51	-7.44	10.58	-0.43	5.08
11/14/10	0	-50.51	-7.44	10.58	-0.43	5.08
11/15/10	0.508	-50.51	-7.44	10.58	-0.43	5.08
11/16/10	0	-50.51	-7.44	10.58	-0.43	5.08
11/17/10	0	-121.61	-16.88	5.85	-1.40	2.23
11/18/10	0	-121.61	-16.88	5.85	-1.40	2.23
11/19/10	7.868	-121.61	-16.88	5.85	-1.40	2.23
11/20/10	1.015	-121.61	-16.88	5.85	-1.40	2.23
11/21/10	9.391	-121.61	-16.88	5.85	-1.40	2.23
11/22/10	2.284	-121.61	-16.88	5.85	-1.40	2.23
11/23/10	5.33	-121.61	-16.88	5.85	-1.40	2.23
11/24/10	0	-142.01	-19.43	5.17	-3.50	0.83
11/25/10	0	-142.01	-19.43	5.17	-3.50	0.83
11/26/10	0	-142.01	-19.43	5.17	-3.50	0.83
11/27/10	4.569	-142.01	-19.43	5.17	-3.50	0.83
11/28/10	5.33	-142.01	-19.43	5.17	-3.50	0.83
11/29/10	0	-142.01	-19.43	5.17	-3.50	0.83
11/30/10	0	-142.01	-19.43	5.17	-3.50	0.83
12/1/10	3.807	-100.23	-13.94	6.58	0.56	3.57
12/2/10	7.36	-100.23	-13.94	6.58	0.56	3.57
12/3/10	16.49	-100.23	-13.94	6.58	0.56	3.57
12/4/10	0	-100.23	-13.94	6.58	0.56	3.57
12/5/10	2.031	-100.23	-13.94	6.58	0.56	3.57
12/6/10	3.553	-100.23	-13.94	6.58	0.56	3.57
12/7/10	0	-100.23	-13.94	6.58	0.56	3.57
12/8/10	2.792	-79.58	-10.58	10.57	3.03	6.80
12/9/10	1.269	-79.58	-10.58	10.57	3.03	6.80
12/10/10	3.046	-79.58	-10.58	10.57	3.03	6.80
12/11/10	1.523	-79.58	-10.58	10.57	3.03	6.80
12/12/10	12.2	-79.58	-10.58	10.57	3.03	6.80
12/13/10	1.269	-79.58	-10.58	10.57	3.03	6.80
12/14/10	17.76	-79.58	-10.58	10.57	3.03	6.80
12/15/10	7.8	-79.58	-10.58	10.57	3.03	6.80
12/16/10	0	-79.58	-10.58	10.57	3.03	6.80
12/17/10	0	-79.58	-10.58	10.57	3.03	6.80
12/18/10	6.599	-79.29	-11.74	6.40	-3.05	1.68

12/19/10	1.269	-79.29	-11.74	6.40	-3.05	1.68
12/20/10	6.853	-79.29	-11.74	6.40	-3.05	1.68
12/21/10	7.8	-79.29	-11.74	6.33	-1.47	2.43
12/22/10	0.508	-156.77	-21.04	6.33	-1.47	2.43
12/23/10	0	-156.77	-21.04	6.33	-1.47	2.43
12/24/10	0	-156.77	-21.04	6.33	-1.47	2.43
12/25/10	0	-156.77	-21.04	6.33	-1.47	2.43
12/26/10	7.107	-156.77	-21.04	6.33	-1.47	2.43
12/27/10	2.031	-156.77	-21.04	6.33	-1.47	2.43
12/28/10	0.761	-156.77	-21.04	6.33	-1.47	2.43
12/29/10	19.79	-145.11	-18.42	5.57	-2.83	1.37
12/30/10	0.508	-145.11	-18.42	5.57	-2.83	1.37
12/31/10	0	-145.11	-18.42	5.57	-2.83	1.37
1/1/11	5.838	-145.11	-18.42	5.57	-2.83	1.37
1/2/11	3.3	-145.11	-18.42	5.57	-2.83	1.37
1/3/11	2.031	-145.11	-18.42	5.57	-2.83	1.37
1/4/11	2.538	-145.11	-18.42	5.57	-2.83	1.37
1/5/11	1.523					
1/6/11	1.523					
1/7/11	2.792					
1/8/11	3.807					
1/9/11	2.538					
1/10/11	2.538					
1/11/11	3.046	-103.03	-13.79	7.58	-4.15	1.71
1/12/11	1.269	-103.03	-13.79	7.58	-4.15	1.71
1/13/11	2.031	-103.03	-13.79	7.58	-4.15	1.71
1/14/11	2.792	-103.03	-13.79	7.58	-4.15	1.71
1/15/11	3.046	-103.03	-13.79	7.58	-4.15	1.71
1/16/11	4.061	-103.03	-13.79	7.58	-4.15	1.71
1/17/11	4.061	-103.03	-13.79	7.58	-4.15	1.71
1/18/11	2.792	-103.03	-13.79	7.58	-4.15	1.71
1/19/11	2.538	-103.03	-13.79	7.58	-4.15	1.71
1/20/11	2.031					
1/21/11	3.3					
1/22/11	2.031					
1/23/11	2.538					
1/24/11	2.792					
1/25/11	1.777					
1/26/11	2.031					
1/27/11	3.046					
1/28/11	2.031					
1/29/11	0.508					
1/30/11	1.777					
1/31/11	1.523					
2/1/11	2.792					
2/2/11	2.031					
2/3/11	2.284					
2/4/11	0.761					
2/5/11	0.761					
2/6/11	0.254					
2/7/11	2.538					
2/8/11	2.538	-76.45	-10.5	10.40	-3.31	3.54
2/9/11	2.031	-76.45	-10.5	10.40	-3.31	3.54
2/10/11	1.523	-76.45	-10.5	10.40	-3.31	3.54
2/11/11	2.031	-76.45	-10.5	10.40	-3.31	3.54
2/12/11	1.269	-76.45	-10.5	10.40	-3.31	3.54
2/13/11	1.523	-76.45	-10.5	10.40	-3.31	3.54

2/14/11	4.061	-76.45	-10.5	10.40	-3.31	3.54
2/15/11	2.031	-76.45	-10.5	10.40	-3.31	3.54
2/16/11	2.284	-123.31	-16.95	10.97	-2.54	4.21
2/17/11	2.538	-123.31	-16.95	10.97	-2.54	4.21
2/18/11	1.523	-123.31	-16.95	10.97	-2.54	4.21
2/19/11	1.777	-123.31	-16.95	10.97	-2.54	4.21
2/20/11	1.523	-123.31	-16.95	10.97	-2.54	4.21
2/21/11	4.061	-123.31	-16.95	10.97	-2.54	4.21
2/22/11	1.269	-123.31	-16.95	10.97	-2.54	4.21
2/23/11	2.538					
2/24/11	1.015					
2/25/11	1.269					
2/26/11	1.015					
2/27/11	1.269					
2/28/11	1.777					
3/1/11	1.523	-143.21	-18.56	12.46	-1.69	5.39
3/2/11	3.3	-143.21	-18.56	12.46	-1.69	5.39
3/3/11	3.046	-143.21	-18.56	12.46	-1.69	5.39
3/4/11	1.015	-143.21	-18.56	12.46	-1.69	5.39
3/5/11	2.031	-143.21	-18.56	12.46	-1.69	5.39
3/6/11	0.508	-143.21	-18.56	12.46	-1.69	5.39
3/7/11	0.761	-143.21	-18.56	12.46	-1.69	5.39
3/8/11	1.269	-143.21	-18.56	12.46	-1.69	5.39
3/9/11	1.015	-83.34	-11.06	14.27	-1.29	6.49
3/10/11	1.269	-83.34	-11.06	14.27	-1.29	6.49
3/11/11	1.015	-83.34	-11.06	14.27	-1.29	6.49
3/12/11	0.761	-83.34	-11.06	14.27	-1.29	6.49
3/13/11	2.284	-83.34	-11.06	14.27	-1.29	6.49
3/14/11	2.031	-83.34	-11.06	14.27	-1.29	6.49
3/15/11	1.015	-113.59	-15.14	15.54	-0.89	7.33
3/16/11	1.269	-113.59	-15.14	15.54	-0.89	7.33
3/17/11	1.523	-113.59	-15.14	15.54	-0.89	7.33
3/18/11	0.761	-113.59	-15.14	15.54	-0.89	7.33
3/19/11	0.254	-113.59	-15.14	15.54	-0.89	7.33
3/20/11	1.015	-113.59	-15.14	15.54	-0.89	7.33
3/21/11	0.254	-113.59	-15.14	15.54	-0.89	7.33
3/22/11	1.269	-113.59	-15.14	15.54	-0.89	7.33
3/23/11	1.777	-112.39	-14.42	15.17	-0.97	7.10
3/24/11	1.269	-112.39	-14.42	15.17	-0.97	7.10
3/25/11	1.269	-112.39	-14.42	15.17	-0.97	7.10
3/26/11	1.269	-112.39	-14.42	15.17	-0.97	7.10
3/27/11	1.523	-112.39	-14.42	15.17	-0.97	7.10
3/28/11	1.523	-112.39	-14.42	15.17	-0.97	7.10
3/29/11	0.254	-112.39	-14.42	15.17	-0.97	7.10
3/30/11	1.523					
3/31/11	2.031					
4/1/11	1.015					
4/2/11	0.254					
4/3/11	1.015					
4/4/11	1.269					
4/5/11	0.508					
4/6/11	0.761					
4/7/11	1.523					
4/8/11	1.523					
4/9/11	1.269					
4/10/11	1.015					
4/11/11	0.508					

4/12/11	0.254					
4/13/11	1.777	-107.38	-12.99	17.60	1.22	9.41
4/14/11	1.777	-107.38	-12.99	17.60	1.22	9.41
4/15/11	0.761	-107.38	-12.99	17.60	1.22	9.41
4/16/11	1.269	-107.38	-12.99	17.60	1.22	9.41
4/17/11	1.015	-107.38	-12.99	17.60	1.22	9.41
4/18/11	1.777	-107.38	-12.99	17.60	1.22	9.41
4/19/11	1.269	-107.38	-12.99	17.60	1.22	9.41
4/20/11	1.777	-84.52	-10.96	18.23	1.84	10.04
4/21/11	1.269	-84.52	-10.96	18.23	1.84	10.04
4/22/11	0.508	-84.52	-10.96	18.23	1.84	10.04
4/23/11	1.015	-84.52	-10.96	18.23	1.84	10.04
4/24/11	1.523	-84.52	-10.96	18.23	1.84	10.04
4/25/11	0.508	-84.52	-10.96	18.23	1.84	10.04
4/26/11	0.761	-84.52	-10.96	18.23	1.84	10.04
4/27/11	1.269					
4/28/11	1.015					
4/29/11	1.015					
4/30/11	1.523					
5/1/11	1.523					
5/2/11	0.761					
5/3/11	2.792					
5/4/11	0.761					
5/5/11	2.792					
5/6/11	0.761					
5/7/11	0.761					
5/8/11	0.508					
5/9/11	2.031					
5/10/11	1.015	-120.15	-16.41	23.00	3.90	13.45
5/11/11	0.254	-120.15	-16.41	23.00	3.90	13.45
5/12/11	0.254	-120.15	-16.41	23.00	3.90	13.45
5/13/11	0.508	-120.15	-16.41	23.00	3.90	13.45
5/14/11	0.761	-120.15	-16.41	23.00	3.90	13.45
5/15/11	0.508	-120.15	-16.41	23.00	3.90	13.45
5/16/11	0.508	-120.15	-16.41	23.00	3.90	13.45
5/17/11	1.777	-102.38	-13.2	23.75	5.06	14.41
5/18/11	1.523	-102.38	-13.2	23.75	5.06	14.41
5/19/11	1.015	-102.38	-13.2	23.75	5.06	14.41
5/20/11	1.777	-102.38	-13.2	23.75	5.06	14.41
5/21/11	1.015	-102.38	-13.2	23.75	5.06	14.41
5/22/11	1.015	-102.38	-13.2	23.75	5.06	14.41
5/23/11	1.015	-102.38	-13.2	23.75	5.06	14.41
5/24/11	0.254	-82.3	-10.96	25.14	6.60	15.87
5/25/11	0.508	-82.3	-10.96	25.14	6.60	15.87
5/26/11	0.508	-82.3	-10.96	25.14	6.60	15.87
5/27/11	0.761	-82.3	-10.96	25.14	6.60	15.87
5/28/11	2.792	-82.3	-10.96	25.14	6.60	15.87
5/29/11	1.269	-82.3	-10.96	25.14	6.60	15.87
5/30/11	0.508	-82.3	-10.96	25.14	6.60	15.87
5/31/11	1.523	-82.3	-10.96	25.14	6.60	15.87
6/1/11	0.508	-94.04	-12.08	24.92	6.95	15.93
6/2/11	1.015	-94.04	-12.08	24.92	6.95	15.93
6/3/11	1.015	-94.04	-12.08	24.92	6.95	15.93
6/4/11	2.031	-94.04	-12.08	24.92	6.95	15.93
6/5/11	2.284	-94.04	-12.08	24.92	6.95	15.93
6/6/11	1.015	-94.04	-12.08	24.92	6.95	15.93
6/7/11	0.254	-94.04	-12.08	24.92	6.95	15.93

6/8/11	2.538					
6/9/11	0.254					
6/10/11	0.508					
6/11/11	0.508					
6/12/11	0.254					
6/13/11	0.254					
6/14/11	1.269					
6/15/11	1.015					
6/16/11	0					
6/17/11	0.508					
6/18/11	0.254					
6/19/11	0.508					
6/20/11	2.031					
6/21/11	0.254	-114.91	-14.53	30.48	8.77	19.63
6/22/11	0.254	-114.91	-14.53	30.48	8.77	19.63
6/23/11	0	-114.91	-14.53	30.48	8.77	19.63
6/24/11	1.523	-114.91	-14.53	30.48	8.77	19.63
6/25/11	1.015	-114.91	-14.53	30.48	8.77	19.63
6/26/11	0.508	-114.91	-14.53	30.48	8.77	19.63
6/27/11	0.761	-114.91	-14.53	30.48	8.77	19.63
6/28/11	0.254	-114.91	-14.53	30.48	8.77	19.63
6/29/11	1.777					
6/30/11	0.761					
7/1/11	0.761					
7/2/11	0.508					
7/3/11	0.254					
7/4/11	0.254					
7/5/11	0					
7/6/11	0.254					
7/7/11	0					
7/8/11	0					
7/9/11	1.015					
7/10/11	0.254					
7/11/11	0.254					
7/12/11	0.254	-76.78	-9.46	33.34	11.19	22.26
7/13/11	0.254	-76.78	-9.46	33.34	11.19	22.26
7/14/11	0.254	-76.78	-9.46	33.34	11.19	22.26
7/15/11	0.508	-76.78	-9.46	33.34	11.19	22.26
7/16/11	0.508	-76.78	-9.46	33.34	11.19	22.26
7/17/11	0.508	-76.78	-9.46	33.34	11.19	22.26
7/18/11	1.523	-76.78	-9.46	33.34	11.19	22.26
7/19/11	1.269	-76.78	-9.46	33.34	11.19	22.26
7/20/11	0.254					
7/21/11	0.254					
7/22/11	0.508					
7/23/11	0.254					
7/24/11	0.254					
7/25/11	0.254					
7/26/11	0.254	-67.59	-9.12	34.46	11.67	23.06
7/27/11	1.269	-67.59	-9.12	34.46	11.67	23.06
7/28/11	0.254	-67.59	-9.12	34.46	11.67	23.06
7/29/11	0.761	-67.59	-9.12	34.46	11.67	23.06
7/30/11	1.269	-67.59	-9.12	34.46	11.67	23.06
7/31/11	0.761	-67.59	-9.12	34.46	11.67	23.06
8/1/11	0.254	-67.59	-9.12	34.46	11.67	23.06
8/2/11	0.254	-67.59	-9.12	34.46	11.67	23.06
8/3/11	0.254					

8/4/11	0.254					
8/5/11	0.254					
8/6/11	0					
8/7/11	0.508					
8/8/11	0.508					
8/9/11	0.508					
8/10/11	0.254					
8/11/11	0					
8/12/11	0.254					
8/13/11	0					
8/14/11	0.254					
8/15/11	0.508					
8/16/11	0.254					
8/17/11	0					
8/18/11	0					
8/19/11	0.254					
8/20/11	1.015					
8/21/11	0.508					
8/22/11	0.254					
8/23/11	0.761					
8/24/11	0.761					
8/25/11	0					
8/26/11	0					
8/27/11	0					
8/28/11	0					
8/29/11	0.254					
8/30/11	0.508					
8/31/11	0.508					
9/1/11	0					
9/2/11	0					
9/3/11	0					
9/4/11	0					
9/5/11	0					
9/6/11	0					
9/7/11	2.538					
9/8/11	0.254					
9/9/11	1.269					
9/10/11	0.254					
9/11/11	0.254					
9/12/11	0.254					
9/13/11	0					
9/14/11	0.761					
9/15/11	0.761					
9/16/11	0					
9/17/11	1.269					
9/18/11	1.269					
9/19/11	0.761					
9/20/11	0.508					
9/21/11	0					
9/22/11	0					
9/23/11	0.508					
9/24/11	0.254					
9/25/11	1.269					
9/26/11	0.254					
9/27/11	0.761	-94.91	-11.74	26.12	4.78	15.45
9/28/11	0.254	-94.91	-11.74	26.12	4.78	15.45
9/29/11	0.254	-94.91	-11.74	26.12	4.78	15.45

9/30/11	0	-94.91	-11.74	26.12	4.78	15.45
10/1/11	0.254	-94.91	-11.74	26.12	4.78	15.45
10/2/11	0.761	-94.91	-11.74	26.12	4.78	15.45
10/3/11	0	-94.91	-11.74	26.12	4.78	15.45
10/4/11	0.508	-94.91	-11.74	26.12	4.78	15.45
10/5/11	0.254	-115.4	-14.9	23.17	3.01	13.09
10/6/11	0.508	-115.4	-14.9	23.17	3.01	13.09
10/7/11	1.269	-115.4	-14.9	23.17	3.01	13.09
10/8/11	0.254	-115.4	-14.9	23.17	3.01	13.09
10/9/11	0.761	-115.4	-14.9	23.17	3.01	13.09
10/10/11	0.761	-115.4	-14.9	23.17	3.01	13.09
10/11/11	0.761	-115.4	-14.9	23.17	3.01	13.09
10/12/11	0.254					
10/13/11	0.254					
10/14/11	0.254					
10/15/11	0.254					
10/16/11	0.254					
10/17/11	0.761					
10/18/11	1.269					
10/19/11	1.777					
10/20/11	1.015					
10/21/11	1.777					
10/22/11	0.254					
10/23/11	3.046					
10/24/11	2.284					
10/25/11	1.269					
10/26/11	1.269					
10/27/11	0.761					
10/28/11	2.538					
10/29/11	1.523					
10/30/11	1.777					
10/31/11	0.761					
11/1/11	0.761	-133.35	-17.39	14.84	-0.50	7.17
11/2/11	2.284	-133.35	-17.39	14.84	-0.50	7.17
11/3/11	3.046	-133.35	-17.39	14.84	-0.50	7.17
11/4/11	1.015	-133.35	-17.39	14.84	-0.50	7.17
11/5/11	1.015	-133.35	-17.39	14.84	-0.50	7.17
11/6/11	2.031	-133.35	-17.39	14.84	-0.50	7.17
11/7/11	2.792	-133.35	-17.39	14.84	-0.50	7.17
11/8/11	2.538	-133.35	-17.39	14.84	-0.50	7.17
11/9/11	2.031					
11/10/11	2.538					
11/11/11	1.269					
11/12/11	2.284					
11/13/11	2.284					
11/14/11	2.792					
11/15/11	1.015					
11/16/11	2.792					
11/17/11	4.315					
11/18/11	3.3					
11/19/11	2.792					
11/20/11	2.284					
11/21/11	3.553					
11/22/11	4.822	-71.65	-9.14	8.40	-3.10	2.65
11/23/11	3.807	-71.65	-9.14	8.40	-3.10	2.65
11/24/11	3.553	-71.65	-9.14	8.40	-3.10	2.65
11/25/11	2.538	-71.65	-9.14	8.40	-3.10	2.65

11/26/11	1.523	-71.65	-9.14	8.40	-3.10	2.65
11/27/11	1.777	-71.65	-9.14	8.40	-3.10	2.65
11/28/11	2.792	-71.65	-9.14	8.40	-3.10	2.65
11/29/11	3.046	-71.65	-9.14	8.40	-3.10	2.65
11/30/11	2.031					
12/1/11	3.553					
12/2/11	3.807					
12/3/11	2.792					
12/4/11	2.792					
12/5/11	2.284					
12/6/11	3.3					
12/7/11	4.061					
12/8/11	5.076					
12/9/11	3.553					
12/10/11	2.792					
12/11/11	2.538					
12/12/11	3.807					
12/13/11	3.553					
12/14/11	4.822					
12/15/11	4.569					
12/16/11	3.046					
12/17/11	3.807					
12/18/11	1.523					
12/19/11	3.553					
12/20/11	4.315					
12/21/11	3.3					
12/22/11	1.777					
12/23/11	1.523					
12/24/11	1.523					
12/25/11	0.761					
12/26/11	1.523					
12/27/11	3.553					
12/28/11	4.569	-67.64	-8.97	6.54	-4.28	1.13
12/29/11	2.792	-67.64	-8.97	6.54	-4.28	1.13
12/30/11	4.061	-67.64	-8.97	6.54	-4.28	1.13
12/31/11	6.853	-67.64	-8.97	6.54	-4.28	1.13
1/1/12	5.838	-67.64	-8.97	6.54	-4.28	1.13
1/2/12	3.3	-67.64	-8.97	6.54	-4.28	1.13
1/3/12	2.031	-67.64	-8.97	6.54	-4.28	1.13
1/4/12	2.538	-67.64	-8.97	6.54	-4.28	1.13
1/5/12	1.523					
1/6/12	1.523					
1/7/12	2.792					
1/8/12	3.807					
1/9/12	2.538					
1/10/12	2.538					
1/11/12	3.046					
1/12/12	1.269					
1/13/12	2.031					
1/14/12	2.792					
1/15/12	3.046					
1/16/12	4.061					
1/17/12	4.061					
1/18/12	2.792	-109.67	-14.28	6.51	-4.33	1.09
1/19/12	2.538	-109.67	-14.28	6.51	-4.33	1.09
1/20/12	2.031	-109.67	-14.28	6.51	-4.33	1.09
1/21/12	3.3	-109.67	-14.28	6.51	-4.33	1.09

1/22/12	2.031	-109.67	-14.28	6.51	-4.33	1.09
1/23/12	2.538	-109.67	-14.28	6.51	-4.33	1.09
1/24/12	2.792	-109.67	-14.28	6.51	-4.33	1.09
1/25/12	1.777	-48.84	-6.74	8.87	-3.74	2.56
1/26/12	2.031	-48.84	-6.74	8.87	-3.74	2.56
1/27/12	3.046	-48.84	-6.74	8.87	-3.74	2.56
1/28/12	2.031	-48.84	-6.74	8.87	-3.74	2.56
1/29/12	0.508	-48.84	-6.74	8.87	-3.74	2.56
1/30/12	1.777	-48.84	-6.74	8.87	-3.74	2.56
1/31/12	1.523	-48.84	-6.74	8.87	-3.74	2.56
2/1/12	2.792	-101.12	-13.02	9.50	-4.11	2.69
2/2/12	2.031	-101.12	-13.02	9.50	-4.11	2.69
2/3/12	2.284	-101.12	-13.02	9.50	-4.11	2.69
2/4/12	0.761	-101.12	-13.02	9.50	-4.11	2.69
2/5/12	0.761	-101.12	-13.02	9.50	-4.11	2.69
2/6/12	0.254	-101.12	-13.02	9.50	-4.11	2.69
2/7/12	2.538	-168.98	-22.36	10.40	-3.40	3.50
2/8/12	2.538	-168.98	-22.36	10.40	-3.40	3.50
2/9/12	2.031	-168.98	-22.36	10.40	-3.40	3.50
2/10/12	1.523	-168.98	-22.36	10.40	-3.40	3.50
2/11/12	2.031	-168.98	-22.36	10.40	-3.40	3.50
2/12/12	1.269	-168.98	-22.36	10.40	-3.40	3.50
2/13/12	1.523	-168.98	-22.36	10.40	-3.40	3.50
2/14/12	4.061	-168.98	-22.36	10.40	-3.40	3.50
2/15/12	2.031					
2/16/12	2.284					
2/17/12	2.538					
2/18/12	1.523					
2/19/12	1.777					
2/20/12	1.523					
2/21/12	4.061					
2/22/12	1.269					
2/23/12	2.538					
2/24/12	1.015					
2/25/12	1.269					
2/26/12	1.015					
2/27/12	1.269					
2/28/12	1.777	-97.59	-13.36	12.46	-1.61	5.42
2/29/12	1.777	-97.59	-13.36	12.46	-1.61	5.42
3/1/12	1.523	-97.59	-13.36	12.46	-1.61	5.42
3/2/12	3.3	-97.59	-13.36	12.46	-1.61	5.42
3/3/12	3.046	-97.59	-13.36	12.46	-1.61	5.42
3/4/12	1.015	-97.59	-13.36	12.46	-1.61	5.42
3/5/12	2.031	-97.59	-13.36	12.46	-1.61	5.42
3/6/12	0.508	-116.79	-15.45	14.10	-1.44	6.33
3/7/12	0.761	-116.79	-15.45	14.10	-1.44	6.33
3/8/12	1.269	-116.79	-15.45	14.10	-1.44	6.33
3/9/12	1.015	-116.79	-15.45	14.10	-1.44	6.33
3/10/12	1.269	-116.79	-15.45	14.10	-1.44	6.33
3/11/12	1.015	-116.79	-15.45	14.10	-1.44	6.33
3/12/12	0.761	-116.79	-15.45	14.10	-1.44	6.33
3/13/12	2.284	-116.79	-15.45	14.10	-1.44	6.33
3/14/12	2.031	-78.92	-10.22	14.91	-1.11	6.90
3/15/12	1.015	-78.92	-10.22	14.91	-1.11	6.90
3/16/12	1.269	-78.92	-10.22	14.91	-1.11	6.90
3/17/12	1.523	-78.92	-10.22	14.91	-1.11	6.90
3/18/12	0.761	-78.92	-10.22	14.91	-1.11	6.90

3/19/12	0.254	-78.92	-10.22	14.91	-1.11	6.90
3/20/12	1.015	-78.92	-10.22	14.91	-1.11	6.90
3/21/12	0.254	-75.96	-9.38	15.40	-0.74	7.33
3/22/12	1.269	-75.96	-9.38	15.40	-0.74	7.33
3/23/12	1.777	-75.96	-9.38	15.40	-0.74	7.33
3/24/12	1.269	-75.96	-9.38	15.40	-0.74	7.33
3/25/12	1.269	-75.96	-9.38	15.40	-0.74	7.33
3/26/12	1.269	-75.96	-9.38	15.40	-0.74	7.33
3/27/12	1.523	-78.75	-10.07	15.89	-0.96	7.46
3/28/12	1.523	-78.75	-10.07	15.89	-0.96	7.46
3/29/12	0.254	-78.75	-10.07	15.89	-0.96	7.46
3/30/12	1.523	-78.75	-10.07	15.89	-0.96	7.46
3/31/12	2.031	-78.75	-10.07	15.89	-0.96	7.46
4/1/12	1.015	-78.75	-10.07	15.89	-0.96	7.46
4/2/12	0.254	-78.75	-10.07	15.89	-0.96	7.46
4/3/12	1.015	-76.77	-10.8	16.59	0.17	8.38
4/4/12	1.269	-76.77	-10.8	16.59	0.17	8.38
4/5/12	0.508	-76.77	-10.8	16.59	0.17	8.38
4/6/12	0.761	-76.77	-10.8	16.59	0.17	8.38
4/7/12	1.523	-76.77	-10.8	16.59	0.17	8.38
4/8/12	1.523	-76.77	-10.8	16.59	0.17	8.38
4/9/12	1.269	-76.77	-10.8	16.59	0.17	8.38
4/10/12	1.015	-106.94	-14.03	17.39	0.57	8.98
4/11/12	0.508	-106.94	-14.03	17.39	0.57	8.98
4/12/12	0.254	-106.94	-14.03	17.39	0.57	8.98
4/13/12	1.777	-106.94	-14.03	17.39	0.57	8.98
4/14/12	1.777	-106.94	-14.03	17.39	0.57	8.98
4/15/12	0.761	-106.94	-14.03	17.39	0.57	8.98
4/16/12	1.269	-106.94	-14.03	17.39	0.57	8.98
4/17/12	1.015	-106.94	-14.03	17.39	0.57	8.98
4/18/12	1.777					
4/19/12	1.269					
4/20/12	1.777					
4/21/12	1.269					
4/22/12	0.508					
4/23/12	1.015					
4/24/12	1.523	-51.59	-5.73	19.84	2.16	11.00
4/25/12	0.508	-51.59	-5.73	19.84	2.16	11.00
4/26/12	0.761	-51.59	-5.73	19.84	2.16	11.00
4/27/12	1.269	-51.59	-5.73	19.84	2.16	11.00
4/28/12	1.015	-51.59	-5.73	19.84	2.16	11.00
4/29/12	1.015	-51.59	-5.73	19.84	2.16	11.00
4/30/12	1.523	-51.59	-5.73	19.84	2.16	11.00
5/1/12	1.523	-51.59	-5.73	19.84	2.16	11.00
5/2/12	0.761					
5/3/12	2.792					
5/4/12	0.761					
5/5/12	2.792					
5/6/12	0.761					
5/7/12	0.761					
5/8/12	0.508					
5/9/12	2.031					
5/10/12	1.015					
5/11/12	0.254					
5/12/12	0.254					
5/13/12	0.508					
5/14/12	0.761					

5/15/12	0.508					
5/16/12	0.508					
5/17/12	1.777					
5/18/12	1.523					
5/19/12	1.015					
5/20/12	1.777					
5/21/12	1.015					
5/22/12	1.015	-123.14	-15.49	24.76	6.11	15.44
5/23/12	1.015	-123.14	-15.49	24.76	6.11	15.44
5/24/12	0.254	-123.14	-15.49	24.76	6.11	15.44
5/25/12	0.508	-123.14	-15.49	24.76	6.11	15.44
5/26/12	0.508	-123.14	-15.49	24.76	6.11	15.44
5/27/12	0.761	-123.14	-15.49	24.76	6.11	15.44
5/28/12	2.792	-123.14	-15.49	24.76	6.11	15.44
5/29/12	1.269	-68.96	-9.16	25.75	6.87	16.31
5/30/12	0.508	-68.96	-9.16	25.75	6.87	16.31
5/31/12	1.523	-68.96	-9.16	25.75	6.87	16.31
6/1/12	0.508	-68.96	-9.16	25.75	6.87	16.31
6/2/12	1.015	-68.96	-9.16	25.75	6.87	16.31
6/3/12	1.015	-68.96	-9.16	25.75	6.87	16.31
6/4/12	2.031	-68.96	-9.16	25.75	6.87	16.31
6/5/12	2.284					
6/6/12	1.015					
6/7/12	0.254					
6/8/12	2.538					
6/9/12	0.254					
6/10/12	0.508					
6/11/12	0.508					
6/12/12	0.254					
6/13/12	0.254					
6/14/12	1.269					
6/15/12	1.015					
6/16/12	0	-79.1	-9.13	30.02	8.32	19.17
6/17/12	0.508	-79.1	-9.13	30.02	8.32	19.17
6/18/12	0.254	-79.1	-9.13	30.02	8.32	19.17
6/19/12	0.508	-79.1	-9.13	30.02	8.32	19.17
6/20/12	2.031	-79.1	-9.13	30.02	8.32	19.17
6/21/12	0.254	-79.1	-9.13	30.02	8.32	19.17
6/22/12	0.254	-79.1	-9.13	30.02	8.32	19.17
6/23/12	0	-79.1	-9.13	30.02	8.32	19.17
6/24/12	1.523	-79.1	-9.13	30.02	8.32	19.17
6/25/12	1.015	-79.1	-9.13	30.02	8.32	19.17
6/26/12	0.508	-78.34	-10.08	30.57	9.62	20.09
6/27/12	0.761	-78.34	-10.08	30.57	9.62	20.09
6/28/12	0.254	-78.34	-10.08	30.57	9.62	20.09
6/29/12	1.777	-78.34	-10.08	30.57	9.62	20.09
6/30/12	0.761	-78.34	-10.08	30.57	9.62	20.09
7/1/12	0.761	-78.34	-10.08	30.57	9.62	20.09
7/2/12	0.508	-78.34	-10.08	30.57	9.62	20.09
7/3/12	0.254					
7/4/12	0.254					
7/5/12	0					
7/6/12	0.254					
7/7/12	0					
7/8/12	0					
7/9/12	1.015					
7/10/12	0.254	-39.25	-4.47	33.57	10.80	22.19

7/11/12	0.254	-39.25	-4.47	33.57	10.80	22.19
7/12/12	0.254	-39.25	-4.47	33.57	10.80	22.19
7/13/12	0.254	-39.25	-4.47	33.57	10.80	22.19
7/14/12	0.254	-39.25	-4.47	33.57	10.80	22.19
7/15/12	0.508	-39.25	-4.47	33.57	10.80	22.19
7/16/12	0.508	-39.25	-4.47	33.57	10.80	22.19
7/17/12	0.508	-39.25	-4.47	33.57	10.80	22.19
7/18/12	1.523					
7/19/12	1.269					
7/20/12	0.254					
7/21/12	0.254					
7/22/12	0.508					
7/23/12	0.254					
7/24/12	0.254					
7/25/12	0.254					
7/26/12	0.254					
7/27/12	1.269					
7/28/12	0.254					
7/29/12	0.761					
7/30/12	1.269					
7/31/12	0.761					
8/1/12	0.254					
8/2/12	0.254					
8/3/12	0.254					
8/4/12	0.254					
8/5/12	0.254					
8/6/12	0					
8/7/12	0.508					
8/8/12	0.508					
8/9/12	0.508					
8/10/12	0.254					
8/11/12	0					
8/12/12	0.254					
8/13/12	0					
8/14/12	0.254					
8/15/12	0.508					
8/16/12	0.254					
8/17/12	0					
8/18/12	0					
8/19/12	0.254					
8/20/12	1.015					
8/21/12	0.508					
8/22/12	0.254					
8/23/12	0.761					
8/24/12	0.761					
8/25/12	0					
8/26/12	0					
8/27/12	0					
8/28/12	0					
8/29/12	0.254					
8/30/12	0.508					
8/31/12	0.508					
9/1/12	0					
9/2/12	0					
9/3/12	0					
9/4/12	0					
9/5/12	0					

9/6/12	0					
9/7/12	2.538					
9/8/12	0.254					
9/9/12	1.269					
9/10/12	0.254					
9/11/12	0.254					
9/12/12	0.254					
9/13/12	0					
9/14/12	0.761					
9/15/12	0.761					
9/16/12	0					
9/17/12	1.269					
9/18/12	1.269					
9/19/12	0.761					
9/20/12	0.508					
9/21/12	0					
9/22/12	0					
9/23/12	0.508					
9/24/12	0.254					
9/25/12	1.269					
9/26/12	0.254					
9/27/12	0.761					
9/28/12	0.254					
9/29/12	0.254					
9/30/12	0					
10/1/12	0.254					
10/2/12	0.761					
10/3/12	0					
10/4/12	0.508					
10/5/12	0.254					
10/6/12	0.508					
10/7/12	1.269					
10/8/12	0.254					
10/9/12	0.761					
10/10/12	0.761					
10/11/12	0.761					
10/12/12	0.254					
10/13/12	0.254					
10/14/12	0.254					
10/15/12	0.254					
10/16/12	0.254	-95.73	-13.8	20.57	1.20	10.89
10/17/12	0.761	-95.73	-13.8	20.57	1.20	10.89
10/18/12	1.269	-95.73	-13.8	20.57	1.20	10.89
10/19/12	1.777	-95.73	-13.8	20.57	1.20	10.89
10/20/12	1.015	-95.73	-13.8	20.57	1.20	10.89
10/21/12	1.777	-95.73	-13.8	20.57	1.20	10.89
10/22/12	0.254	-95.73	-13.8	20.57	1.20	10.89
10/23/12	3.046	-95.73	-13.8	20.57	1.20	10.89
10/24/12	2.284	-78.32	-11.89	18.01	0.74	9.38
10/25/12	1.269	-78.32	-11.89	18.01	0.74	9.38
10/26/12	1.269	-78.32	-11.89	18.01	0.74	9.38
10/27/12	0.761	-78.32	-11.89	18.01	0.74	9.38
10/28/12	2.538	-78.32	-11.89	18.01	0.74	9.38
10/29/12	1.523	-78.32	-11.89	18.01	0.74	9.38
10/30/12	1.777	-78.32	-11.89	18.01	0.74	9.38
10/31/12	0.761	-79.08	-10.25	15.34	-0.33	7.51
11/1/12	0.761	-79.08	-10.25	15.34	-0.33	7.51

11/2/12	2.284	-79.08	-10.25	15.34	-0.33	7.51
11/3/12	3.046	-79.08	-10.25	15.34	-0.33	7.51
11/4/12	1.015	-79.08	-10.25	15.34	-0.33	7.51
11/5/12	1.015	-79.08	-10.25	15.34	-0.33	7.51
11/6/12	2.031	-79.08	-10.25	15.34	-0.33	7.51
11/7/12	2.792	-83.57	-11.79	12.54	-0.81	5.86
11/8/12	2.538	-83.57	-11.79	12.54	-0.81	5.86
11/9/12	2.031	-83.57	-11.79	12.54	-0.81	5.86
11/10/12	2.538	-83.57	-11.79	12.54	-0.81	5.86
11/11/12	1.269	-83.57	-11.79	12.54	-0.81	5.86
11/12/12	2.284	-83.57	-11.79	12.54	-0.81	5.86
11/13/12	2.284	-83.57	-11.79	12.54	-0.81	5.86
11/14/12	2.792	-78.77	-10.34	11.29	-1.83	4.73
11/15/12	1.015	-78.77	-10.34	11.29	-1.83	4.73
11/16/12	2.792	-78.77	-10.34	11.29	-1.83	4.73
11/17/12	4.315	-78.77	-10.34	11.29	-1.83	4.73
11/18/12	3.3	-78.77	-10.34	11.29	-1.83	4.73
11/19/12	2.792	-78.77	-10.34	11.29	-1.83	4.73
11/20/12	2.284	-78.77	-10.34	11.29	-1.83	4.73
11/21/12	3.553	-24.33	-4.01	8.89	-2.77	3.06
11/22/12	4.822	-24.33	-4.01	8.89	-2.77	3.06
11/23/12	3.807	-24.33	-4.01	8.89	-2.77	3.06
11/24/12	3.553	-24.33	-4.01	8.89	-2.77	3.06
11/25/12	2.538	-24.33	-4.01	8.89	-2.77	3.06
11/26/12	1.523	-24.33	-4.01	8.89	-2.77	3.06
11/27/12	1.777	-24.33	-4.01	8.89	-2.77	3.06
11/28/12	2.792	-100.04	-13.09	8.23	-3.33	2.45
11/29/12	3.046	-100.04	-13.09	8.23	-3.33	2.45
11/30/12	2.031	-100.04	-13.09	8.23	-3.33	2.45
12/1/12	3.553	-100.04	-13.09	8.23	-3.33	2.45
12/2/12	3.807	-100.04	-13.09	8.23	-3.33	2.45
12/3/12	2.792	-100.04	-13.09	8.23	-3.33	2.45
12/4/12	2.792	-100.04	-13.09	8.23	-3.33	2.45
12/5/12	2.284	-103.58	-13.37	8.63	-3.01	2.81
12/6/12	3.3	-103.58	-13.37	8.63	-3.01	2.81
12/7/12	4.061	-103.58	-13.37	8.63	-3.01	2.81
12/8/12	5.076	-103.58	-13.37	8.63	-3.01	2.81
12/9/12	3.553	-103.58	-13.37	8.63	-3.01	2.81
12/10/12	2.792	-103.58	-13.37	8.63	-3.01	2.81
12/11/12	2.538	-103.58	-13.37	8.63	-3.01	2.81
12/12/12	3.807	-77.33	-9.93	7.07	-3.79	1.64
12/13/12	3.553	-77.33	-9.93	7.07	-3.79	1.64
12/14/12	4.822	-77.33	-9.93	7.07	-3.79	1.64
12/15/12	4.569	-77.33	-9.93	7.07	-3.79	1.64
12/16/12	3.046	-77.33	-9.93	7.07	-3.79	1.64
12/17/12	3.807	-77.33	-9.93	7.07	-3.79	1.64
12/18/12	1.523	-77.33	-9.93	7.07	-3.79	1.64
12/19/12	3.553	-99.24	-14.61	5.96	-5.40	0.28
12/20/12	4.315	-99.24	-14.61	5.96	-5.40	0.28
12/21/12	3.3	-99.24	-14.61	5.96	-5.40	0.28
12/22/12	1.777	-99.24	-14.61	5.96	-5.40	0.28
12/23/12	1.523	-99.24	-14.61	5.96	-5.40	0.28
12/24/12	1.523	-99.24	-14.61	5.96	-5.40	0.28
12/25/12	0.761	-99.24	-14.61	5.96	-5.40	0.28
12/26/12	1.523	-151.02	-19.59	6.39	-4.85	0.77
12/27/12	3.553	-151.02	-19.59	6.39	-4.85	0.77
12/28/12	4.569	-151.02	-19.59	6.39	-4.85	0.77

12/29/12	2.792	-151.02	-19.59	6.39	-4.85	0.77
12/30/12	4.061	-151.02	-19.59	6.39	-4.85	0.77
12/31/12	6.853	-151.02	-19.59	6.39	-4.85	0.77
1/1/13	5.838	-151.02	-19.59	6.39	-4.85	0.77
1/2/13	3.3	-151.02	-19.59	6.39	-4.85	0.77
1/3/13	2.031	-114.63	-15.99	6.97	-4.23	1.37
1/4/13	2.538	-114.63	-15.99	6.97	-4.23	1.37
1/5/13	1.523	-114.63	-15.99	6.97	-4.23	1.37
1/6/13	1.523	-114.63	-15.99	6.97	-4.23	1.37
1/7/13	2.792	-114.63	-15.99	6.97	-4.23	1.37
1/8/13	3.807	-114.63	-15.99	6.97	-4.23	1.37
1/9/13	2.538	-77.16	-10.94	7.69	-3.70	1.99
1/10/13	2.538	-77.16	-10.94	7.69	-3.70	1.99
1/11/13	3.046	-77.16	-10.94	7.69	-3.70	1.99
1/12/13	1.269	-77.16	-10.94	7.69	-3.70	1.99
1/13/13	2.031	-77.16	-10.94	7.69	-3.70	1.99
1/14/13	2.792	-77.16	-10.94	7.69	-3.70	1.99
1/15/13	3.046	-77.16	-10.94	7.69	-3.70	1.99
1/16/13	4.061					
1/17/13	4.061					
1/18/13	2.792					
1/19/13	2.538					
1/20/13	2.031					
1/21/13	3.3					
1/22/13	2.031	-126.99	-16.42	8.49	-3.74	2.37
1/23/13	2.538	-126.99	-16.42	8.49	-3.74	2.37
1/24/13	2.792	-126.99	-16.42	8.49	-3.74	2.37
1/25/13	1.777	-126.99	-16.42	8.49	-3.74	2.37
1/26/13	2.031	-126.99	-16.42	8.49	-3.74	2.37
1/27/13	3.046	-126.99	-16.42	8.49	-3.74	2.37
1/28/13	2.031	-126.99	-16.42	8.49	-3.74	2.37
1/29/13	0.508	-126.99	-16.42	8.49	-3.74	2.37
1/30/13	1.777					
1/31/13	1.523					
2/1/13	2.792					
2/2/13	2.031					
2/3/13	2.284					
2/4/13	0.761					
2/5/13	0.761	-94.19	-13.13	10.07	-3.80	3.14
2/6/13	0.254	-94.19	-13.13	10.07	-3.80	3.14
2/7/13	2.538	-94.19	-13.13	10.07	-3.80	3.14
2/8/13	2.538	-94.19	-13.13	10.07	-3.80	3.14
2/9/13	2.031	-94.19	-13.13	10.07	-3.80	3.14
2/10/13	1.523	-94.19	-13.13	10.07	-3.80	3.14
2/11/13	2.031	-94.19	-13.13	10.07	-3.80	3.14
2/12/13	1.269	-94.19	-13.13	10.07	-3.80	3.14
2/13/13	1.523					
2/14/13	4.061					
2/15/13	2.031					
2/16/13	2.284					
2/17/13	2.538					
2/18/13	1.523					
2/19/13	1.777					
2/20/13	1.523					
2/21/13	4.061					
2/22/13	1.269					
2/23/13	2.538					

2/24/13	1.015					
2/25/13	1.269					
2/26/13	1.015					
2/27/13	1.269					
2/28/13	1.777					
3/1/13	1.523					
3/2/13	3.3					
3/3/13	3.046					
3/4/13	1.015					
3/5/13	2.031					
3/6/13	0.508					
3/7/13	0.761					
3/8/13	1.269					
3/9/13	1.015					
3/10/13	1.269					
3/11/13	1.015					
3/12/13	0.761					
3/13/13	2.284					
3/14/13	2.031					
3/15/13	1.015					
3/16/13	1.269					
3/17/13	1.523					
3/18/13	0.761					
3/19/13	0.254	-62.23	-7.97	15.64	-0.74	7.45
3/20/13	1.015	-62.23	-7.97	15.64	-0.74	7.45
3/21/13	0.254	-62.23	-7.97	15.64	-0.74	7.45
3/22/13	1.269	-62.23	-7.97	15.64	-0.74	7.45
3/23/13	1.777	-62.23	-7.97	15.64	-0.74	7.45
3/24/13	1.269	-62.23	-7.97	15.64	-0.74	7.45
3/25/13	1.269	-62.23	-7.97	15.64	-0.74	7.45
3/26/13	1.269	-62.23	-7.97	15.64	-0.74	7.45
3/27/13	1.523	-129.61	-17.03	15.73	-1.11	7.31
3/28/13	1.523	-129.61	-17.03	15.73	-1.11	7.31
3/29/13	0.254	-129.61	-17.03	15.73	-1.11	7.31
3/30/13	1.523	-129.61	-17.03	15.73	-1.11	7.31
3/31/13	2.031	-129.61	-17.03	15.73	-1.11	7.31
4/1/13	1.015	-129.61	-17.03	15.73	-1.11	7.31
4/2/13	0.254	-129.61	-17.03	15.73	-1.11	7.31
4/3/13	1.015	-68.05	-7.49	16.59	0.17	8.38
4/4/13	1.269	-68.05	-7.49	16.59	0.17	8.38
4/5/13	0.508	-68.05	-7.49	16.59	0.17	8.38
4/6/13	0.761	-68.05	-7.49	16.59	0.17	8.38
4/7/13	1.523	-68.05	-7.49	16.59	0.17	8.38
4/8/13	1.523	-68.05	-7.49	16.59	0.17	8.38
4/9/13	1.269					
4/10/13	1.015					
4/11/13	0.508					
4/12/13	0.254					
4/13/13	1.777					
4/14/13	1.777					
4/15/13	0.761					
4/16/13	1.269					
4/17/13	1.015					
4/18/13	1.777					
4/19/13	1.269					
4/20/13	1.777					
4/21/13	1.269					

4/22/13	0.508					
4/23/13	1.015					
4/24/13	1.523					
4/25/13	0.508					
4/26/13	0.761					
4/27/13	1.269					
4/28/13	1.015					
4/29/13	1.015					
4/30/13	1.523	-54.99	-7.23	20.74	2.70	11.72
5/1/13	1.523	-54.99	-7.23	20.74	2.70	11.72
5/2/13	0.761	-54.99	-7.23	20.74	2.70	11.72
5/3/13	2.792	-54.99	-7.23	20.74	2.70	11.72
5/4/13	0.761	-54.99	-7.23	20.74	2.70	11.72
5/5/13	2.792	-54.99	-7.23	20.74	2.70	11.72
5/6/13	0.761	-54.99	-7.23	20.74	2.70	11.72
5/7/13	0.761	-54.99	-7.23	20.74	2.70	11.72
5/8/13	0.508	-60.96	-7.83	22.00	3.10	12.55
5/9/13	2.031	-60.96	-7.83	22.00	3.10	12.55
5/10/13	1.015	-60.96	-7.83	22.00	3.10	12.55
5/11/13	0.254	-60.96	-7.83	22.00	3.10	12.55
5/12/13	0.254	-60.96	-7.83	22.00	3.10	12.55
5/13/13	0.508	-60.96	-7.83	22.00	3.10	12.55
5/14/13	0.761	-60.96	-7.83	22.00	3.10	12.55
5/15/13	0.508					
5/16/13	0.508					
5/17/13	1.777					
5/18/13	1.523					
5/19/13	1.015					
5/20/13	1.777					
5/21/13	1.015	-74.34	-7.62	24.60	5.79	15.19
5/22/13	1.015	-74.34	-7.62	24.60	5.79	15.19
5/23/13	1.015	-74.34	-7.62	24.60	5.79	15.19
5/24/13	0.254	-74.34	-7.62	24.60	5.79	15.19
5/25/13	0.508	-74.34	-7.62	24.60	5.79	15.19
5/26/13	0.508	-74.34	-7.62	24.60	5.79	15.19
5/27/13	0.761	-74.34	-7.62	24.60	5.79	15.19
5/28/13	2.792	-74.34	-7.62	24.60	5.79	15.19
5/29/13	1.269					
5/30/13	0.508					
5/31/13	1.523					
6/1/13	0.508					
6/2/13	1.015					
6/3/13	1.015					
6/4/13	2.031					
6/5/13	2.284					
6/6/13	1.015					
6/7/13	0.254					
6/8/13	2.538					
6/9/13	0.254					
6/10/13	0.508					
6/11/13	0.508					
6/12/13	0.254					
6/13/13	0.254					
6/14/13	1.269					
6/15/13	1.015					
6/16/13	0					
6/17/13	0.508					

6/18/13	0.254	-98.35	-11.87	29.63	8.05	18.84
6/19/13	0.508	-98.35	-11.87	29.63	8.05	18.84
6/20/13	2.031	-98.35	-11.87	29.63	8.05	18.84
6/21/13	0.254	-98.35	-11.87	29.63	8.05	18.84
6/22/13	0.254	-98.35	-11.87	29.63	8.05	18.84
6/23/13	0	-98.35	-11.87	29.63	8.05	18.84
6/24/13	1.523	-98.35	-11.87	29.63	8.05	18.84
6/25/13	1.015	-98.35	-11.87	29.63	8.05	18.84
6/26/13	0.508					
6/27/13	0.761					
6/28/13	0.254					
6/29/13	1.777					
6/30/13	0.761					
7/1/13	0.761					
7/2/13	0.508					
7/3/13	0.254					
7/4/13	0.254					
7/5/13	0					
7/6/13	0.254					
7/7/13	0					
7/8/13	0					
7/9/13	1.015					
7/10/13	0.254					
7/11/13	0.254					
7/12/13	0.254					
7/13/13	0.254					
7/14/13	0.254					
7/15/13	0.508					
7/16/13	0.508					
7/17/13	0.508					
7/18/13	1.523					
7/19/13	1.269					
7/20/13	0.254					
7/21/13	0.254					
7/22/13	0.508					
7/23/13	0.254					
7/24/13	0.254					
7/25/13	0.254					
7/26/13	0.254					
7/27/13	1.269					
7/28/13	0.254					
7/29/13	0.761					
7/30/13	1.269					
7/31/13	0.761					
8/1/13	0.254					
8/2/13	0.254					
8/3/13	0.254					
8/4/13	0.254					
8/5/13	0.254					
8/6/13	0	-64.3	-8.49	0.41	11.00	5.70
8/7/13	0.508	-64.3	-8.49	0.41	11.00	5.70
8/8/13	0.508	-64.3	-8.49	0.41	11.00	5.70
8/9/13	0.508	-64.3	-8.49	0.41	11.00	5.70
8/10/13	0.254	-64.3	-8.49	0.41	11.00	5.70
8/11/13	0	-64.3	-8.49	0.41	11.00	5.70
8/12/13	0.254	-64.3	-8.49	0.41	11.00	5.70
8/13/13	0	-64.3	-8.49	0.41	11.00	5.70

8/14/13	0.254					
8/15/13	0.508					
8/16/13	0.254					
8/17/13	0					
8/18/13	0					
8/19/13	0.254					
8/20/13	1.015	-59.64	-7.61	31.80	9.78	20.79
8/21/13	0.508	-59.64	-7.61	31.80	9.78	20.79
8/22/13	0.254	-59.64	-7.61	31.80	9.78	20.79
8/23/13	0.761	-59.64	-7.61	31.80	9.78	20.79
8/24/13	0.761	-59.64	-7.61	31.80	9.78	20.79
8/25/13	0	-59.64	-7.61	31.80	9.78	20.79
8/26/13	0	-59.64	-7.61	31.80	9.78	20.79
8/27/13	0	-59.64	-7.61	31.80	9.78	20.79
8/28/13	0					
8/29/13	0.254					
8/30/13	0.508					
8/31/13	0.508					
9/1/13	0					
9/2/13	0					
9/3/13	0					
9/4/13	0					
9/5/13	0					
9/6/13	0					
9/7/13	2.538					
9/8/13	0.254					
9/9/13	1.269					
9/10/13	0.254					
9/11/13	0.254					
9/12/13	0.254					
9/13/13	0					
9/14/13	0.761					
9/15/13	0.761					
9/16/13	0					
9/17/13	1.269	-58.66	-8.49	26.66	5.80	16.23
9/18/13	1.269	-58.66	-8.49	26.66	5.80	16.23
9/19/13	0.761	-58.66	-8.49	26.66	5.80	16.23
9/20/13	0.508	-58.66	-8.49	26.66	5.80	16.23
9/21/13	0	-58.66	-8.49	26.66	5.80	16.23
9/22/13	0	-58.66	-8.49	26.66	5.80	16.23
9/23/13	0.508	-58.66	-8.49	26.66	5.80	16.23
9/24/13	0.254	-51.38	-6.64	26.87	5.20	16.03
9/25/13	1.269	-51.38	-6.64	26.87	5.20	16.03
9/26/13	0.254	-51.38	-6.64	26.87	5.20	16.03
9/27/13	0.761	-51.38	-6.64	26.87	5.20	16.03
9/28/13	0.254	-51.38	-6.64	26.87	5.20	16.03
9/29/13	0.254	-51.38	-6.64	26.87	5.20	16.03
9/30/13	0	-51.38	-6.64	26.87	5.20	16.03
10/1/13	0.254	-51.38	-6.64	26.87	5.20	16.03
10/2/13	0.761					
10/3/13	0					
10/4/13	0.508					
10/5/13	0.254					
10/6/13	0.508					
10/7/13	1.269					
10/8/13	0.254					
10/9/13	0.761					

10/10/13	0.761					
10/11/13	0.761					
10/12/13	0.254					
10/13/13	0.254					
10/14/13	0.254					
10/15/13	0.254					
10/16/13	0.254					
10/17/13	0.761					
10/18/13	1.269					
10/19/13	1.777					
10/20/13	1.015					
10/21/13	1.777					
10/22/13	0.254					
10/23/13	3.046					
10/24/13	2.284					
10/25/13	1.269					
10/26/13	1.269					
10/27/13	0.761					
10/28/13	2.538					
10/29/13	1.523					
10/30/13	1.777					
10/31/13	0.761					
11/1/13	0.761					
11/2/13	2.284					
11/3/13	3.046					
11/4/13	1.015					
11/5/13	1.015					
11/6/13	2.031					
11/7/13	2.792					
11/8/13	2.538					
11/9/13	2.031					
11/10/13	2.538					
11/11/13	1.269					
11/12/13	2.284					
11/13/13	2.284					
11/14/13	2.792					
11/15/13	1.015					
11/16/13	2.792					
11/17/13	4.315					
11/18/13	3.3					
11/19/13	2.792	-88.82	-11.62	9.36	-2.54	3.41
11/20/13	2.284	-88.82	-11.62	9.36	-2.54	3.41
11/21/13	3.553	-88.82	-11.62	9.36	-2.54	3.41
11/22/13	4.822	-88.82	-11.62	9.36	-2.54	3.41
11/23/13	3.807	-88.82	-11.62	9.36	-2.54	3.41
11/24/13	3.553	-88.82	-11.62	9.36	-2.54	3.41
11/25/13	2.538	-88.82	-11.62	9.36	-2.54	3.41
11/26/13	1.523	-88.82	-11.62	9.36	-2.54	3.41
11/27/13	1.777					
11/28/13	2.792					
11/29/13	3.046					
11/30/13	2.031					
12/1/13	3.553					
12/2/13	3.807					
12/3/13	2.792	-110.3	-16.13	8.63	-3.01	2.81
12/4/13	2.792	-110.3	-16.13	8.63	-3.01	2.81
12/5/13	2.284	-110.3	-16.13	8.63	-3.01	2.81

12/6/13	3.3	-110.3	-16.13	8.63	-3.01	2.81
12/7/13	4.061	-110.3	-16.13	8.63	-3.01	2.81
12/8/13	5.076	-110.3	-16.13	8.63	-3.01	2.81
12/9/13	3.553	-110.3	-16.13	8.63	-3.01	2.81
12/10/13	2.792	-110.3	-16.13	8.63	-3.01	2.81
12/11/13	2.538					
12/12/13	3.807					
12/13/13	3.553					
12/14/13	4.822					
12/15/13	4.569					
12/16/13	3.046					
12/17/13	3.807					
12/18/13	1.523					
12/19/13	3.553					
12/20/13	4.315					
12/21/13	3.3					
12/22/13	1.777					
12/23/13	1.523					
12/24/13	1.523					
12/25/13	0.761					
12/26/13	1.523					
12/27/13	3.553					
12/28/13	4.569					
12/29/13	2.792					
12/30/13	4.061					
12/31/13	6.853					
1/1/14	5.838					
1/2/14	3.3					
1/3/14	2.031					
1/4/14	2.538					
1/5/14	1.523					
1/6/14	1.523					
1/7/14	2.792					
1/8/14	3.807					
1/9/14	2.538					
1/10/14	2.538					
1/11/14	3.046					
1/12/14	1.269					
1/13/14	2.031					
1/14/14	2.792					
1/15/14	3.046					
1/16/14	4.061					
1/17/14	4.061					
1/18/14	2.792					
1/19/14	2.538					
1/20/14	2.031					
1/21/14	3.3					
1/22/14	2.031					
1/23/14	2.538					
1/24/14	2.792					
1/25/14	1.777					
1/26/14	2.031					
1/27/14	3.046					
1/28/14	2.031					
1/29/14	0.508					
1/30/14	1.777					
1/31/14	1.523					

2/1/14	2.792					
2/2/14	2.031					
2/3/14	2.284					
2/4/14	0.761	-144.73	-18.14	9.83	-4.03	2.9
2/5/14	0.761	-144.73	-18.14	9.83	-4.03	2.9
2/6/14	0.254	-144.73	-18.14	9.83	-4.03	2.9
2/7/14	2.538	-144.73	-18.14	9.83	-4.03	2.9
2/8/14	2.538	-144.73	-18.14	9.83	-4.03	2.9
2/9/14	2.031	-144.73	-18.14	9.83	-4.03	2.9
2/10/14	1.523	-144.73	-18.14	9.83	-4.03	2.9
2/11/14	2.031	-144.73	-18.14	9.83	-4.03	2.9
2/12/14	1.269	-71.93	-9.68	10.66	-3.01	3.82
2/13/14	1.523	-71.93	-9.68	10.66	-3.01	3.82
2/14/14	4.061	-71.93	-9.68	10.66	-3.01	3.82
2/15/14	2.031	-71.93	-9.68	10.66	-3.01	3.82
2/16/14	2.284	-71.93	-9.68	10.66	-3.01	3.82
2/17/14	2.538	-71.93	-9.68	10.66	-3.01	3.82
2/18/14	1.523	-71.93	-9.68	10.66	-3.01	3.82
2/19/14	1.777					
2/20/14	1.523					
2/21/14	4.061					
2/22/14	1.269					
2/23/14	2.538					
2/24/14	1.015					
2/25/14	1.269	-91.58	-12.01	12.43	-1.96	5.23
2/26/14	1.015	-91.58	-12.01	12.43	-1.96	5.23
2/27/14	1.269	-91.58	-12.01	12.43	-1.96	5.23
2/28/14	1.777	-91.58	-12.01	12.43	-1.96	5.23
3/1/14	1.523	-91.58	-12.01	12.43	-1.96	5.23
3/2/14	3.3	-91.58	-12.01	12.43	-1.96	5.23
3/3/14	3.046	-91.58	-12.01	12.43	-1.96	5.23
3/4/14	1.015	-91.58	-12.01	12.43	-1.96	5.23
3/5/14	2.031	-95.87	-12.03	13.63	-1.44	6.09
3/6/14	0.508	-95.87	-12.03	13.63	-1.44	6.09
3/7/14	0.761	-95.87	-12.03	13.63	-1.44	6.09
3/8/14	1.269	-95.87	-12.03	13.63	-1.44	6.09
3/9/14	1.015	-95.87	-12.03	13.63	-1.44	6.09
3/10/14	1.269	-95.87	-12.03	13.63	-1.44	6.09
3/11/14	1.015	-95.87	-12.03	13.63	-1.44	6.09
3/12/14	0.761	-95.87	-12.03	13.63	-1.44	6.09
3/13/14	2.284					
3/14/14	2.031					
3/15/14	1.015					
3/16/14	1.269					
3/17/14	1.523					
3/18/14	0.761					
3/19/14	0.254					
3/20/14	1.015					
3/21/14	0.254					
3/22/14	1.269					
3/23/14	1.777					
3/24/14	1.269					
3/25/14	1.269	-86.09	-10.61	15.56	-1.05	7.26
3/26/14	1.269	-86.09	-10.61	15.56	-1.05	7.26
3/27/14	1.523	-86.09	-10.61	15.56	-1.05	7.26
3/28/14	1.523	-86.09	-10.61	15.56	-1.05	7.26
3/29/14	0.254	-86.09	-10.61	15.56	-1.05	7.26

3/30/14	1.523	-86.09	-10.61	15.56	-1.05	7.26
3/31/14	2.031	-86.09	-10.61	15.56	-1.05	7.26
4/1/14	1.015	-86.09	-10.61	15.56	-1.05	7.26
4/2/14	0.254					
4/3/14	1.015					
4/4/14	1.269	-62.89	-8.76	16.75	0.20	8.48
4/5/14	0.508	-62.89	-8.76	16.75	0.20	8.48
4/6/14	0.761	-62.89	-8.76	16.75	0.20	8.48
4/7/14	1.523	-62.89	-8.76	16.75	0.20	8.48
4/8/14	1.523	-62.89	-8.76	16.75	0.20	8.48
4/9/14	1.269					
4/10/14	1.015					
4/11/14	0.508					
4/12/14	0.254					
4/13/14	1.777					
4/14/14	1.777					
4/15/14	0.761	-59.07	-8.1	17.46	1.43	9.44
4/16/14	1.269	-59.07	-8.1	17.46	1.43	9.44
4/17/14	1.015	-59.07	-8.1	17.46	1.43	9.44
4/18/14	1.777	-59.07	-8.1	17.46	1.43	9.44
4/19/14	1.269	-59.07	-8.1	17.46	1.43	9.44
4/20/14	1.777	-59.07	-8.1	17.46	1.43	9.44
4/21/14	1.269	-59.07	-8.1	17.46	1.43	9.44
4/22/14	0.508	-59.07	-8.1	17.46	1.43	9.44
4/23/14	1.015					
4/24/14	1.523					
4/25/14	0.508					
4/26/14	0.761					
4/27/14	1.269					
4/28/14	1.015					
4/29/14	1.015					
4/30/14	1.523					
5/1/14	1.523					
5/2/14	0.761					
5/3/14	2.792					
5/4/14	0.761					
5/5/14	2.792					
5/6/14	0.761	-38.86	-4.29	21.81	3.01	12.41
5/7/14	0.761	-38.86	-4.29	21.81	3.01	12.41
5/8/14	0.508	-38.86	-4.29	21.81	3.01	12.41
5/9/14	2.031	-38.86	-4.29	21.81	3.01	12.41
5/10/14	1.015	-38.86	-4.29	21.81	3.01	12.41
5/11/14	0.254	-38.86	-4.29	21.81	3.01	12.41
5/12/14	0.254	-38.86	-4.29	21.81	3.01	12.41
5/13/14	0.508	-60.89	-7.34	23.31	4.84	14.08
5/14/14	0.761	-60.89	-7.34	23.31	4.84	14.08
5/15/14	0.508	-60.89	-7.34	23.31	4.84	14.08
5/16/14	0.508	-60.89	-7.34	23.31	4.84	14.08
5/17/14	1.777	-60.89	-7.34	23.31	4.84	14.08
5/18/14	1.523	-60.89	-7.34	23.31	4.84	14.08
5/19/14	1.015	-60.89	-7.34	23.31	4.84	14.08
5/20/14	1.777	-60.89	-7.34	23.31	4.84	14.08
5/21/14	1.015					
5/22/14	1.015					
5/23/14	1.015					
5/24/14	0.254					
5/25/14	0.508					

5/26/14	0.508					
5/27/14	0.761					
5/28/14	2.792					
5/29/14	1.269					
5/30/14	0.508					
5/31/14	1.523					
6/1/14	0.508					
6/2/14	1.015					
6/3/14	1.015					
6/4/14	2.031					
6/5/14	2.284					
6/6/14	1.015					
6/7/14	0.254					
6/8/14	2.538					
6/9/14	0.254					
6/10/14	0.508					
6/11/14	0.508					
6/12/14	0.254					
6/13/14	0.254					
6/14/14	1.269					
6/15/14	1.015					
6/16/14	0					
6/17/14	0.508					
6/18/14	0.254					
6/19/14	0.508					
6/20/14	2.031					
6/21/14	0.254					
6/22/14	0.254					
6/23/14	0					
6/24/14	1.523	-77.45	-9.01	30.50	9.43	19.96
6/25/14	1.015	-77.45	-9.01	30.50	9.43	19.96
6/26/14	0.508	-77.45	-9.01	30.50	9.43	19.96
6/27/14	0.761	-77.45	-9.01	30.50	9.43	19.96
6/28/14	0.254	-77.45	-9.01	30.50	9.43	19.96
6/29/14	1.777	-77.45	-9.01	30.50	9.43	19.96
6/30/14	0.761	-77.45	-9.01	30.50	9.43	19.96
7/1/14	0.761	-77.45	-9.01	30.50	9.43	19.96
7/2/14	0.508					
7/3/14	0.254					
7/4/14	0.254					
7/5/14	0					
7/6/14	0.254					
7/7/14	0					
7/8/14	0					
7/9/14	1.015					
7/10/14	0.254					
7/11/14	0.254					
7/12/14	0.254					
7/13/14	0.254					
7/14/14	0.254					
7/15/14	0.508	-38.33	-5.04	33.11	11.34	22.23
7/16/14	0.508	-38.33	-5.04	33.11	11.34	22.23
7/17/14	0.508	-38.33	-5.04	33.11	11.34	22.23
7/18/14	1.523	-38.33	-5.04	33.11	11.34	22.23
7/19/14	1.269	-38.33	-5.04	33.11	11.34	22.23
7/20/14	0.254	-38.33	-5.04	33.11	11.34	22.23
7/21/14	0.254	-38.33	-5.04	33.11	11.34	22.23

7/22/14	0.508	-38.33	-5.04	33.11	11.34	22.23
7/23/14	0.254					
7/24/14	0.254					
7/25/14	0.254					
7/26/14	0.254					
7/27/14	1.269					
7/28/14	0.254					
7/29/14	0.761					
7/30/14	1.269					
7/31/14	0.761					
8/1/14	0.254					
8/2/14	0.254					
8/3/14	0.254					
8/4/14	0.254					
8/5/14	0.254					
8/6/14	0					
8/7/14	0.508					
8/8/14	0.508					
8/9/14	0.508					
8/10/14	0.254					
8/11/14	0					
8/12/14	0.254					
8/13/14	0					
8/14/14	0.254					
8/15/14	0.508					
8/16/14	0.254					
8/17/14	0					
8/18/14	0					
8/19/14	0.254					
8/20/14	1.015					
8/21/14	0.508					
8/22/14	0.254					
8/23/14	0.761					
8/24/14	0.761					
8/25/14	0					
8/26/14	0					
8/27/14	0					
8/28/14	0					
8/29/14	0.254					
8/30/14	0.508					
8/31/14	0.508					
9/1/14	0					
9/2/14	0					
9/3/14	0					
9/4/14	0					
9/5/14	0					
9/6/14	0					
9/7/14	2.538					
9/8/14	0.254					
9/9/14	1.269					
9/10/14	0.254					
9/11/14	0.254					
9/12/14	0.254					
9/13/14	0					
9/14/14	0.761					
9/15/14	0.761					
9/16/14	0					

9/17/14	1.269					
9/18/14	1.269					
9/19/14	0.761					
9/20/14	0.508					
9/21/14	0					
9/22/14	0					
9/23/14	0.508	-77.68	-10.82	26.91	5.17	16.04
9/24/14	0.254	-77.68	-10.82	26.91	5.17	16.04
9/25/14	1.269	-77.68	-10.82	26.91	5.17	16.04
9/26/14	0.254	-77.68	-10.82	26.91	5.17	16.04
9/27/14	0.761	-77.68	-10.82	26.91	5.17	16.04
9/28/14	0.254	-77.68	-10.82	26.91	5.17	16.04
9/29/14	0.254	-77.68	-10.82	26.91	5.17	16.04
9/30/14	0	-77.68	-10.82	26.91	5.17	16.04
10/1/14	0.254					
10/2/14	0.761					
10/3/14	0					
10/4/14	0.508					
10/5/14	0.254					
10/6/14	0.508					
10/7/14	1.269					
10/8/14	0.254					
10/9/14	0.761					
10/10/14	0.761					
10/11/14	0.761					
10/12/14	0.254					
10/13/14	0.254					
10/14/14	0.254	-38.03	-5.24	21.13	1.20	11.16
10/15/14	0.254	-38.03	-5.24	21.13	1.20	11.16
10/16/14	0.254	-38.03	-5.24	21.13	1.20	11.16
10/17/14	0.761	-38.03	-5.24	21.13	1.20	11.16
10/18/14	1.269	-38.03	-5.24	21.13	1.20	11.16
10/19/14	1.777	-38.03	-5.24	21.13	1.20	11.16
10/20/14	1.015	-38.03	-5.24	21.13	1.20	11.16
10/21/14	1.777	-80.52	-10.52	19.11	0.89	10.00
10/22/14	0.254	-80.52	-10.52	19.11	0.89	10.00
10/23/14	3.046	-80.52	-10.52	19.11	0.89	10.00
10/24/14	2.284	-80.52	-10.52	19.11	0.89	10.00
10/25/14	1.269	-80.52	-10.52	19.11	0.89	10.00
10/26/14	1.269	-80.52	-10.52	19.11	0.89	10.00
10/27/14	0.761	-80.52	-10.52	19.11	0.89	10.00
10/28/14	2.538	-107.42	-14.33	15.67	-0.07	7.8
10/29/14	1.523	-107.42	-14.33	15.67	-0.07	7.8
10/30/14	1.777	-107.42	-14.33	15.67	-0.07	7.8
10/31/14	0.761	-107.42	-14.33	15.67	-0.07	7.8
11/1/14	0.761	-107.42	-14.33	15.67	-0.07	7.8
11/2/14	2.284	-107.42	-14.33	15.67	-0.07	7.8
11/3/14	3.046	-107.42	-14.33	15.67	-0.07	7.8
11/4/14	1.015	-107.42	-14.33	15.67	-0.07	7.8
11/5/14	1.015					
11/6/14	2.031					
11/7/14	2.792					
11/8/14	2.538					
11/9/14	2.031					
11/10/14	2.538					
11/11/14	1.269					
11/12/14	2.284	-45.54	-7.06	11.58	-1.58	5.00

11/13/14	2.284	-45.54	-7.06	11.58	-1.58	5.00
11/14/14	2.792	-45.54	-7.06	11.58	-1.58	5.00
11/15/14	1.015	-45.54	-7.06	11.58	-1.58	5.00
11/16/14	2.792	-45.54	-7.06	11.58	-1.58	5.00
11/17/14	4.315	-45.54	-7.06	11.58	-1.58	5.00
11/18/14	3.3	-45.54	-7.06	11.58	-1.58	5.00
11/19/14	2.792	-71.3	-8.76	9.69	-2.39	3.65
11/20/14	2.284	-71.3	-8.76	9.69	-2.39	3.65
11/21/14	3.553	-71.3	-8.76	9.69	-2.39	3.65
11/22/14	4.822	-71.3	-8.76	9.69	-2.39	3.65
11/23/14	3.807	-71.3	-8.76	9.69	-2.39	3.65
11/24/14	3.553	-71.3	-8.76	9.69	-2.39	3.65
11/25/14	2.538	-71.3	-8.76	9.69	-2.39	3.65
11/26/14	1.523					
11/27/14	1.777					
11/28/14	2.792					
11/29/14	3.046					
11/30/14	2.031					
12/1/14	3.553					
12/2/14	3.807	-82.07	-10.98	8.40	-3.01	2.69
12/3/14	2.792	-82.07	-10.98	8.40	-3.01	2.69
12/4/14	2.792	-82.07	-10.98	8.40	-3.01	2.69
12/5/14	2.284	-82.07	-10.98	8.40	-3.01	2.69
12/6/14	3.3	-82.07	-10.98	8.40	-3.01	2.69
12/7/14	4.061	-82.07	-10.98	8.40	-3.01	2.69
12/8/14	5.076	-82.07	-10.98	8.40	-3.01	2.69
12/9/14	3.553	-82.07	-10.98	8.40	-3.01	2.69
12/10/14	2.792	-119.34	-15.36	7.61	-3.40	2.11
12/11/14	2.538	-119.34	-15.36	7.61	-3.40	2.11
12/12/14	3.807	-119.34	-15.36	7.61	-3.40	2.11
12/13/14	3.553	-119.34	-15.36	7.61	-3.40	2.11
12/14/14	4.822	-119.34	-15.36	7.61	-3.40	2.11
12/15/14	4.569	-119.34	-15.36	7.61	-3.40	2.11
12/16/14	3.046	-89.26	-11.37	6.38	-4.80	0.79
12/17/14	3.807	-89.26	-11.37	6.38	-4.80	0.79
12/18/14	1.523	-89.26	-11.37	6.38	-4.80	0.79
12/19/14	3.553	-89.26	-11.37	6.38	-4.80	0.79
12/20/14	4.315	-89.26	-11.37	6.38	-4.80	0.79
12/21/14	3.3	-89.26	-11.37	6.38	-4.80	0.79
12/22/14	1.777	-89.26	-11.37	6.38	-4.80	0.79
12/23/14	1.523	-99.26	-12.81	6.04	-5.64	0.2
12/24/14	1.523	-99.26	-12.81	6.04	-5.64	0.2
12/25/14	0.761	-99.26	-12.81	6.04	-5.64	0.2
12/26/14	1.523	-99.26	-12.81	6.04	-5.64	0.2
12/27/14	3.553	-99.26	-12.81	6.04	-5.64	0.2
12/28/14	4.569	-99.26	-12.81	6.04	-5.64	0.2
12/29/14	2.792	-99.26	-12.81	6.04	-5.64	0.2
12/30/14	4.061					
12/31/14	6.853					
1/1/15	5.838					
1/2/15	3.3					
1/3/15	2.031					
1/4/15	2.538					
1/5/15	1.523					
1/6/15	1.523	-82.49	-10.92	7.61	-3.77	1.92
1/7/15	2.792	-82.49	-10.92	7.61	-3.77	1.92
1/8/15	3.807	-82.49	-10.92	7.61	-3.77	1.92

1/9/15	2.538	-82.49	-10.92	7.61	-3.77	1.92
1/10/15	2.538	-82.49	-10.92	7.61	-3.77	1.92
1/11/15	3.046	-82.49	-10.92	7.61	-3.77	1.92
1/12/15	1.269	-82.49	-10.92	7.61	-3.77	1.92
1/13/15	2.031	-82.49	-10.92	7.61	-3.77	1.92
1/14/15	2.792	-67.68	-8.64	7.54	-4.20	1.67
1/15/15	3.046	-67.68	-8.64	7.54	-4.20	1.67
1/16/15	4.061	-67.68	-8.64	7.54	-4.20	1.67
1/17/15	4.061	-67.68	-8.64	7.54	-4.20	1.67
1/18/15	2.792	-67.68	-8.64	7.54	-4.20	1.67
1/19/15	2.538	-67.68	-8.64	7.54	-4.20	1.67
1/20/15	2.031	-67.68	-8.64	7.54	-4.20	1.67
1/21/15	3.3					
1/22/15	2.031					
1/23/15	2.538					
1/24/15	2.792					
1/25/15	1.777					
1/26/15	2.031					
1/27/15	3.046	-67.05	-9.42	9.19	-3.89	2.65
1/28/15	2.031	-67.05	-9.42	9.19	-3.89	2.65
1/29/15	0.508	-67.05	-9.42	9.19	-3.89	2.65
1/30/15	1.777	-67.05	-9.42	9.19	-3.89	2.65
1/31/15	1.523	-67.05	-9.42	9.19	-3.89	2.65
2/1/15	2.792	-67.05	-9.42	9.19	-3.89	2.65
2/2/15	2.031	-67.05	-9.42	9.19	-3.89	2.65
2/3/15	2.284	-67.05	-9.42	9.19	-3.89	2.65
2/4/15	0.761	-75.67	-10.19	9.83	-4.11	2.86
2/5/15	0.761	-75.67	-10.19	9.83	-4.11	2.86
2/6/15	0.254	-75.67	-10.19	9.83	-4.11	2.86
2/7/15	2.538	-75.67	-10.19	9.83	-4.11	2.86
2/8/15	2.538	-75.67	-10.19	9.83	-4.11	2.86
2/9/15	2.031	-75.67	-10.19	9.83	-4.11	2.86
2/10/15	1.523	-75.67	-10.19	9.83	-4.11	2.86
2/11/15	2.031					
2/12/15	1.269					
2/13/15	1.523					
2/14/15	4.061					
2/15/15	2.031					
2/16/15	2.284					
2/17/15	2.538					
2/18/15	1.523					
2/19/15	1.777					
2/20/15	1.523					
2/21/15	4.061					
2/22/15	1.269					
2/23/15	2.538					
2/24/15	1.015					
2/25/15	1.269					
2/26/15	1.015					
2/27/15	1.269					
2/28/15	1.777					
3/1/15	1.523					
3/2/15	3.3					
3/3/15	3.046	-87.7	-10.3	13.04	-1.55	5.74
3/4/15	1.015	-87.7	-10.3	13.04	-1.55	5.74
3/5/15	2.031	-87.7	-10.3	13.04	-1.55	5.74
3/6/15	0.508	-87.7	-10.3	13.04	-1.55	5.74

3/7/15	0.761	-87.7	-10.3	13.04	-1.55	5.74
3/8/15	1.269	-87.7	-10.3	13.04	-1.55	5.74
3/9/15	1.015	-87.7	-10.3	13.04	-1.55	5.74
3/10/15	1.269	-87.7	-10.3	13.04	-1.55	5.74
3/11/15	1.015	-78.52	-9.74	14.43	-1.22	6.61
3/12/15	0.761	-78.52	-9.74	14.43	-1.22	6.61
3/13/15	2.284	-78.52	-9.74	14.43	-1.22	6.61
3/14/15	2.031	-78.52	-9.74	14.43	-1.22	6.61
3/15/15	1.015	-78.52	-9.74	14.43	-1.22	6.61
3/16/15	1.269	-78.52	-9.74	14.43	-1.22	6.61
3/17/15	1.523	-41.53	-5.47	15.80	-0.81	7.49
3/18/15	0.761	-41.53	-5.47	15.80	-0.81	7.49
3/19/15	0.254	-41.53	-5.47	15.80	-0.81	7.49
3/20/15	1.015	-41.53	-5.47	15.80	-0.81	7.49
3/21/15	0.254	-41.53	-5.47	15.80	-0.81	7.49
3/22/15	1.269	-41.53	-5.47	15.80	-0.81	7.49
3/23/15	1.777	-41.53	-5.47	15.80	-0.81	7.49
3/24/15	1.269	-41.53	-5.47	15.80	-0.81	7.49
3/25/15	1.269					
3/26/15	1.269					
3/27/15	1.523					
3/28/15	1.523					
3/29/15	0.254					
3/30/15	1.523					
3/31/15	2.031					
4/1/15	1.015	-124.22	-16.63	16.74	0.01	8.38
4/2/15	0.254	-124.22	-16.63	16.74	0.01	8.38
4/3/15	1.015	-124.22	-16.63	16.74	0.01	8.38
4/4/15	1.269	-124.22	-16.63	16.74	0.01	8.38
4/5/15	0.508	-124.22	-16.63	16.74	0.01	8.38
4/6/15	0.761	-124.22	-16.63	16.74	0.01	8.38
4/7/15	1.523	-124.22	-16.63	16.74	0.01	8.38
4/8/15	1.523	-124.22	-16.63	16.74	0.01	8.38
4/9/15	1.269					
4/10/15	1.015					
4/11/15	0.508					
4/12/15	0.254					
4/13/15	1.777					
4/14/15	1.777					
4/15/15	0.761					
4/16/15	1.269					
4/17/15	1.015					
4/18/15	1.777					
4/19/15	1.269					
4/20/15	1.777					
4/21/15	1.269					
4/22/15	0.508					
4/23/15	1.015					
4/24/15	1.523					
4/25/15	0.508					
4/26/15	0.761					
4/27/15	1.269					
4/28/15	1.015					
4/29/15	1.015					
4/30/15	1.523					
5/1/15	1.523					
5/2/15	0.761					

5/3/15	2.792					
5/4/15	0.761					
5/5/15	2.792	-29.98	-3.83	21.59	2.93	12.26
5/6/15	0.761	-29.98	-3.83	21.59	2.93	12.26
5/7/15	0.761	-29.98	-3.83	21.59	2.93	12.26
5/8/15	0.508	-29.98	-3.83	21.59	2.93	12.26
5/9/15	2.031	-29.98	-3.83	21.59	2.93	12.26
5/10/15	1.015	-29.98	-3.83	21.59	2.93	12.26
5/11/15	0.254	-29.98	-3.83	21.59	2.93	12.26
5/12/15	0.254	-50.75	-7.26	23.39	4.53	13.96
5/13/15	0.508	-50.75	-7.26	23.39	4.53	13.96
5/14/15	0.761	-50.75	-7.26	23.39	4.53	13.96
5/15/15	0.508	-50.75	-7.26	23.39	4.53	13.96
5/16/15	0.508	-50.75	-7.26	23.39	4.53	13.96
5/17/15	1.777	-50.75	-7.26	23.39	4.53	13.96
5/18/15	1.523	-50.75	-7.26	23.39	4.53	13.96
5/19/15	1.015	-50.75	-7.26	23.39	4.53	13.96
5/20/15	1.777					
5/21/15	1.015					
5/22/15	1.015					
5/23/15	1.015					
5/24/15	0.254					
5/25/15	0.508					
5/26/15	0.508					
5/27/15	0.761	-78.44	-9.51	25.27	6.87	16.07
5/28/15	2.792	-78.44	-9.51	25.27	6.87	16.07
5/29/15	1.269	-78.44	-9.51	25.27	6.87	16.07
5/30/15	0.508	-78.44	-9.51	25.27	6.87	16.07
5/31/15	1.523	-78.44	-9.51	25.27	6.87	16.07
6/1/15	0.508	-78.44	-9.51	25.27	6.87	16.07
6/2/15	1.015	-78.44	-9.51	25.27	6.87	16.07
6/3/15	1.015					
6/4/15	2.031					
6/5/15	2.284					
6/6/15	1.015					
6/7/15	0.254					
6/8/15	2.538					
6/9/15	0.254					
6/10/15	0.508					
6/11/15	0.508					
6/12/15	0.254					
6/13/15	0.254					
6/14/15	1.269					
6/15/15	1.015					
6/16/15	0					
6/17/15	0.508					
6/18/15	0.254					
6/19/15	0.508					
6/20/15	2.031					
6/21/15	0.254					
6/22/15	0.254					
6/23/15	0					
6/24/15	1.523					
6/25/15	1.015					
6/26/15	0.508					
6/27/15	0.761					
6/28/15	0.254					

6/29/15	1.777					
6/30/15	0.761					
7/1/15	0.761					
7/2/15	0.508					
7/3/15	0.254					
7/4/15	0.254					
7/5/15	0					
7/6/15	0.254					
7/7/15	0	-39.99	-5.24	33.44	10.46	21.95
7/8/15	0	-39.99	-5.24	33.44	10.46	21.95
7/9/15	1.015	-39.99	-5.24	33.44	10.46	21.95
7/10/15	0.254	-39.99	-5.24	33.44	10.46	21.95
7/11/15	0.254	-39.99	-5.24	33.44	10.46	21.95
7/12/15	0.254	-39.99	-5.24	33.44	10.46	21.95
7/13/15	0.254	-39.99	-5.24	33.44	10.46	21.95
7/14/15	0.254	-39.99	-5.24	33.44	10.46	21.95
7/15/15	0.508					
7/16/15	0.508					
7/17/15	0.508					
7/18/15	1.523					
7/19/15	1.269					
7/20/15	0.254					
7/21/15	0.254					
7/22/15	0.508					
7/23/15	0.254					
7/24/15	0.254					
7/25/15	0.254					
7/26/15	0.254					
7/27/15	1.269					
7/28/15	0.254					
7/29/15	0.761					
7/30/15	1.269					
7/31/15	0.761					
8/1/15	0.254					
8/2/15	0.254					
8/3/15	0.254					
8/4/15	0.254					
8/5/15	0.254					
8/6/15	0					
8/7/15	0.508					
8/8/15	0.508					
8/9/15	0.508					
8/10/15	0.254					
8/11/15	0					
8/12/15	0.254					
8/13/15	0					
8/14/15	0.254					
8/15/15	0.508					
8/16/15	0.254					
8/17/15	0					
8/18/15	0					
8/19/15	0.254					
8/20/15	1.015					
8/21/15	0.508					
8/22/15	0.254					
8/23/15	0.761					
8/24/15	0.761					

8/25/15	0					
8/26/15	0					
8/27/15	0					
8/28/15	0					
8/29/15	0.254					
8/30/15	0.508					
8/31/15	0.508					
9/1/15	0					
9/2/15	0					
9/3/15	0					
9/4/15	0					
9/5/15	0					
9/6/15	0					
9/7/15	2.538					
9/8/15	0.254					
9/9/15	1.269					
9/10/15	0.254					
9/11/15	0.254					
9/12/15	0.254					
9/13/15	0					
9/14/15	0.761					
9/15/15	0.761					
9/16/15	0					
9/17/15	1.269					
9/18/15	1.269					
9/19/15	0.761					
9/20/15	0.508					
9/21/15	0					
9/22/15	0					
9/23/15	0.508					
9/24/15	0.254					
9/25/15	1.269					
9/26/15	0.254					
9/27/15	0.761					
9/28/15	0.254					
9/29/15	0.254					
9/30/15	0					
10/1/15	0.254					
10/2/15	0.761					
10/3/15	0					
10/4/15	0.508					
10/5/15	0.254					
10/6/15	0.508					
10/7/15	1.269					
10/8/15	0.254					
10/9/15	0.761					
10/10/15	0.761					
10/11/15	0.761					
10/12/15	0.254					
10/13/15	0.254					
10/14/15	0.254	-56.53	-7.14	21.36	1.11	11.24
10/15/15	0.254	-56.53	-7.14	21.36	1.11	11.24
10/16/15	0.254	-56.53	-7.14	21.36	1.11	11.24
10/17/15	0.761	-56.53	-7.14	21.36	1.11	11.24
10/18/15	1.269	-56.53	-7.14	21.36	1.11	11.24
10/19/15	1.777	-56.53	-7.14	21.36	1.11	11.24
10/20/15	1.015	-56.53	-7.14	21.36	1.11	11.24

REFERENCES

Antinao, J.L., and McDonald, E., 2013, An enhanced role for the Tropical Pacific on the humid Pleistocene-Holocene transition in southwestern North America: Quat. Sci. Rev.,vol. 78, p.319-342.

Asmerom, Yemane, Victor J. Polyak, and Stephen J. Burns, 2010, Variable winter moisture in the southwestern United States linked to rapid glacial climate shifts: Nature Geoscience vol.3, no.2, p.114-117.

Banner, Jay L., et al., 1996, High-resolution temporal record of Holocene ground-water chemistry: Tracing links between climate and hydrology: Geology, vol. 24, no.11, p. 1049-1053.

Berkelhammer, M; Stott, L; Yoshimura, K; Johnson, K; & Sinha, A., 2012, Synoptic and mesoscale controls on the isotopic composition of precipitation in the western United States: Climate Dynamics, vol.38, p. 433 - 454. doi: 10.1007/s00382-011-1262-3. UC Irvine: 532522.Retrieved from http://escholarship.org/uc/item/9kd7g7mf

Berkelhammer, M, A Sinha, M. Mudelsee, H. Cheng, R. Edwards and K. Cannariato, 2010, Persistent multidecadal power of the Indian Summer Monsoon: Earth and Planetary Science Letters. doi:10.1016/j.epsl.2009.12.017

Breitenbach, S.F.M., Rehfeld, K., Goswami, B., Baldini, J.U.L., Ridley, H.E., Kennett, D.J., Prufer, K.M., Aquino, V.V., Asmerom, Y., Polyak, V.J., Cheng, H., Kurths, J., and Marwan, N., 2012, COnstructing Proxy Records from Age models (COPRA): Climate of the Past, v. 8, p. 1765–1779, doi: 10.5194/cp-8-1765-2012.

Briles, C.E., Whitlock, C. and Bartlein, P.J., 2005. Postglacial vegetation, fire, and climate history of the Siskiyou Mountains, Oregon, USA: Quaternary Research, vol.64, no.1, p.44-56.

Broecker, W.S., McGee, D., Adams, K.D., Cheng, H., Edwards, R.L., Oviatt, C.G. and Quade, J., 2009. A Great Basin-wide dry episode during the first half of the Mystery Interval?: Quaternary Science Reviews, vol.28, no.25, p.2557-2563.

Broecker, W. and Putnam, A.E., 2012. How did the hydrologic cycle respond to the two-phase mystery interval?: Quaternary Science Reviews, vol.57, p.17-25.

Bond, G., Broecker, W., Johnsen, S., McManus, J., Labeyrie, L., Jouzel, J. and Bonani, G., 1993. Correlations between climate records from North Atlantic sediments and Greenland ice: Nature, vol.365, no. 6442, p.143-147.

Bond, G., Broecker, W., Lotti, R. and McManus, J., 1992. Abrupt color changes in isotope stage 5 in North Atlantic deep sea cores: implications for rapid change of climate-driven events: In Start of a Glacial p. 185-205. Springer, Berlin, Heidelberg.

Cheng, H., Edwards, R.L., Shen, C.C., Polyak, V.J., Asmerom, Y., Woodhead, J., Hellstrom, J., Wang, Y., Kong, X., Spötl, C. and Wang, X., 2013. Improvements in 230 Th dating, 230 Th and 234 U half-life values, and U–Th isotopic measurements by multi-collector inductively coupled plasma mass spectrometry: Earth and Planetary Science Letters, vol. 371, p.82-91.

Clark, P.U., Shakun, J.D., Baker, P.A., Bartlein, P.J., Brewer, S., Brook, E., Carlson, A.E., Cheng, H., Kaufman, D.S., Liu, Z. and Marchitto, T.M., 2012. Global climate evolution during the last deglaciation: Proceedings of the National Academy of Sciences, vol.109, no.19, p.E1134-E1142.

Cross, M., McGee, D., Broecker, W.S., Quade, J., Shakun, J.D., Cheng, H., Lu, Y. and Edwards, R.L., 2015. Great Basin hydrology, paleoclimate, and connections with the North Atlantic: A speleothem stable isotope and trace element record from Lehman Caves, NV: Quaternary Science Reviews, vol.127, p.186-198.

Deininger, M., Fohlmeister, J., Scholz, D. and Mangini, A., 2012. Isotope disequilibrium effects: The influence of evaporation and ventilation effects on the carbon and oxygen isotope composition of speleothems–A model approach: Geochimica et Cosmochimica Acta, vol. 96, p.57-79.

Dettinger, Michael D., et al., 1998, North-south precipitation patterns in western North America on interannual-to-decadal timescales: Journal of Climate, vol.11, no.12, p. 3095-3111.

Dettinger, M.D., Cayan, D.R., Meyer, M.K. and Jeton, A.E., 2004. Simulated hydrologic responses to climate variations and change in the Merced, Carson, and American River basins, Sierra Nevada, California, 1900–2099: Climatic Change, vol.62, no.1, p.283-317.

Denton, G.H., Anderson, R.F., Toggweiler, J.R., Edwards, R.L., Schaefer, J.M. and Putnam, A.E., 2010. The last glacial termination: Science, vol.328, no.5986, p.1652-1656.

Draxler, R.R. and Hess, G.D., 1998. An overview of the HYSPLIT_4 modelling system for trajectories: Australian meteorological magazine, vol.47, p.295-308.

Dreybrodt, W. and Scholz, D., 2011. Climatic dependence of stable carbon and oxygen isotope signals recorded in speleothems: From soil water to speleothem calcite: Geochimica et Cosmochimica Acta, vol.*75*, no.3, p.734-752.

Epstein, S., Buchsbaum, R., Lowenstam, H.A. and Urey, H.C., 1953. Revised carbonate-water isotopic temperature scale: Geological Society of America Bulletin, vol.64, no.11, pp.1315-1326.

Ersek, V., Mix, A.C. and Clark, P.U., 2010. Variations of δ18O in rainwater from southwestern Oregon: Journal of Geophysical Research: Atmospheres, vol. 115, no.D9.

Ersek, Vasile, et al., 2012 Holocene winter climate variability in mid-latitude western North America: Nature communications vol.3 p.1219.

Fairchild, Ian J., 2006, Modification and preservation of environmental signals in speleothems: Earth Sci.Rev., vol. 75, p.105-153.

Fairchild, Ian J., and Andy Baker, 2012 Speleothem science: from process to past environments. vol.3. John Wiley & Sons.

Feng, W., Banner, J.L., Guilfoyle, A.L., Musgrove, M. and James, E.W., 2012. Oxygen isotopic fractionation between drip water and speleothem calcite: A 10-year monitoring study, central Texas, USA: Chemical Geology, vol. 304, p.53-67.

Feng, W., Casteel, R.C., Banner, J.L., and Heinze-Fry, A., 2014, Oxygen isotope variations in rainfall, drip-water and speleothem calcite from a well-ventilated cave in Texas, USA: Assessing a new speleothem temperature proxy: Geochimica et Cosmochimica Acta, vol. 127, p. 233–250, doi:10.1016/j.gca.2013.11.039.

Fleitmann, D., Burns, S.J., Mudelsee, M., Neff, U., Kramers, J., Mangini, A. and Matter, A., 2003. Holocene forcing of the Indian monsoon recorded in a stalagmite from southern Oman: Science, vol.300, no.5626, p.1737-1739.

Friedman, I., Smith, G.I., Gleason, J.D., Warden, A. and Harris, J.M., 1992. Stable isotope composition of waters in southeastern California 1. Modern precipitation. Journal of Geophysical Research: Atmospheres, vol. 97, p.5795-5812.

Genty, D., Blamart, D., Ouahdi, R., Gilmour, M., Baker, A., Jouzel, J. and Van-Exter, S., 2003. Precise dating of Dansgaard–Oeschger climate oscillations in western Europe from stalagmite data: Nature, vol.421, no.6925, p.833-837.

Griffin, D., and K. J. Anchukaitis, 2014, How unusual is the 2012–2014 California drought?: Geophys. Res. Lett., vol.41, p. 9017–9023, doi:10.1002/2014GL062433.

Gehre, M., Geilmann, H., Richter, J., Werner, R.A. and Brand, W.A., 2004. Continuous flow 2H/1H and 18O/16O analysis of water samples with dual inlet precision. Rapid Communications in Mass Spectrometry, vol.18, p.2650-2660.

Gutjahr, M., and J. Lippold 2011, Early arrival of Southern Source Water in the deep North Atlantic prior to Heinrich event 2, Paleoceanography, 26, PA2101, doi:10.1029/2011PA002114.

Harvey, F.E., 2001, Use of NADP Archive Samples to Determine the Isotope Composition of Precipitation: Characterizing the Meteoric Input Function for Use in Ground Water Studies: Groundwater, vol. 39, p.380-390, http://onlinelibrary.wiley.com/doi/10.1111/j.1745- 6584.2001.tb02322.x/abstract

Harvey, F. E., and J. M. Welker, 2000, Stable isotopic composition of precipitation in the semi-arid north- central portion of the US Great Plains: J. Hydrol., vol.238, p.90–109, doi:1016/S0022-1694(00)00316-4.

Hendy, C.H., 1971. The isotopic geochemistry of speleothems—I. The calculation of the effects of different modes of formation on the isotopic composition of speleothems and their applicability as palaeoclimatic indicators: Geochimica et cosmochimica Acta, vol.35, no.8, p.801-824.

Holden, N.E., 1989. Total and spontaneous fission half-lives for uranium, plutonium, americium and curium nuclides. Pure and Applied Chemistry, vol. 61, p.1483-1504.

Hostetler, S.W. and Benson, L.V., 1994. Stable isotopes of oxygen and hydrogen in the Truckee River–Pyramid Lake surface-water system. 2. A predictive model of δ18O and 182H in Pyramid Lake: Limnology and Oceanography, vol.39, n.2, p.356-364

Howitt, Richard, et al., 2014 Economic analysis of the 2014 drought for California agriculture. Center for Watershed Sciences, University of California, Davis.

Ibarra, D.E., Egger, A.E., Weaver, K.L., Harris, C.R. and Maher, K., 2014. Rise and fall of late Pleistocene pluvial lakes in response to reduced evaporation and precipitation: Evidence from Lake Surprise, California. Geological Society of America Bulletin, p. B31014-1.

Jaffey, A.H., Flynn, K.F., Glendenin, L.E., Bentley, W.T. and Essling, A.M., 1971. Precision measurement of half-lives and specific activities of U 235 and U 238. Physical Review C, vol. 4, no.5, p.1889.

Johnsen, R., Chen, A. and Biondi, M.A., 1980. Dissociative charge transfer of He+ ions with H2 and D2 molecules from 78 to 330 K: The Journal of Chemical Physics, vol. 72, no.5, p.3085-3088.

Johnsen, S.J., Clausen, H.B., Dansgaard, W., Fuhrert, K., Gundestrup, N., Hammer, C.U., Iversen, P., Jouzel, I. and Stauffer, B., 1992. Irregular glacial interstadials, recorded in a new Greenland: Nature, vol.3, p.311-313.

Kendall, C. and Coplen, T.B., 2001. Distribution of oxygen-18 and deuterium in river waters across the United States. Hydrological processes, vol.15, p.1363-1393.

Kirby, Matthew E., et al., 2013, "Latest Pleistocene to Holocene hydroclimates from Lake Elsinore, California: Quaternary Science Reviews vol.76, p. 1-15.

Lachniet, Matthew S., 2009, Climatic and environmental controls on speleothem oxygen-isotope values: Quaternary Science Reviews vol.28, p. 412-432.

Lachniet, M.S., Denniston, R.F., Asmerom, Y. and Polyak, V.J., 2014. Orbital control of western North America atmospheric circulation and climate over two glacial cycles: Nature communications, vol.5.

Lyle M., Heusser L., Ravelo C., Yamamoto M., Barron J., Diffenbaugh N. S., Herbert T., Andreasen D., 2012, Out of the tropics: The Pacific, Great Basin Lakes, and Late Pleistocene water cycle in the western United States: Science, v. 337, n. 6102, p. 1629–1633, doi:http://dx.doi.org/10.1126/science.1218390

Lora, J.M., Mitchell, J.L. and Tripati, A.E., 2016. Abrupt reorganization of North Pacific and western North American climate during the last deglaciation: Geophysical Research Letters.

McGee, D., Quade, J., Edwards, R.L., Broecker, W.S., Cheng, H., Reiners, P.W. and Evenson, N., 2012. Lacustrine cave carbonates: novel archives of paleohydrologic change in the Bonneville Basin (Utah, USA): Earth and Planetary Science Letters, vol. 351, p.182-194.

Merlivat, L. and Jouzel, J., 1979. Global climatic interpretation of the deuterium-oxygen 18 relationship for precipitation: Journal of Geophysical Research: Oceans, vol. 84, no.C8, pp.5029-5033.

Mickler, P.J., Banner, J.L., Stern, L., Asmerom, Y., Edwards, R.L. and Ito, E., 2004. Stable isotope variations in modern tropical speleothems: evaluating equilibrium vs. kinetic isotope effects: Geochimica et Cosmochimica Acta,vol. 6821, p.4381-4393.

Munroe, Jeffrey S., and Benjamin JC Laabs., 2013, Temporal correspondence between pluvial lake highstands in the southwestern US and Heinrich Event 1: Journal of Quaternary Science vol. 28, no.1, p. 49-58.

Medellín-Azuara J., 2016 The California Case: Managing Groundwater in Irrigated Agriculture: Harvard College Review of Environment and Society, v.3, p.11-12.

Musgrove, M., Banner, J.L., Mack, L.E., Combs, D.M., James, E.W., Cheng, H. and Edwards, R.L., 2001. Geochronology of late Pleistocene to Holocene speleothemsfrom central Texas: Implications for regional paleoclimate: Geological Society of America Bulletin, vol.113, n.12, p.1532-1543.

North Greenland Ice Core Project members, 2004. North Greenland ice core project oxygen isotope data: IGBP PAGES/World Data Center for Paleoclimatology Data Contribution Series, 59.

Oster, Jessica L., Montanez I., Sharp W., and Cooper K., 2009 Late Pleistocene California droughts during deglaciation and Arctic warming: Earth Planet. Sci. Lett., vol.288, p.434-443.

Oster, J.L., Montañez, I.P. and Kelley, N.P., 2012. Response of a modern cave system to large seasonal precipitation variability: Geochimica et Cosmochimica Acta,vol. 91, p.92-108.

Oster, J.L., Montañez, I.P., Mertz-Kraus, R., Sharp, W.D., Stock, G.M., Spero, H.J., Tinsley, J. and Zachos, J.C., 2014. Millennial-scale variations in western Sierra Nevada precipitation during the last glacial cycle MIS 4/3 transition: Quaternary Research, vol.82, no.1, p.236-248.

Oster, J.L., Montanez, I.P., Santare, L.R., Sharp, W.D., Wong, C., Cooper, K.M., 2015. Stalagmite records of hydroclimate in central California during termination 1 Quaternary Science Reviews, 127, 199 214. http://www.sciencedirect.com/science/ article/pii/ S0277379115300627
Oster, Jessica L., et al., 2015, Steering of westerly storms over western North America at the Last Glacial Maximum: Nature Geoscience vol.8.3, p.201-205.

Oviatt, C.G., 1997. Lake Bonneville fluctuations and global climate change: Geology, vol.25, n.2, p.155-158.

Pfahl, S. and Wernli, H., 2008. Air parcel trajectory analysis of stable isotopes in water vapor in the eastern Mediterranean: Journal of Geophysical Research: Atmospheres, vol. 113, no.D20.

Polyak, V.J., Asmerom, Y., Burns, S.J. and Lachniet, M.S., 2012. Climatic backdrop to the terminal Pleistocene extinction of North American mammals: Geology, vol.40, n.11, p.1023-1026.

Redmond, K. T., and R. W. Koch, 1991, Surface Climate and Streamflow Variability in the Western United States and Their Relationship to Large-Scale Circulation Indices:Water Resour. Res., vol.27,p.2381–2399, doi:10.1029/91WR00690.

Romanov, D., Kaufmann, G. and Dreybrodt, W., 2008. δ 13 C profiles along growth layers of stalagmites: comparing theoretical and experimental results: Geochimica et Cosmochimica Acta, vol.72, no.2, p.438-448.

Stein, A.F., Draxler, R.R, Rolph, G.D., Stunder, B.J.B., Cohen, M.D., and Ngan, F., 2015, NOAA's HYSPLIT atmospheric transport and dispersion modeling system: Bull. Amer.Meteor.Soc.,v o1. 96,p . 2059-2077, http://dx.doi.org/10.1175/BAMS-D-14-00110.1

Street, J.H., Anderson, R.S. and Paytan, A., 2012. An organic geochemical record of Sierra Nevada climate since the LGM from Swamp Lake, Yosemite: Quaternary Science Reviews, vol.40, p.89-106.

Tremaine, D.M., Froelich, P.N. and Wang, Y., 2011. Speleothem calcite farmed in situ: modern calibration of δ 18 O and δ 13 C paleoclimate proxies in a continuously-monitored natural cave system: Geochimica et Cosmochimica Acta, vol.75, n.17, p.4929-4950.

US Climate data, Temperature - Precipitation - Sunshine – Snowfall, http://www.usclimatedata.com

Vacco, D.A., Clark, P.M., Mix, A.C., Cheng, H., and Edwards, R.L., 2005, A speleothem record of Younger Dryas cooling, Klamath Mountains, Oregon, USA, Quaternary Res., vol. 64, p.249-256, http://dx.doi.org/10.1016/j.yqres.2005.06.008

Vachon, R. W., J. W. C. White, E. Gutmann, and J. M. Welker 2007, Amount-weighted annual isotopic (δ18O) values are affected by the seasonality of precipitation: A sensitivity study: Geophys. Res. Lett., vol. 34, L21707, doi:10.1029/2007GL030547.

Vachon, R. W., J. M. Welker, J. W. C. White, and B.H. Vaughn 2010a, Monthly precipitation isoscapes (δ18O) of the United States: Connections with surface temperatures, moisture source conditions, and air mass trajectories: J. Geophys. Res., vol.115, D21126, doi:10.1029/2010JD014105.

Vachon, R. W., J. M. Welker, J. W. C. White, and B.H. Vaughn 2010b, Moisture source temperatures and precipitation δ18O-temperature relationships across the US: Water Resour. Res., vol.46, W07523, doi:10.1029/2009WR008558.

Wagner, J. D. M., et al., 2010, Moisture variability in the southwestern United States linked to abrupt glacial climate change: Nature Geoscience, vol.3, p.110-113.

Welker, J. M., 2000, Isotopic (δ18O) characteristics of weekly precipitation collected across the United States: An initial analysis with application to water source studies: Hydrol. Processes, vol.14, p.1449–1464, doi:10.1002/1099-1085(20000615)14:8<1449::AID-HYP993>3.0.CO;2-7.

Wise, E. K., 2010, Spatiotemporal variability of the precipitation dipole transition zone in the western United States: Geophys. Res. Lett., vol. 37, L07706, doi:10.1029/2009GL04